Communication over Asynchronous Networks: Signaling and Rate-Reliability Analysis

by

Mehdi Torbatian

A thesis
presented to the University of Waterloo
in fulfillment of the
thesis requirement for the degree of
Doctor of Philosophy
in
Electrical and Computer Engineering

Waterloo, Ontario, Canada, 2011

Author's Declaration

I hereby declare that I am the sole author of this thesis. This is a true copy of the thesis, including any required final revisions, as accepted by my examiners.

I understand that my thesis may be made electronically available to the public.

Abstract

Asynchronism *inherently* exists in many communication systems specially in multi-terminal networks mainly due to the effect of multi-path and propagation delay. While in theoretical analysis of communication systems perfect synchronization of the terminals is often presumed, in some cases in which the nodes are randomly distributed over a geometrical area, it might be impossible to synchronize the nodes even if an ideal infrastructure service provider is used. In this work, two major categories of multi-user communication systems, i.e., relay networks and interference channels, are considered and the effect of the asynchronism among the terminals on characteristic properties of these channels are investigated.

In Chapter 2, the construction of distributed space-time codes for a general two-hop *asynchronous* cooperative relay network is considered. A novel algebraic structure is proposed and shown to achieve full diversity for arbitrary number of relays, arbitrary input alphabets, and arbitrary delay profiles among the relays. Unlike previously proposed delay tolerant schemes, the new design has minimum length which translates into smaller decoding complexity at the same transmission rate. Full-rate and full-diversity are achieved by the new designs with or without the use of guard intervals between successive transmissions. Simulation results confirm the mathematical analysis of the proposed codes.

In Chapter 3, the underlying asynchronous network is examined for various relaying protocols such as non-orthogonal selection decode-and-forward, orthogonal selection decode-and-forward, non-orthogonal amplify-and-forward (NAF), and orthogonal amplify-and-forward (OAF). The transmitter nodes send pulse amplitude modulation (PAM) signals, in which information symbols are linearly modulated by a shaping waveform to be sent to the destination, asynchronously. We consider two different cases with respect to the type of the shaping waveforms used in the structure of the PAM signals. In the theoretical case where band-limited shaping waveforms are used, it is shown that the asynchronism does not affect the DMT performance of the system and the same DMT as that of the corresponding synchronous network is obtained for all the aforementioned protocols. In the practical case where time-limited shaping waveforms are used, it is shown that

better diversity gains can be achieved at the expense of a bandwidth expansion. More precisely, in the decode-and-forward type protocols, the asynchronous network provides a better diversity gain than that of the corresponding synchronous network throughout the range of the multiplexing gain. In the amplify-and-forward type protocols, the asynchronous network provides the same DMT as that of the corresponding synchronous counterpart under the OAF protocol; however, a better diversity gain is achieved under the NAF protocol throughout the range of the multiplexing gain. In particular, in the single relay asynchronous network, the NAF protocol provides the same DMT as that of the 2×1 multiple-input single-output channel.

In Chapter 4, a constant K-user interference channel in which the users are not symbol-synchronous is considered. It is shown that the asynchronism among the users does not affect the total number of degrees of freedom (DOF) of this channel; however, it facilitates aligning interfering signals at each receiver node. To achieve the total $K/2$ DOF of this channel when single antenna nodes are used, a novel practical interference alignment scheme is proposed wherein the alignment task is performed with the help of asynchronous delays which inherently exist among the received signals at each receiver node. The asynchronism causes inter-symbol-interference (ISI) among transmitted symbols by different transmitters resulting in the underlying quasi-static links to be converted to ISI and accordingly into time varying channels. It is proved that this conversion solves the lack of channel variation required for the interference alignment in quasi-static scenarios. When each node is equipped with $M > 1$ antennas, it is argued that the same alignment scheme proposed for the single antenna nodes' interference channel is sufficient to achieve the total $MK/2$ DOF of the medium provided that each pair of the transmitters and the receivers experience the same asynchronous delay for all the corresponding antennas. In contrast to previously proposed alignment schemes, the channel state information of the links does not need to be known at the transmitter nodes. Instead, the relative delays among the received signals at each receiver node are globally known to the entire network.

While the asynchronism is usually treated as a troublesome factor in communication systems, in this dissertation, we are interested to introduce it as a useful property of the wireless medium similar to the fading which can improve the system performance in some communication scenarios or facilitate signaling over the medium in some other scenarios.

Acknowledgements

I am indebted to many individuals who helped me during the course of my Ph.D. studies. This work would not exist without their generous support.

I owe my deepest gratitude to my supervisor, Professor Mohamed Oussama Damen for his guidance and inspiration from the beginning to the end of my Ph.D. studies. I was fortunate to work with such a brilliant, insightful, creative, and knowledgeable supervisor. I would like to thank him for his care and support. I learnt many valuable lessons, not restricted to the research work, from him.

I wish to thank the members of my dissertation committee, Professors Frank Kschischang, Liang Liang Xie, Murat Uysal, and David Jao for carefully reading my thesis and for providing me with insightful questions and constructive suggestions. I wish to express my gratitude and thanks to Professor Catherine Rosenberg for attending my Ph.D. examination as a delegate of Professor Liang Liang Xie who was not able to attend the session.

I am pleased to thank my friends and colleagues Hossein Najafi and Walid Abediseid whom I have enjoyed discussing and sharing ideas with them.

My special thank and appreciation is to Sahar Molla-Aghajanzadeh, my beautiful wife, for all her love, support, and patient throughout the completion of this work.

I humbly thank my parents and my sibling for their endless love and unconditional support without which I could not get to this stage.

This is a great opportunity to thank my wonderful friends, Ehsan Fathi, Adel Izadbakhsh, Siamak Fouladi, Majid Safari, Behzad Behravesh, Sivash Bayat, Ali Hosseini, Fereidoon Rezanejad, Babak Alipanahi, Arash Tabibiazar, Tohid Ahadifard, and Alireza Shasttiri, with whom I have shared many happy moments of my life.

To my beloved wife:

Sahar Molla Aghajanzadeh

and

To my parents:

Mehri Toghian and *Rasool Torbatian*

Table of Contents

List of Figures

List of Abbreviations

SNR	Signal to Noise Ratio
CSI	Channel State Information
PAM	Pulse Amplitude Modulation
QAM	Quadrature Amplitude Modulation
SISO	Single-Input Single-Output
MISO	Multiple-Input Single-Output
MIMO	Multiple-Input Multiple-Output
STC	Space-Time Codes
STTC	Space-Time Trellis Codes
STBC	Space-Time Block Codes
OFDM	Orthogonal Frequency Division Multiplexing
FT	Fourier Transform
DFT	Discrete Fourier Transform
IDFT	Inverse Discrete Fourier Transform
DTFT	Discrete Time Fourier Transform
DMT	Diversity Multiplexing Tradeoff
DF	Decode-and-Forward
AF	Amplify-and-Forward
NSDF	Non-orthogonal Selection Decode-and-Forward
OSDF	Orthogonal Selection Decode-and-Forward
NAF	Non-orthogonal Amplify-and-Forward
OAF	Orthogonal Amplify-and-Forward
IC	Interference Channel
DOF	Degrees of Freedom
ISI	Inter-Symbol-Interference

Notation

$\underline{x}, \underline{X}$	Letters with underline denote vectors
$\mathbf{x}, \mathbf{X}$	Boldface letters denote matrices
$\underline{x}^T, \mathbf{X}^T$	Transpose of $\underline{x}, \mathbf{X}$
$\underline{x}^*, \mathbf{X}^*$	Conjugate of $\underline{x}, \mathbf{X}$
$\underline{x}^\dagger, \mathbf{X}^\dagger$	Transpose conjugate of $\underline{x}, \mathbf{X}$
$\mathbf{X} \succeq 0$	Matrix $\mathbf{X}$ is positive semi-definite
$\mathbf{X} \succeq \mathbf{Y}$	Matrix $\mathbf{X} - \mathbf{Y}$ is positive semi-definite
$\mathbf{I}_n$	Identity matrix of dimension n
ξ	$\sqrt{-1}$
$\mathbb{R}$	Field of real numbers
$\mathbb{Q}$	Field of rational numbers
$\mathbb{C}$	Field of complex numbers
$\mathbb{Z}$	Ring of integers
$\mathbb{Z}[\xi]$	Ring of Gaussian integers
$\mathbb{Z}[j]$	Ring of Eisenstein integers
$\mathtt{span}\,\mathbf{X}$	Vector space spanned by matrix $\mathbf{X}$
$\mathtt{rank}\,\mathbf{X}$	Rank of matrix $\mathbf{X}$
$\mathtt{trace}\,\mathbf{X}$	Trace of matrix $\mathbf{X}$
$\mathtt{diag}\{\cdot\}$	A diagonal or a block diagonal matrix of arguments
$(x)^+$	$\max\{0, x\}$

Chapter 1

Introduction

Asynchronism *inherently* exists in many communication systems mainly due to the effect of multi-path and propagation delay. In particular, in multi-terminal networks, the nodes are at different locations, which results in different propagation delays, and they have their own local oscillators with no common timing reference. Hence, the signaling over such channels is naturally asynchronous. As a fundamental issue in design of communication systems, asynchronism can detrimentally affect the system performance if it is ignored or not dealt with properly. Although in most cases, it is assumed that terminals are synchronized by an infrastructure service provider, which itself causes a large amount of overhead on the overall throughput of the system, this assumption cannot be held in many communication scenarios such as the interference channels in which terminals are randomly distributed over a geometrical area. In such a scenario, only one of the receivers can possibly receive a synchronized version of the transmitted signals (if an infrastructure synchronizing center exists) and the rest receive random asynchronous linear combinations of the transmitted signals.

Various techniques have been deployed in practice to mange the asynchronism in communication networks. The major approaches are briefly discussed in the following. The traditional approach is to employ a central control unit with proper controlling signals to synchronize the terminals. As it was discussed earlier, this approach causes a large amount of overhead on the throughput of the system specially in networks with large number of nodes. More importantly, it cannot be used in communication networks in which multiple distributed and independent receivers exist. Another approach which will be discussed more in the next section is to design signals such that they provide the required properties such as the diversity gain regardless of the existence of the natural asynchronism among the terminals. Various design methods of *distributed space-time codes*, which provide the maximum diversity gain over a wireless channel at

the presence of the asynchronism, are examples of this approach. Although this might be an ideal solution to combat the synchronization error in a communication system, in practice, it is not feasible often to design such signals for any arbitrary profiles of the asynchronism. For example, in design of delay-tolerant space-time codes, it is usually assumed that the asynchronism among the nodes are integer multiples of the symbol intervals which is in fact often unrealistic. The third approach is to use orthogonal frequency division multiplexing (OFDM) to offset the effect of the synchronization error. Using OFDM, the asynchronous delays in the time domain are converted to phase shifts in the frequency domain and appear as multiplicative factors of the fading coefficients. This might be the best option to handle the asynchronism in most cases; however, it is at the cost of a rate loss due to inserting cyclic prefix symbols at the beginning of each OFDM symbol. Time sharing among transmitting nodes followed by zero-padding the transmitted frames is also another way of combating the asynchronism which again results in a rate loss and delay in decoding.

While many research works exist on how to offset the effect of the asynchronism in communication networks, some examples have been reported wherein the asynchronism has helped to improve the system performance [1–8]. For example in [3], it is shown that asynchronous pulse amplitude modulation (PAM) can exploit the total existing degrees of freedom (DOF) of a multiple-input multiple output (MIMO) system which communicates over a spectral mask with infinite support, while synchronous PAM can exploit only finite number of DOF of this channel. In this thesis, we are interested to introduce the asynchronism as a useful property of the wireless medium which can be exploited to improve the system performance in some cases or to facilitate signaling over the channel in some others. We begin with design of the delay tolerant space-time codes for two-hop asynchronous relay networks. Then, the effect of the asynchronism on diversity multiplexing tradeoff (DMT) of these channels is examined. Asynchronous interference channels are considered at the end.

1.1 Delay-Tolerant Space-Time Codes

Reliable data transmission over wireless channels can be achieved by diversity techniques. Among them, spatial diversity using multiple transmit and receive antennas has gained much interest in the last decade (e.g., [9–17] and references therein). However, in some cases such as mobile handsets and sensor networks, transmitters and receivers are restricted in size and power consumption. Hence, it may not be feasible or cost effective to equip them with additional RF hardware. In these cases, *cooperative diversity* allows the source to use nearby nodes as virtual antennas. In other words, the nearby transmitters act as relay nodes for the original transmitter [18, 19].

Cooperative diversity opened a new research area for designing distributed space-time codes which provide specific diversity and coding gain. Although these codes follow the well-known *rank* and *determinant* criteria [9], the lack of a common timing reference can affect the structure of the code matrix and result in a rank deficient space-time code. Hence, the previously designed fully diverse space-time codes are no longer valid for cooperative diversity unless they provide the desired diversity gain not only when the transmitters are synchronous, but also when they transmit their symbols with arbitrary relative delays. Such codes that preserve the diversity gain regardless of the relative delays among the rows of the codeword's matrix are called *delay-tolerant* space-time codes.

1.1.1 Prior Works

Many previously proposed space-time codes are adapted to use in *synchronous* cooperative scenarios [20, 21]. For example, inspired by linear dispersion (LD) codes [12], Jing and Hassibi introduced distributed LD codes [20]. In their proposed construction, each relay multiplies the received block of the signal by a specific unitary matrix and sends it toward the receiver without decoding. They showed that these codes can provide the same rate and diversity gain as those of the original LD codes at very high signal to noise ratio (SNR). The main advantage of these codes is that the transmitted symbols from the source do not need to be decoded at the relay nodes. Therefore, there does not exist a bottleneck on the rate by requiring the relays to decode. However, such codes cannot realize the capabilities of the cooperative diversity when they apply to practical asynchronous cases.

In [22], intentional delays are introduced in different terminals. At the destination, the minimum mean square error estimator is used to exploit the cooperative diversity. Full-diversity order is not guaranteed in this method. In [23], Mei, et al. considered the effect of the synchronization error for two cooperative relays when the Alamouti scheme [24] is used to transmit information symbols over a block fading channel. The authors showed that the synchronization error turns a frequency-flat channel into a frequency-selective one with correlated channel coefficients. They proposed to use either time reverse space-time coding (TR-STC) or OFDM signaling to combat synchronization error between relay nodes. The proposed schemes achieve full-diversity for two relays at the expense of a rate loss resulted from either adding cyclic prefix to OFDM symbols or inserting guard intervals between blocks of symbols in the TR-STC technique. Latter in [25], the OFDM based scheme was generalized for a network with arbitrary number of relays. In [26], Xia, et al. proposed a MIMO-OFDM scheme to use in cooperative networks which achieves a diversity gain equal to the number of active relays provided that the length of the added cyclic prefix is

not smaller than the maximum length of the frequency selective channels plus the asynchronous delays.

Many distributed space-time schemes have been proposed to provide cooperative diversity gains in the presence of the asynchronizm among the relays [27–33]. For example, inspired by ElGamal-Hammons stacking construction [11], Li and Xia [29] considered the design of binary space-time trellis codes (STTC) that are full-diversity and delay tolerant for any number of cooperating relays. The authors extended their proposed structures to multilevel space-time codes for higher order constellations using the generalized stacking construction proposed in [15]. In [28], Shang and Xia extended the proposed structures of [29] to full-diversity delay tolerant STTCs of minimum delay length. In [30] and [31], Hammons showed that codes obtained from generalization of the construction of [15] from PAM and QAM to AM-PSK constellations preserve the diversity gain despite the timing offset among the relay nodes. He also showed that certain binary space-time block codes (STBCs) derived from the stacking construction [11] are delay tolerant. In [32], he proposed a delay tolerant transmission scheme of STBCs of short length to be used in asynchronous cooperative communications. In [33], Damen and Hammons extended the class of threaded algebraic space-time (TAST) codes [13] to the case of delay tolerant codes for cooperative diversity. Their proposed codes are based on delay tolerant threaded structures of length growing exponentially with the number of relays. Different threads are separated by different algebraic or transcendental numbers which guarantee that the difference of every two distinct codewords is full rank. Although these codes provide full-rate and full-diversity gain simultaneously, they are not minimum delay length and are no longer delay tolerant if one deletes one column of the codeword matrix.

A common assumption in all the aforementioned distributed space-time code is that the asynchronous delays are integer multiples of the symbol interval and fractional delays (i.e., the non-integer part of the delay) are absorbed in multi path. In contrast, the OFDM based scheme proposed in [23] allows the synchronization error to be any factor of the symbol interval.

1.1.2 Contributions

We introduce a novel delay tolerant algebraic structure to achieve full diversity for arbitrary number of relays, arbitrary input alphabets, and arbitrary delay profiles among the relays. Our work can be considered as an extension of the delay tolerant TAST codes proposed in [33] which itself is originated from the TAST framework in [13]. Similarly to [33], we consider the scenario of decode-and-forward single-carrier asynchronous relay transmission, wherein the source node first transmits to the relays. Then each relay, after decoding the source message, encodes the message

and retransmits it to the destination. Unlike previously proposed delay tolerant schemes, the new design has minimum length which translates into smaller decoding complexity at the same transmission rate. in difference to [33], we restrict ourselves to square matrices (i.e., the temporal span of the code equals the number of transmit antennas) and use a full-diversity single input single output (SISO) code to fill all the threads in the space-time codeword matrix. Then, by properly choosing algebraic or transcendental numbers [13] with increasing powers in some elements of the codeword matrix, we ensure full-diversity regardless of the delay profile. Full-rate and full-diversity are achieved by the new designs with or without the use of guard intervals between successive transmissions. The mathematical analysis of the code design procedure are supported by the simulation results.

1.2 Diversity Multiplexing Tradeoff of Asynchronous Relay Networks

Diversity multiplexing tradeoff is an information theoretic performance measure in multiple antenna quasi-static communication systems and space-time coding which characterizes the tradeoff between the multiplexing gain as a measure of the transmission rate and the diversity gain as a measure of the reliability of the transmission [34]. Since the relay networks mimics the behavior of multiple antenna systems, DMT is a fundamental performance measure in such networks under various relaying protocols. A relaying protocol characterizes the rules that the nodes follow to cooperatively send the source message to the destination. Various relaying protocols have been introduced [35, 36]. The most important ones, which are in fact the building blocks of other existing protocols, are listed below.

- Decode-and-Forward (DF): each relay decode the received signal from the source and independently re-encodes and re-sends it to the destination.
- Amplify-and-Forward (AF): each relay performs linear processing (not decoding) on the received signal from the source and retransmits it to the destination.
- Compress-and-Forward (CF): each relay compressed the received signal, which contains the source message and noise, into a new codeword and sends it to the destination.
- Compute-and-Map: each relay quantizes the received signal at the noise level and re-encodes and retransmits it to the destination.

Definition 1.1. *A relaying protocol is called orthogonal if the source and the relays transmit over two non-overlapping time intervals, otherwise it is called non-orthogonal.*

In a class of DF type protocols, only those relays that can fully decode the source message error free re-encode and re-transmit it to the destination. In other words, only successful relays in decoding are *selected* to contribute in the cooperation process. In this case, the protocol is called the *selection* DF relaying protocol.

In Chapter 3, we focus on the two first aforementioned protocols when they apply to a two-hop *asynchronous* cooperative network with arbitrary number of parallel relays. The DMT performance is calculated for special classes of these protocols to determine the effect of the asynchronism on this performance measure and to compare with that of the corresponding synchronous networks.

1.2.1 Prior Works

The outage probability and the DMT performances of various space-time cooperative schemes and relaying protocols over two-hop *synchronous* cooperative relay networks have extensively been considered in the literature (see [37–42] and references therein). It is shown that the DMT performance of such networks is upper bounded by the transmit diversity bound which is in fact the DMT of a multiple-input single-output (MISO) channel with the number of transmitter antennas equal to the number of the transmitting nodes in the corresponding relay network. More precisely, the DMT performance of a *synchronous* two-hop relay network containing one source, one destination, and M parallel relays for any relaying protocol is upper bounded as follows.

$$d^*(r) \leq (M+1)(1-r)^+, \tag{1.1}$$

where $(1-r)^+ = \max\{0, 1-r\}$. For a *synchronous* two-hop cooperative relay network with arbitrary number of relays, the DMT performance is calculated in [42] for various relaying protocols such as the orthogonal and the non-orthogonal selection decode-and-forward (OSDF and NSDF) and the orthogonal amplify-and-forward (OAF). In each case, a DMT optimal code is constructed using cyclic division algebra space-time codes [16], [17]. It is shown that by allowing the source and the relays to transmit over proper asymmetric portions of a cooperative frame, a larger diversity gain may be achieved at each multiplexing gain.

The effect of the asynchronism on the DMT performance of two-hop rely networks has been considered for various relaying protocols (see [2, 43–45] and references therein). In [2], the effect of the asynchronism on the DMT of an orthogonal DF cooperative network consisting of two

parallel relays is examined, in which the transmitting nodes use shaping waveforms spanned over two symbol intervals. The author shows that for large length codewords, the same DMT performance as that of the corresponding synchronous network is achieved. Moreover, when both relays can fully decode the source message, the equivalent channel from the relays to the destination at high values of SNR behaves similar to a parallel channel with two independent links. The outage probability and the DMT of an asynchronous relay network containing two parallel relays without the direct source-destination link are considered in [43]. It is shown that the same DMT performance as that of the corresponding synchronous network is achieved. In [44], under the assumption of having integer delays, two different models of asynchronism in a cooperative relay network with at least two relays are considered. For each model, a variant of the slotted amplify-and-forward (SAF) relaying protocol [46] is proposed which asymptotically achieves the transmit diversity bound in the absence of a direct source-destination link. In the presence of this link, it is shown in [45] that the SAF protocol is asymptotically optimal under both models of asynchronism. It is worth noting that in the SAF protocol, the relays are assumed to be isolated from each other, i.e., they do not interfere each other, which is in fact often unrealistic.

1.2.2 Contributions

We analyze the DMT performance of a general two-hop *asynchronous* cooperative network containing one source, one destination, and M parallel relays for various relaying protocols such as the OSDF, NSDF, OAF, and the non-orthogonal amplify-and-forward (NAF). Similar to [42], we let the source and the relays to transmit over asymmetric portions of a cooperative frame in order to maximize the diversity gain at each multiplexing gain and we avoid the cooperation whenever it reduces the diversity gain compared to the case that the source transmits alone. in difference to [45], we consider the more practical AF and DF types protocols with real (not integer) asynchronous delays and examine the effect of the asynchronism on the DMT of the system from both the theoretical and the practical points of views.

The transmitter nodes send PAM signals in which information symbols are linearly modulated by a shaping waveform to be sent to the destination. We consider two different cases with respect to the type of the shaping waveforms used in the structure of the PAM signals. In case that the shaping waveforms are band-limited resulting in infinite support in the time domain, for example when the "sinc" waveform is used, it is shown that asynchronism does not affect the DMT performance of the system. However, when time-limited shaping waveforms are used which is in fact the case in practice, the transmitted signals in the frequency domain lie in a spectral mask which does not have a limited support. Although the tails of the spectrum are usually

neglected because they are below the noise level, they may expand the bandwidth when the system is analyzed at high values of signal to noise ratio (SNR). In this case, it is argued that:

- Both the OSDF and the NSDF protocols provide better diversity gains throughout the range of the multiplexing gain over the asynchronous network compared to those of the corresponding synchronous network. In addition, similar to what was reported in [2], the equivalent channel model becomes the same as a parallel channel with the number of independent links equal to the number of transmitting nodes.
- The NAF protocol provides a better diversity gain in the asynchronous scenario compared to the synchronous scenario throughout the range of the multiplexing gain. In particular, this protocol results in the same DMT as that of the 2×1 MISO channel in a single relay asynchronous cooperative network.
- The OAF protocol provides the same diversity gain over both asynchronous and the corresponding synchronous networks for all multiplexing gains.

1.3 Asynchronous Interference Channels

The problem of finding the capacity region of the Gaussian interference channel is still open. The best achievable rate for this channel in the two-user case is given in [47] and is known as the Han-Kobayashi scheme. Recently, significant progress has been made containing new capacity results for the strong and the weak interference regimes [48–50]. Moreover, it is shown in [51] that the Han-Kobayashi scheme achieves the capacity of the two-user Gaussian interference channel within one bit for all ranges of channel coefficients. For such channels where the capacity region is unknown, to approximate the capacity at least for large values of SNR, the region of degrees of freedom and the total number of DOF of the channel are studied. The DOF region, roughly speaking, determines the shape of the capacity region at high values of SNR. It is defined as the limit of the logarithm of the capacity region over the logarithm of SNR when SNR goes to infinity. Similarly, the total number of DOF of a channel is defined as the pre-log factor of the sum-capacity when SNR goes to infinity.

Since it is unknown itself, there has not been much interest yet to investigate the effect of the *asynchronism* on the capacity region of this channel. However, the interference channel is inherently an asynchronous medium. Moreover, since there are multiple independent receivers randomly distributed over a geometrical area, the nodes cannot be synchronized even if an infrastructure service provider is used. In Chapter 4, we investigate the effect of the asynchronism, which

naturally exists among the users, on the total number of DOF of a K-user symbol-asynchronous interference channel.

1.3.1 Prior Works

In [52], it is shown that the total DOF of the K-user *synchronous* interference channel is $K/2$ if fading coefficients are time/frequency/space varying, that is, each pair can benefit from half of its original DOF with no interference from other pairs. This upper bound is achieved by a technique called *Interference Alignment*. The key idea of interference alignment is to design signals such that interfering signals at each receiver overlap while the desired signal remains distinct from the interferences [53, 54]. In [55], it is shown that in a K-user interference channel with ergodic channel coefficients a simple pairing scheme of particular channel matrices is sufficient to achieve the total $K/2$ degrees of freedom.

In practice, however, the transmission rate is usually much faster than rate of channel variation resulting in quasi-static (constant) or block fading channel models. For such channels where the link coefficients are fixed for a long period of time, it is shown in [56] that the total multiplexing gain is upper bounded by $K/2$. However, the authors conjuncture that it cannot be more than one regardless of the number of users. This is known as the Høst-Madsen-Nosratinia conjecture. Inspired by the idea of interference alignment for varying fading channels, many efforts have been made to generalize the idea to more practical constant interference channel and equivalently to settle this conjecture in the negative. However, it is not a trivial extension of the work in [52] because the assumption of having time varying channels is necessary for the proposed achieving algorithm to work. In [57], it is shown that in a quasi-static K-user interference channel with real fading coefficients, there are $K/2$ degrees of freedom if the direct fading coefficients are irrational and the crossing gains are rational numbers, while it is strictly less than $K/2$ when all the coefficients are rational numbers. Although interference signals are perfectly aligned using the proposed lattice based scheme, the necessary assumption on the values of the channel coefficients in this work restricts the result to a subset of measure zero of all possible channel coefficients. In [58], using asymmetric complex signaling over constant interference channel, it is shown that a minimum total DOF equal to 1.2 is achievable for almost all values of channel coefficients (unless for a subset of measure zero) of an interference channel with three or more users led to reject the Høst-Masden-Nosratinia conjecture. Inspired by [57], the authors in [59] take advantage of the properties of the rational and the irrational numbers to virtually increase the number of DOF of a quasi-static single-input single-output channel. The results are applied to a constant K-user interference channel to align the users' interferences and to achieve the total $K/2$ DOF of this

channel. While the proposed scheme, which is known as the real-interference-alignment, performs the alignment task almost surely at infinite SNR with infinite quantization precision, it does not suggest a feasible solution to implement the algorithm for practical values of SNR with a finite number of quantization levels.

A common assumption in all of the aforementioned schemes is that the users are synchronous and the received signal at each receiver node is a synchronized linear combination of the transmitted signals. However, this is not a feasible assumption even if an infrastructure service provider exists to synchronize the terminals.

Propagation delay based interference alignment was first proposed in a toy example to clarify the idea of interference alignment [60]. It was then explored more in [61] via an example of proper node placement in a wireless network containing four nodes to align the interference signals based on their propagation delays. In [62], a fully connected K-user interference channel is modeled by a time indexed interference graph and the alignment task is associated with finding the maximal independent set of the graph via a dynamic programming algorithm. As a simplifying assumption in this work, asynchronous delays among the received signals at each receiver are assumed to be integer multiples of the symbol interval which is unrealistic. In addition, the "sinc" waveform is approximated by the "rectangular" waveform while at the same time the system is contradictory assumed to be strictly bandwidth limited.

1.3.2 Contributions

We consider a K-user interference channel wherein users are not symbol synchronous and we investigate the effect of the asynchronism existing among the users on the total DOF of this channel. We show that the asynchronism does not affect the total DOF of the system; however, it facilitates aligning interfering signals at each receiver node. As an achieving scheme for the total DOF equal to $K/2$, we propose a novel interference alignment algorithm for this channel by taking advantage of asynchronous delays which inherently exist among the received signals at each receiver node. The asynchronism causes inter-symbol-interference (ISI) among transmitted symbols by different transmitters. In this case, the underlying quasi-static links are converted to ISI and accordingly into time varying channels solving the lack of channel variation required for the interference alignment in quasi-static scenarios. For simplicity and ease of understanding, we present the scheme first for the three-user interference channel with single antenna nodes. The results are then extended to a general single antenna nodes' interference channel with arbitrary number of users. Later, it is argued that the same scheme can be used in a K-user asynchronous interference channel with terminals each equipped with M antennas to achieve the total $MK/2$

DOF of the medium provided that each pair of the transmitters and the receivers experience the same asynchronous delay for all the corresponding antennas. In contrast to previously proposed alignment schemes, the channel state information of the links does not need to be known at the transmitter nodes. Instead, the relative delays among the received signals at each receiver node are globally known to the entire network.

Chapter 2

Delay Tolerant Space-Time Codes

2.1 Introduction

The construction of distributed space-time codes for asynchronous relays is considered in this chapter. A novel algebraic structure is proposed and shown to achieve full diversity for arbitrary number of relays, arbitrary input alphabets, and arbitrary delay profiles among the relays. Unlike previously proposed delay tolerant schemes, the new design has minimum length which translates into smaller decoding complexity at the same transmission rate. Full-rate and full-diversity are achieved by the new designs with or without the use of guard intervals between successive transmissions. Simulation results confirm the mathematical analysis of the proposed codes.

2.1.1 System Model

Consider a cooperative network containing one source node, one destination node, and M parallel relay nodes. The source communicates with the destination in two steps. In the first step, the source broadcasts its message to the relays. Those relays that can decode the received signals error free participate in the second step (in what follows, we assume that all of the M relays are able to decode the received signals error free). In the second step, the relays send their symbols toward the destination. Since the relay nodes use common time slots and frequency bandwidth for their signal transmission, they cooperatively implement a space-time code. We consider the design and performance evaluation of distributed space-time codes used by the relays. This can be considered as a MIMO system model with M transmit antennas corresponding to M relays and N receive antennas at the destination. At time instant t, the received signal vector $\underline{y}_t \in \mathbb{C}^{N\times 1}$

is modeled as

$$\underline{y}_t = \mathbf{H}_t \underline{x}_t + \underline{z}_t, \tag{2.1}$$

where $\underline{x}_t \in \mathbb{C}^{M\times 1}$ is the modulated signal vector transmitted during the t-th symbol interval. $\mathbf{H}_t \in \mathbb{C}^{N\times M}$ and $\underline{z}_t \in \mathbb{C}^{N\times 1}$ denote the channel matrix and the additive white Gaussian noise vector, respectively. The channel is assumed to be quasi-static, i.e. the channel matrix $\mathbf{H}_t$ is constant over a codeword interval but is independent from codeword to codeword. The modulated signal vectors $\underline{x}_t, t = 1, \ldots, T$, span the space-time codeword $\mathbf{X}$ of size $M \times T$ over T symbol intervals. The transmitted symbols are generated from a finite constellation. Let $\mathcal{A}$ denote a two-dimensional constellation chosen from the ring of Gaussian integers or Eisenstein integers, respectively denoted by $\mathbb{Z}[\xi]$, $i = \sqrt{-1}$, and $\mathbb{Z}[j], j = e^{2\pi\xi/3}$. Let $\mathbb{F} = \mathbb{Q}(\xi)$, or $\mathbb{Q}(j)$, denote the field of complex Gaussian rational numbers, or complex Eisenstein rational numbers, respectively.[1] Let $\mathbb{F}(\theta)$ be an extension field of degree $[\mathbb{F}(\theta) : \mathbb{F}]$ over $\mathbb{F}$. The input alphabet for our construction is given by

$$\Omega = \left\{ x = \sum_{n=0}^{P-1} u_n \theta^n : u_n \in \mathcal{A} \right\}, \tag{2.2}$$

where integer $P \leq [\mathbb{F}(\theta) : \mathbb{F}]$. Each transmitted symbol is from Ω, or more generally, from its image $f(\Omega)$ under some specified one-to-one mapping $f : \Omega \to \mathbb{C}$.

2.1.2 Delay Tolerance of Space-Time Codes

Let $\mathcal{X}$ be a STBC with codewords of size $M \times T$. Assume $\mathbf{X}_1$ and $\mathbf{X}_2$ are two distinct codewords of $\mathcal{X}$. The diversity order of $\mathcal{X}$ is the minimum rank of the difference matrix, $\mathbf{X}_1 - \mathbf{X}_2$, over all pairs of distinct codewords in $\mathcal{X}$ (*rank* criterion) [9].

We assume that the fractional delays are absorbed in multi path, so asynchronous delays are integer multiples of the symbol interval. Delays are unknown at the relays, but are known at the destination. Here, we consider the transmission of either one single codeword or consecutive codewords with sufficient guard interval between them such that the earlier and the latter transmitted codewords do not interfere with the codeword under consideration.

The space-time code $\mathcal{X}$ is τ-delay tolerant for the asynchronous cooperative diversity scenario if for all distinct codewords $\mathbf{X}_1, \mathbf{X}_2 \in \mathcal{X}$, the difference matrix $\mathbf{X}_1 - \mathbf{X}_2$ retains full-rank even though the rows of the codewords are transmitted with arbitrary delays of duration at most τ symbols. To make this definition more precise, suppose that the $M \times T$ modulated codeword

[1] For simplicity of notation, we restrict ourselves to $\mathbb{Z}[i]$ or $\mathbb{Z}[j]$; however, as in [33], the input alphabet $\mathcal{A}$ can be chosen from any cyclotomic ring $\mathbb{Z}[\exp(2i\pi/n)]$, with n integer.

matrix $\mathbf{X} \in \mathcal{X}$, containing the rows $\underline{x}_1, \underline{x}_2, \ldots, \underline{x}_M$, is transmitted by M relays with delay profile $\Delta = (\delta_1, \delta_2, \ldots, \delta_M)$. Here, δ_i denotes the relative delay of the signal received from the i-th relay with respect to the earliest received signal. This is equivalent to receive the $M \times (T + \delta_{max})$ matrix

$$\mathbf{X}^{\Delta} = \begin{bmatrix} \underline{0}^{\delta_1} & \underline{x}_1 & \underline{0}^{\delta_{max}-\delta_1} \\ \underline{0}^{\delta_2} & \underline{x}_2 & \underline{0}^{\delta_{max}-\delta_2} \\ \vdots & \vdots & \vdots \\ \underline{0}^{\delta_M} & \underline{x}_M & \underline{0}^{\delta_{max}-\delta_M} \end{bmatrix}, \tag{2.3}$$

where $\underline{0}^{\delta_i}, i = 1, \ldots, M$, and δ_{max} denote an all-zero vector of length δ_i and the maximum of the relative delays, respectively. Now, a space-time code $\mathcal{X}$ is called τ-delay tolerant if for all delay profiles Δ with $\delta_{max}(\Delta) \leq \tau$, the effective space-time code $\mathcal{X}^{\Delta}$ achieves the same spatial diversity as that of $\mathcal{X}$. A space-time code is fully delay tolerant if it is delay tolerant for any positive integer τ.

2.1.3 Threaded Code Structure

Definition 2.1. *A layer is a mapping that assigns a unique transmit antenna to be used at each individual time interval of a codeword. It is called a thread if its domain and range include all possible transmit antennas and all possible symbol intervals, respectively [10].*

The proposed delay tolerant TAST codes in [33] are based on using three different threaded structures which are intrinsically delay tolerant: running use (RU), naive double use (NDU), and optimum double use (ODU). The latter has the smallest delay length. For $M = 4$, an ODU threading is given by

$$\mathbf{1}_{ODU} = \begin{bmatrix} 1 & 0 & 0 & 0 & 0 & 0 & 0 \\ 0 & 0 & 0 & 0 & 1 & 1 & 0 \\ 0 & 1 & 0 & 1 & 0 & 0 & 0 \\ 0 & 0 & 1 & 0 & 0 & 0 & 1 \end{bmatrix}. \tag{2.4}$$

As the rows of this matrix are linearly independent for every delay profile, it follows that the space-time code is delay tolerant. The structure can contain four different threads which are individually delay tolerant; However, when they join together in a matrix, it is not guaranteed that the resulted structure is full-diversity delay tolerant. This is guaranteed by multiplying all of the threads by different powers of an appropriate algebraic or a transcendental number, ϕ. It was proved in [33] that for $M \geq 5$, the delay length of the code is $T_M^{ODU} = 2^{M-2} + 1$. Clearly, this code is not minimum delay length, and its length grows exponentially with the number of

relay nodes. Unlike the ODU threaded structure, in this chapter, we propose a minimum length delay-tolerant TAST-like code.

2.2 Construction of the Proposed Delay Tolerant STBCs

In this section, we develop our new design of delay tolerant space-time codes with minimum delay length $T = M$. The minimum rank of the difference of distinct codewords is the diversity order of a space-time code. One simple way to verify the rank of a matrix is to find the largest square sub-matrix with nonzero determinant.

Remark 2.1. *The Leibniz formula for the determinant of any $M \times M$ matrix $\mathbf{X}$ is given by*

$$\det \mathbf{X} = \sum_{\sigma \in \mathcal{P}_M} \mathtt{sgn}(\sigma) \prod_{k=1}^{M} \mathbf{X}(k, \sigma(k)), \tag{2.5}$$

where $\mathcal{P}_M$ is the set of all permutations, σ, of the numbers $\{1, 2, \ldots, M\}$, $\mathtt{sgn}(\sigma)$ is the signature of the permutation σ which depends on the number of exchanges in σ, and $\mathbf{X}(k, \sigma(k))$ is the $(k, \sigma(k))$-th entry of matrix $\mathbf{X}$ [63].

First, we observe that randomly generated Gaussian space-time codes are delay tolerant with probability 1. As all the entries of the code matrix are chosen independently from a Gaussian distribution, the difference of distinct codewords does not have zero entry with probability one (except the zeros due to the delay of the rows). Thus, one can find an $M \times M$ sub-matrix $\mathbf{T}$ such that the i-th column $i = 1, \ldots, M$, has nonzero entry at the i-th row. In this case, $\mathbf{T}$ has at least one thread with all nonzero entries. According to Remark 2.1, the determinant of $\mathbf{T}$ contains linear combination of the terms which are equal to the multiplication of the elements of the threads of $\mathbf{T}$. Since these terms are independent random variables with at least one nonzero term corresponding to the main diagonal thread, $\det \mathbf{T}$ is nonzero with probability 1. Thus, this code which supports full spatial diversity is delay tolerant for every delay profile with probability 1.

Such a Gaussian code has two major drawbacks. First, as it does not have a specific structure, the decoding procedure is exponentially complex. Second, the codebook has to be saved in both transmitters and receiver places for encoding and decoding procedures which requires a large amount of memory in both sides. Our proposed scheme in this chapter avoids these drawbacks while preserving the advantages of random Gaussian codes.

The general guidelines for the construction of our codes are described in the following. Let $\mathcal{C}$ be a one dimensional full-diversity block code of length MT suitable for SISO channels (i.e.,

it achieves full diversity, MT, when sent over an i.i.d. SISO fading channel [13]). Let $\mathbf{G}$ be a fixed $M \times T$ matrix with elements as powers of some complex number $\phi \neq 1$ on the unit circle. By parsing the entries of a codeword vector $\underline{c} \in \mathcal{C}$ to an $M \times T$ matrix $\mathbf{C}$ (whose entries are a rearrangement of those of $\underline{c}$), a space-time matrix codeword is formed as follows

$$\mathbf{X} = \mathbf{C} \odot \mathbf{G}, \tag{2.6}$$

where $\odot$ denotes the component-wise product. In this chapter, matrix $\mathbf{G}$ is designed such that the resulted space-time code achieves full-diversity and is delay tolerant for arbitrary delay profile and arbitrary number of transmitter antennas. Note that finding full diversity SISO codes is well documented in the literature, e.g., [64] and references therein. Two main families of codes are proposed in the sequel based on two different structures of matrix $\mathbf{G}$ in (2.6).

In the first family, $\mathbf{G} \triangleq \mathbf{A}_M$, where $\mathbf{A}_M$ is given by

$$\mathbf{A}_M \triangleq \begin{bmatrix} \phi^{b_{1,1}} & \dots & \phi^{b_{1,M}} \\ \phi^{b_{2,1}} & \dots & \phi^{b_{2,M}} \\ \vdots & \ddots & \vdots \\ \phi^{b_{M,1}} & \dots & \phi^{b_{M,M}} \end{bmatrix}, \tag{2.7}$$

where $b_{i,j} \geq 0, i, j = 1, \dots, M$ are non-negative integers, and ϕ is an appropriate number with properties detailed in the sequel. One can show that by an appropriate choice of the parameters ϕ and $b_{i,j}$'s followed by using proper one dimensional code $\mathcal{C}$, the resulting space-time code is delay tolerant for every delay profile.

Define Ξ as the set which contains those M-tuples of $b_{i,j}$ that have been chosen from different rows of $\mathbf{A}_M$. Ξ contains M^M vectors of length M, i.e., $\Xi = \{\underline{b}_1, \underline{b}_2, \dots, \underline{b}_{M^M}\}$. Define b_{max} as

$$b_{max} = \max_q \sum_{j=1}^{M} b_q(j), \quad \underline{b}_q \in \Xi, q = 1, \dots, M^M, \tag{2.8}$$

where $b_q(j)$ is the j-th element of $\underline{b}_q$.

At the beginning, for ease of understanding, we consider a case that $\mathcal{C}$ is a repetition code over Ω and there are only three relays in the network, $M = 3$. Let $b_{i,j}$'s be defined as consecutive integer powers of 2. $\mathbf{A}_3$ is given by

$$\mathbf{A}_3 = \begin{bmatrix} 1 & \phi & \phi^2 \\ \phi^4 & \phi^8 & \phi^{16} \\ \phi^{32} & \phi^{64} & \phi^{128} \end{bmatrix}. \tag{2.9}$$

As can be seen, the summation of the elements of every 3-tuple in Ξ is unique. Since $\mathcal{C}$ is a repetition code, all differences between distinct codewords are multiples of $\mathbf{A}_3$. Therefore, to verify the diversity order of this code for a delay profile $\Delta = (\delta_1, \delta_2, \delta_3)$, one only needs to find the largest full-ranked square sub-matrix of $\mathbf{A}_3^{\Delta}$. Assume $\mathbf{T}$ is a 3×3 sub-matrix of $\mathbf{A}_3^{\Delta}$ (columns of $\mathbf{T}$ are chosen from columns of $\mathbf{A}_M^{\Delta}$) with at least one thread with all nonzero entries. According to (2.5), the summation of $b_{i,j}$'s corresponding to this thread will appear as a power of ϕ in the determinant value. Since this value is unique, the corresponding term in the determinant value is not interfered by the other terms showed in (2.5) if ϕ is chosen such that the numbers $\{1, \phi, \ldots, \phi^{b_{max}}\}$ are algebraically independent over the set $\{-1, 1\}$. Note that the coefficients of the ϕ terms in the determinant value are all in $\{-1, 1\}$. By definition, the largest power of ϕ that may appear in the determinant value for all delay profiles is b_{max}. Hence, the determinant value is not zero and the code achieves full diversity for every delay profile. Here, $b_{max} = 146$ and the numbers $\{1, \phi, \ldots, \phi^{146}\}$ should be algebraically independent over the set $\{-1, 1\}$ in order to generate a full-diversity and delay tolerant code. Theorem 2.1 concludes the results.

Theorem 2.1. *Let $\mathcal{X}$ denote the space-time code in which the repetition code with codewords of length M^2 over alphabet Ω is used as the one dimensional SISO code in conjunction with matrix $\mathbf{A}_M$. Then $\mathcal{X}$ achieves full spatial diversity and is fully delay tolerant if the following conditions are satisfied:*

1- ϕ is chosen as an algebraic or a transcendental number such that the numbers $\{1, \phi, ..., \phi^{b_{max}}\}$ are algebraically independent over the set $\{-1, 1\}$.

2- The $b_{i,j}$ parameters are chosen such that the summation of the elements of every $\underline{b}_q \in \Xi$ is a unique value.

Proof. Since all differences between distinct codewords in $\mathcal{X}$ are multiples of $\mathbf{A}_M$, it suffices to show that $\mathbf{A}_M^{\Delta}$ is full rank for every arbitrary delay profile $\Delta = \{\delta_1, \delta_2, \ldots, \delta_M\}$. To verify the diversity order of the code, one needs to find the largest full-ranked square sub-matrix $\mathbf{T}$ of $\mathbf{A}_M^{\Delta}$. $\mathbf{T}$ is constructed by taking a column of $\mathbf{A}_M^{\Delta}$ with a nonzero entry at the i-th ($i = 1, 2, \ldots, M$) row as the i-th column. Assume that construction of $\mathbf{T}$ is started by choosing the first column. Since $\mathbf{A}_M$ is an $M \times M$ matrix with all nonzero entries, at the i-th ($i = 1, \ldots, M$) step of the process, there exists at least $M - i + 1$ columns that contain a nonzero entry at the i-th row. Therefore, this form of column selection is feasible. As a result, $\mathbf{T}$ is of size $M \times M$ and all the elements on its main diagonal thread are nonzero. If the sum of the parameters $b_{i,j}$ corresponding to this thread is α, we get

$$\det(\mathbf{T}) = g(\phi) \pm \phi^{\alpha}, \tag{2.10}$$

where $g(\phi)$ is a polynomial of ϕ with degree less than or equal to b_{max} with all constant coefficients in $\{-1, 1\}$. Since α is unique, $g(\phi)$ does not contain any term in ϕ^{α}. As a result, if the numbers $\{1, \phi, \ldots, \phi^{b_{max}}\}$ are algebraically independent over $\{-1, 1\}$, $\det(\mathbf{T})$ is not zero and the code achieves full-diversity for every delay profile. □

It is worth noting that the second condition of Theorem 2.1 is a sufficient condition. It guarantees that every nonzero thread (a thread with all nonzero entries) of $\mathbf{T}$ will appear with a unique power of ϕ in the determinant value. On the other hand, having only one nonzero thread of $\mathbf{T}$ with unique power of ϕ in the determinant value is enough for a full diversity delay tolerant code. Therefore, there may exist some other schemes for assigning $b_{i,j}$ parameters that cause a full diversity delay tolerant code, while they do not follow the second condition of Theorem 2.1.

While there may exist a lot of choices for the parameters $b_{i,j}, i, j = 1, \ldots, M$, those that result in a smaller value for b_{max} are of interest. In this case, one can design the code with smaller degree extension of the base field. A simple choice is to use consecutive integer powers of 2.

The previous family of the codes assigns a specific power of ϕ to every element of the codeword matrix resulting in a complex code structure which might be more than what is necessary to guarantee a full diversity delay tolerant code. The second family of the codes, which we call it the proposed code, is based on a simpler structure for matrix $\mathbf{G}$ and more relaxed conditions for the $b_{i,j}$ parameters. Let $\mathbf{G} \triangleq \mathbf{B}_M$, where $\mathbf{B}_M$ is defined as

$$\mathbf{B}_M \triangleq \begin{bmatrix} 1 & \phi^{b_{1,2}} & \phi^{b_{1,3}} & \cdots & \phi^{b_{1,M}} \\ 1 & 1 & \phi^{b_{2,3}} & \cdots & \phi^{b_{2,M}} \\ \vdots & \vdots & & \ddots & \vdots \\ 1 & 1 & 1 & \cdots & \phi^{b_{M-1,M}} \\ 1 & 1 & 1 & \cdots & 1 \end{bmatrix}. \tag{2.11}$$

The space-time code $\mathcal{X}$ is constructed as explained in the general guidelines for the code construction. Similarly, Ξ is defined as the set which contains those M-tuples of $b_{i,j}$ in $\mathbf{B}_M$ that have been chosen from different rows of this matrix. By considering that the diagonal and the lower triangular entries of $\mathbf{B}_M$ are all ϕ^0, Ξ and b_{max} are defined as before. Theorem 2.2 characterizes sufficient conditions that make the resulted code full-diversity and delay tolerant when the one dimensional SISO code $\mathcal{C}$ is a repetition code over Ω.

Theorem 2.2. *Let $\mathcal{X}$ denote the space-time code in which the repetition code with codewords of length M^2 over alphabet Ω is used as the one dimensional SISO code in conjunction with matrix $\mathbf{B}_M$. Then $\mathcal{X}$ achieves full spatial diversity and is fully delay tolerant if the following conditions are satisfied:*

1- ϕ is chosen as an algebraic or a transcendental number such that the numbers $\{1, \phi, ..., \phi^{b_{max}}\}$ are algebraically independent over integers.

2- The parameters $b_{i,j} \geq 0, i = 1, \ldots, M-1, j = i+1, \ldots, M$, are chosen such that the summation of the entries of every M-tuple in Ξ with $M-1$ non-zero entries is unique and different from that of other M-tuples in Ξ.

Proof. Since the one-dimensional code $\mathcal{C}$ is a repetition code, it suffices to show that $\mathbf{B}_M^{\Delta}$ is full rank for every arbitrary delay profiles $\Delta = \{\delta_1, \delta_2, \ldots, \delta_M\}$. To verify the diversity order of the code, one needs to find the largest full-ranked square sub-matrix $\mathbf{T}$ of $\mathbf{B}_M^{\Delta}$. $\mathbf{T}$ is constructed by choosing the $(M-i+1)$-th column, $i = 1, \ldots, M-1$, such that it contains a non-zero power of ϕ at the $(M-i)$-th row. The first column is chosen such that it contains a nonzero element, 1, at the M-th row. To show that this form of column selection is feasible, assume that construction of $\mathbf{T}$ is carried out by choosing its columns in a reverse order, i.e., the M-th column is selected first, the $(M-1)$-th column is selected second, and similarly up to the first column which is selected at last. Due to the original form of the matrix $\mathbf{B}_M$, at the i-th step of the process, there are i entries containing ϕ factor at the $(M-i)$-th row. Since $(i-1)$ columns have been chosen beforehand, there is at least one column containing ϕ factor at this row. Thus, the aforementioned form of column selection is feasible for $\mathbf{T}$ for every delay profile. As can be seen, $\mathbf{T}$ is an $M \times M$ matrix that has at least one thread ℓ with all nonzero entries containing $(M-1)$ entries of powers of ϕ. It is given by

$$\mathbf{T} = \begin{bmatrix} \star & \phi^{b_{\ell_{1,2}}} & \star & \cdots & \star \\ \star & \star & \phi^{b_{\ell_{2,3}}} & \cdots & \star \\ \vdots & \vdots & & \ddots & \vdots \\ \star & \star & \star & \cdots & \phi^{b_{\ell_{M-1,M}}} \\ 1 & \star & \star & \cdots & \star \end{bmatrix}, \tag{2.12}$$

where $\star$ can be zero due to the delay profile Δ or any one of the entries of $\mathbf{B}_M$ which may or may not contain the factor ϕ. Let α be the summation of the powers of ϕ existing in the thread ℓ, $\alpha = b_{\ell_{1,2}} + b_{\ell_{2,3}} + \ldots + b_{\ell_{M-1,M}}$, then the determinant of $\mathbf{T}$ is

$$\det(\mathbf{T}) = g(\phi) \pm \phi^{\alpha}, \tag{2.13}$$

where $g(\phi)$ is a polynomial of ϕ with degree less than or equal to b_{max} and with integer coefficients. Since α is unique, $g(\phi)$ does not contain any term in ϕ^{α}. Therefore, if the numbers $\{1, \phi, \ldots, \phi^{b_{max}}\}$ are algebraically independent over integers, $\det(\mathbf{T})$ is not zero, and the constructed code achieves full-diversity for every delay profile. □

There is an infinite number of schemes to select proper values for the $b_{i,j}$ parameters ; however, one simple choice is to use geometric series of integer powers of 2 as

$$\begin{aligned} b_{i,j} &= 2^{\frac{(M-i)(M-i-1)}{2}+M-j} \\ & \quad i=1,\ldots,M-1, \quad j=i+1,\ldots,M. \end{aligned} \tag{2.14}$$

For example, for $M=3$ we have,

$$\mathbf{B}_3 = \begin{bmatrix} 1 & \phi^4 & \phi^2 \\ 1 & 1 & \phi \\ 1 & 1 & 1 \end{bmatrix}. \tag{2.15}$$

The results of Theorems 2.1, 2.2 can be generalized to any full-diversity SISO code [64]. In general, one-to-one functions $f_{i,j}, i,j=1,\ldots,M$ of $x\in\Omega$, $f_{i,j}:\Omega\to\mathbb{C}$, are used instead of x at the (i,j)-th element of the codeword matrix. Having $\mathcal{C}$ as a general full diversity SISO code, the space time-code $\mathcal{X}$ is constructed as explained in the general guidelines of the code construction. The generalized codeword matrix of the proposed code is shown in (2.16).

$$\mathbf{X}_M(x) \triangleq \begin{bmatrix} f_{1,1}(x) & \phi^{b_{1,2}} f_{1,2}(x) & \phi^{b_{1,3}} f_{1,3}(x) & \cdots & \phi^{b_{1,M}} f_{1,M}(x) \\ f_{2,1}(x) & f_{2,2}(x) & \phi^{b_{2,3}} f_{2,3}(x) & \cdots & \phi^{b_{2,M}} f_{2,M}(x) \\ \vdots & \vdots & & \ddots & \vdots \\ f_{M-1,1}(x) & f_{M-1,2}(x) & f_{M-1,3}(x) & \cdots & \phi^{b_{M-1,M}} f_{M-1,M}(x) \\ f_{M,1}(x) & f_{M,2}(x) & f_{M,3}(x) & \cdots & f_{M,M}(x) \end{bmatrix}. \tag{2.16}$$

By proceeding in the same procedure of the original repetition code, one can prove that $\mathcal{X}$ is full-diversity and delay tolerant for every delay profile. The following theorem formulates the results.

Theorem 2.3. *Let $\mathcal{X}$ denote the space-time code with codewords of the form $\mathbf{X}_M(x), x\in\Omega$ wherein a general full diversity code with codewords of length M^2 is used as the one dimensional SISO code in conjunction with matrix $\mathbf{B}_M$. Then $\mathcal{X}$ achieves full spatial diversity and is fully delay tolerant if the following conditions are satisfied:*

1- *ϕ is chosen as an algebraic or a transcendental number such that the numbers $\{1,\phi,...,\phi^{b_{max}}\}$ are algebraically independent over the field that contains $f_{i,j}(x), i,j=1,\ldots,M, x\in\Omega$.*

2- *The parameters $b_{i,j}\geq 0, i=1,\ldots,M-1, j=i+1,\ldots,M$, are chosen such that the summation of the entries of every M-tuple in Ξ with $M-1$ non-zero entries is a unique value and different from that of other M-tuples in Ξ.*

The proof is similar to the one of Theorem 2.2 and is omitted for brevity. Note that the constant coefficients of the ϕ factors in the determinant value in this case are in the field that contains $f_{i,j}(x), i, j = 1, \ldots, M, x \in \Omega$. $b_{i,j}$'s are chosen the same as before.

Remark 2.2. *It is worth noting that the required condition for the numbers* $\{1, \phi, \ldots, \phi^{b_{\max}}\}$ *to be algebraically independent over the field that contains the elements of the code matrices is just a sufficient condition. In some cases, having the numbers* $\{1, \phi, \ldots, \phi^{b_{max}}\}$ *be algebraically independent over a field contained in that field with smaller degree is enough to achieve full-diversity. Typically,* ϕ *can be chosen as a cyclotomic number, i.e., the* n*-th root of unity* $\zeta_n = e^{2\pi\xi/n}$ *(in this case,* ϕ *is an algebraic number). The order of* ζ_n *over* $\mathbb{Q}$ *is determined by Euler function* $\phi(n)$ *which represents the number of integers both less than and identically prime with* n*.*

Remark 2.3. *By assuming that the proposed code is designed to be used in a system containing* M *relay nodes, the full transmit diversity gain* M *is achieved provided that all the relays correctly decode the source messages. To this end, the relays are equipped with an error detection mechanism (e.g., cyclic redundancy check codes), only those relays that have not detected any error at the end of the first step will participate in the second step of the process. However, it is easy to check that the elements of any subset of the rows of the proposed structure are linearly independent for every delay profile. Therefore, the resulted space-time code provides the full diversity gain which is equal to the number of active relays.*

2.3 Delay Tolerant Space-Time Codes with Overlapped Codewords

Thus far, we assumed that the relay nodes insert enough guard interval (i.e., filling symbols) between every two consecutive codewords to ensure that the constructed space-time code is received without any interference from either the next or the previous codewords. This assumption limits the transmission rate and confines the applications of the proposed codes to low transmission rate scenarios. In this section, we consider the case that every relay transmits its symbols continuously without any delay guard between codewords.

In the problem under consideration, there exists $k \geq 1$ vectors of information symbols $\underline{u}_1, \underline{u}_2, \ldots, \underline{u}_k$, where $\underline{u}_i = (u_i(1), u_i(2), \ldots, u_i(MT)), i = 1, \ldots, k$. x_i is the constellation point in Ω corresponding to $\underline{u}_i$ generated using (2.2). The matrices of the space-time codewords are constructed according to Theorem 2.2 or 2.3 and transmitted over the channel one codeword after another without any guard interval.

While it is difficult to prove (or disprove) that the overlapped code is still delay tolerant for every delay profile, we propose in the following a simple modification that guarantees delay-tolerance regardless of the use of guard intervals. We propose to use different algebraic or transcendental numbers for different blocks of the overlapped codeword. One can show that when the maximum possible delay between relay nodes is confined to the delay length of the code T, only two different numbers, ϕ_1, ϕ_2, are required to make the resulted overlapped code delay tolerant. When k (number of codewords transmitted over the channel without guard interval) is large, the rate loss of the code due to the required guard interval at both end of the overlapped codeword becomes negligible.

As a simple example, let $\underline{u}_1$, $\underline{u}_2$ be two vectors of information symbols. x_1, x_2 are the corresponding constellation points in Ω, and $\mathbf{X}_1, \mathbf{X}_2$ are the corresponding repetition space-time codewords according to Theorem 2.2. For $M = 3$, the resulted overlapped codeword $\mathbf{X}_{1,2} = (\mathbf{X}_1, \mathbf{X}_2)$ is given below.

$$\mathbf{X}_{1,2} = \left[\begin{array}{ccc|ccc} x_1 & \phi_1^4 x_1 & \phi_1^2 x_1 & x_2 & \phi_2^4 x_2 & \phi_2^2 x_2 \\ x_1 & x_1 & \phi_1 x_1 & x_2 & x_2 & \phi_2 x_2 \\ x_1 & x_1 & x_1 & x_2 & x_2 & x_2 \end{array}\right], \tag{2.17}$$

where ϕ_1, and ϕ_2 are two different numbers such that the numbers $\{1, \phi_1, \ldots, \phi_1^5\}$ are algebraically independent over integers and the numbers $\{1, \phi_2, \ldots, \phi_2^5\}$ are algebraically independent over the field that contains the elements of the first block. In this case, by proceeding the same proof of Theorem 2.2, one can show that the resulted overlapped code is delay tolerant for every delay profile. This is formulated more precisely in the following.

Theorem 2.4. *Let $\underline{u}_1, \underline{u}_2, \ldots, \underline{u}_k$, $k \geq 1$, be vectors of information symbols, where $\underline{u}_i = (u_i(1), u_i(2), \ldots, u_i(MT)), i = 1, \ldots k$. Let $x_1, x_2, \ldots, x_k$ be the corresponding constellation points in Ω, and $\mathbf{X}_1, \mathbf{X}_2, \ldots, \mathbf{X}_k$ be the corresponding code matrices constructed as explained in Theorem 2.2. Assuming $\delta_{max} \leq T$, the overlapped code $\mathcal{X}$ with codewords of the form $\mathbf{X}_{1,2,\ldots,k} = (\mathbf{X}_1, \mathbf{X}_2, \ldots, \mathbf{X}_k)$ (constructed by concatenation of $\mathbf{X}_i, i = 1, \ldots, k$ without guard interval) achieves full-diversity and is delay tolerant for every delay profile if the following conditions are satisfied:*

1- *ϕ_1 is an appropriate algebraic or a transcendental number such that the numbers $\{1, \phi_1, ..., \phi_1^{b_{max}}\}$ are algebraically independent over integers.*

2- *ϕ_2 is chosen such that the numbers $\{1, \phi_2, ..., \phi_2^{b_{max}}\}$ are algebraically independent over the field that contains the elements of the first block. ϕ_1, ϕ_2 are alternately used for every other blocks.*

The proof is similar to the proof of Theorem 2.2 and is omitted for brevity. As in the non-overlapped scenario, the results can be generalized from repetition codes to any full-diversity SISO code [13, 64].

2.4 Examples

In this section, we give some examples of the new designed codes proposed in Theorem 2.3. The construction of these codes is carried out by properly choosing the SISO code and the ϕ number.

The required full-diversity SISO codes over fading channels can be constructed by applying full-diversity unitary transformations to input signals drawn from lattices or multidimensional constellations carved from a ring. In [65], Damen et al. provided an explicit construction of $M \times M$ fully diverse unitary transformations $\mathbf{U}_M$ over the field that contains the elements of information symbols.

$$\mathbf{W}_M = \mathbf{U}_M^{\dagger} \mathbf{D}_\theta, \tag{2.18}$$

where $\mathbf{U}_M^{\dagger}$ is the conjugate transpose of the $M \times M$ Discrete Fourier Transform (DFT) matrix and $\mathbf{D}_\theta = \text{diag}\left\{1, \theta^{\frac{1}{M}}, \ldots, \theta^{\frac{M-1}{M}}\right\}$, where θ is a transcendental or an algebraic number of suitable degree to guarantee the full-diversity of the rotation [65].

We consider design of the new proposed codes for $M = 2$, and 3 active relays. The required full-diversity rotations are of size 4×4 and 9×9, respectively. To benefit from optimum rotations, information symbols are chosen from $\mathbb{Z}[\xi]$, and $\mathbb{Z}[j]$ for $M = 2$, and 3, respectively. Two explicit examples of the new proposed codes are given below.

1. For $M = N = T = 2$, one has the delay tolerant STBC with codeword matrices of the form

$$\begin{bmatrix} x_1 & \phi x_3 \\ x_2 & x_4 \end{bmatrix}, \tag{2.19}$$

where $\underline{x} = (x_1, x_2, \ldots, x_4)^T = \Theta \underline{u}$, $\underline{u}$ is a 4×1 vector of QAM symbols, and $\Theta = \mathbf{W}_4$ is the optimal 4×4 complex rotation according to (2.18). By setting $\phi = e^{2\pi\xi/3}$, this code provides the rate of 2 QAM symbols per channel use and achieves a transmit diversity of 2 regardless of the delay profile among its rows.

2. For $M = T = 3, N = 2$, one has the delay tolerant STBC with codeword matrices of the form

$$\begin{bmatrix} x_1 & \phi^4 x_4 & \phi^2 x_7 \\ x_2 & x_5 & \phi x_8 \\ x_3 & x_6 & x_9 \end{bmatrix}, \tag{2.20}$$

where $\underline{x} = (x_1, x_2, \ldots, x_9)^T = \Theta \underline{u}$, $\underline{u}$ is 9×1 vector of information symbols belong to the 4-array constellation in $\mathbb{Z}[j]$, and $\Theta = \mathbf{W}_9$ is the optimal 9×9 complex rotation according to (2.18). By setting $\phi = e^{2\pi\xi/7}$, this code provides the rate of 3 symbols per channel use and achieves a transmit diversity of 3 regardless of the delay profile among its rows.

2.5 Simulation Results

In this section, we show some performance results of the proposed codes for $M = 2$ and 3 active relays. The decoding procedure is performed by sphere decoding [66]. We assume that the destination is equipped with two receive antennas. This results in an under determined system for $M = 3$ transmit antennas. In this case, we benefit from the minimum mean square error decision feedback equalizer (MMSE-DFE) as the preprocessing stage followed by the sphere decoding algorithm [66]. The figures show bit and codeword error rates as a function of E_b/N_0 in dB which is adjusted as follows.

$$\left.\frac{E_b}{N_0}\right|_{dB} = \left.\frac{E_s}{N_0}\right|_{dB} - 10\log_{10} R, \tag{2.21}$$

where E_s is the average signal energy per receive antenna and R is the code rate in bit per channel use (bpcu).

Figures 2.1 and 2.2 show the bit error rate (BER) and the word error rate (WER) performances of the new proposed code with codewords of the form (2.19) for both cases of synchronous and asynchronous relays. At the latter case, the second row is shifted to the right by one symbol interval. The results are compared with the results of the Golden code [67] as well as the results of the delay tolerant 2×2 code (matrix $\mathbf{D}$) proposed by Damen in [68]. Here, $M = N = T = 2$ and $\phi = e^{2\pi\xi/3}$. Information symbols are chosen from the 4-QAM constellation to adjust the rate of $\frac{8}{2+\delta_{max}}$ bpcu, where $\delta_{max} = 0$ when the relays are synchronous (see Fig. 2.1), and 1 when they are asynchronous (see Fig. 2.2). As can be seen, the proposed code outperforms the matrix $\mathbf{D}$ in both cases of synchronous and asynchronous relays. For example, at the BER of 10^{-4}, the proposed code has about 0.6 dB gain over $\mathbf{D}$ when $\delta_{max} = 0$. When $\delta_{max} = 1$, the performances of the two codes are almost the same at low SNR regime; however, our code outperforms the other one at high SNR regime. This confirms that our proposed code achieves the diversity gain of 2 and is delay tolerant. In addition, the performance of the proposed code is quite close to the one of the Golden code when the relays are synchronous, and is much better than that when they are asynchronous (the latter is not delay tolerant).

Figures 2.3, 2.4, show the BER and the WER performances of the proposed code with codewords of the form (2.20) when $M = T = 3$ and $N = 2$ with and without delay, respectively.

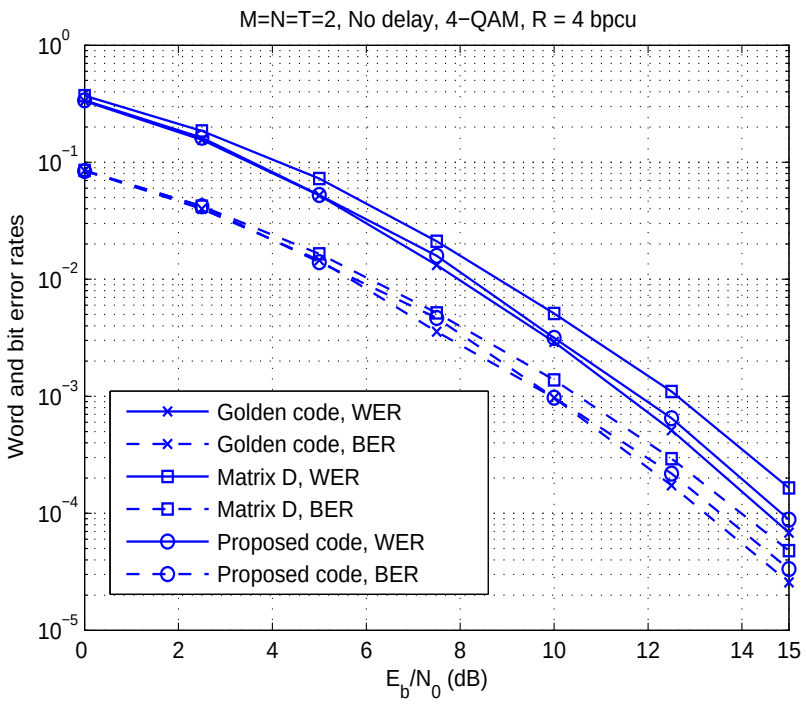

Figure 2.1: WER and BER performances of the Golden code, matrix **D** code, and the proposed code when the relays are synchronous.

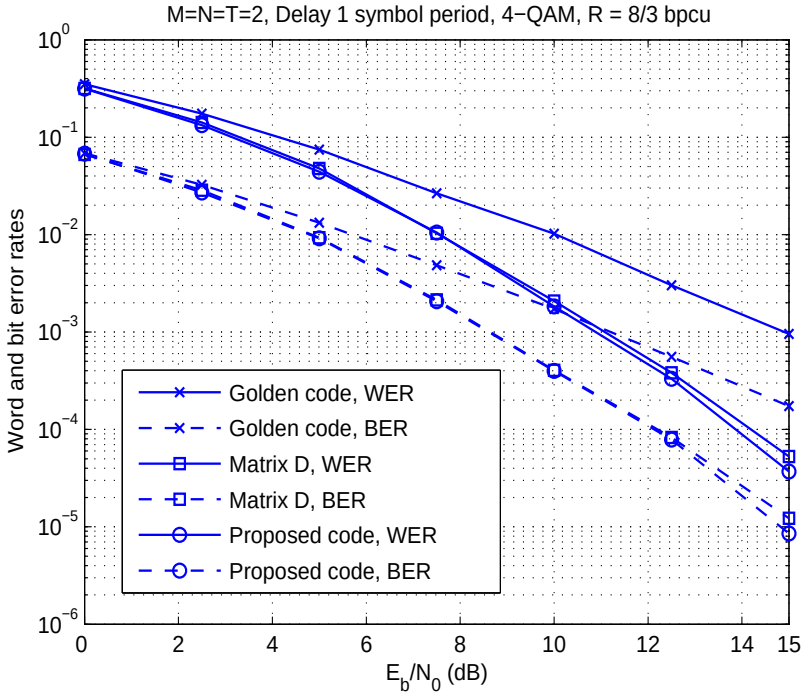

Figure 2.2: WER and BER performances of the Golden code, matrix **D** code, and the proposed code when the relays are asynchronous.

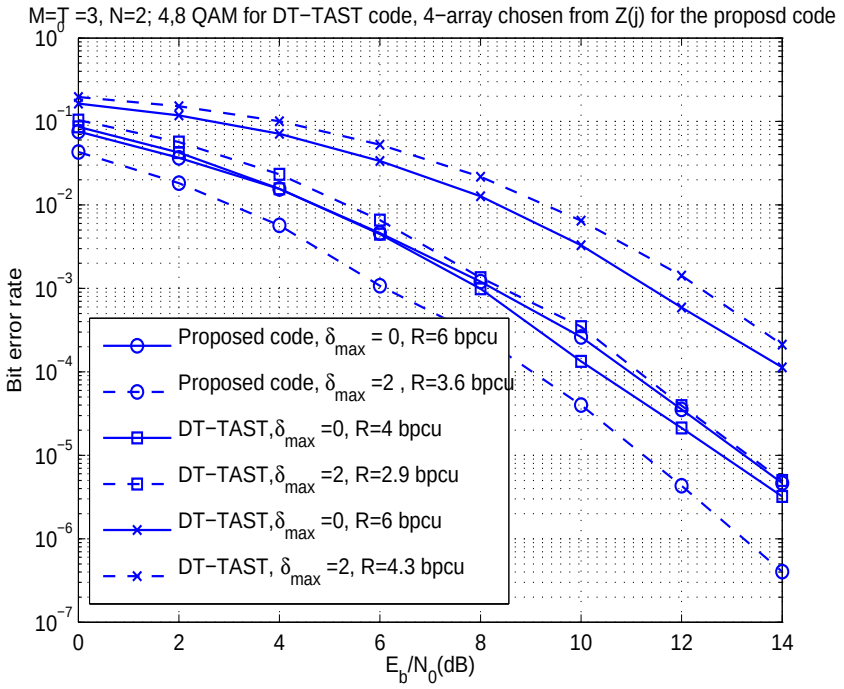

Figure 2.3: BER performance of the proposed code and DT-TAST code for both cases of synchronous and asynchronous relays.

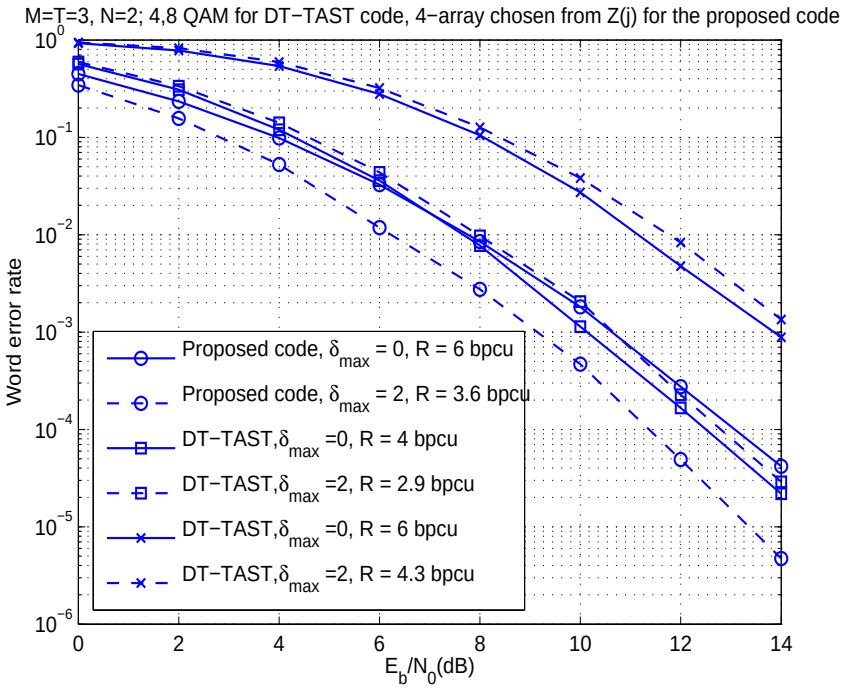

Figure 2.4: WER performance of the proposed code and the DT-TAST code for both cases of synchronous and asynchronous relays.

At the latter case, the first and the second rows are shifted once and twice to the right. The 9×9 optimal rotation is applied to the vector of information symbols which are carved from a four point constellation of $\mathbb{Z}[j]$. This code provides the rates 6, and 3.6 bpcu corresponding to $\delta_{max} = 0, 2$, respectively. The results are compared with the one of the delay tolerant TAST (DT-TAST) codes proposed in [33], where the code matrix of size 3×5 with two nonzero threads are used to transmit 4, and 8-QAM symbols over the channel. As can be seen, the proposed code performs much better than the equivalent DT-TAST code at the same rate in both synchronous and asynchronous cases. For example, at the BER of 10^{-5}, and $\delta_{max} = 0$ ($R = 6$ bpcu), it has 5 dB gain over the DT-TAST code and even more when $\delta_{max} = 2$ (R = 3.6 bpcu). These figures show that the proposed code at the rates 6 and 3.6 bpcu (corresponding to the synchronous and the asynchronous cases) performs almost the same as the DT-TAST code which has smaller rates of 4 and 2.9 bpcu, respectively. The results confirm that $\mathbf{B}_3$ is delay tolerant.

In another scenario, we assume that the proposed distributed space-time code is designed for $M = 3$ relays; however, one of the relays is not able to decode the source messages error free. In this case, it will not participate in the second step of the process, and the resulted space-time code is of size 2×3 instead of 3×3. Figure 2.5 shows the BER and the WER performances of the proposed structure under this condition. The numerical results are provided for both synchronous and asynchronous cases. In the latter case, the second relay has one symbol interval relative delay with reference to the first relay. The decoding procedure is carried out by MMSE-DFE followed by the sphere decoder. As can be seen, the maximum diversity gain of two is achieved in both cases.

2.6 Discussion and Conclusion

A novel design for the construction of full-diversity full-rate delay tolerant distributed space-time codes with minimum temporal length was introduced for cooperative diversity in wireless networks. The new codes achieve full-diversity for arbitrary number of active relays, arbitrary delay profiles and arbitrary input alphabets. Due to their minimal temporal span, the new codes enjoy smaller decoding complexity compared to those proposed in [29] and [33] while they achieve the same diversity gain.

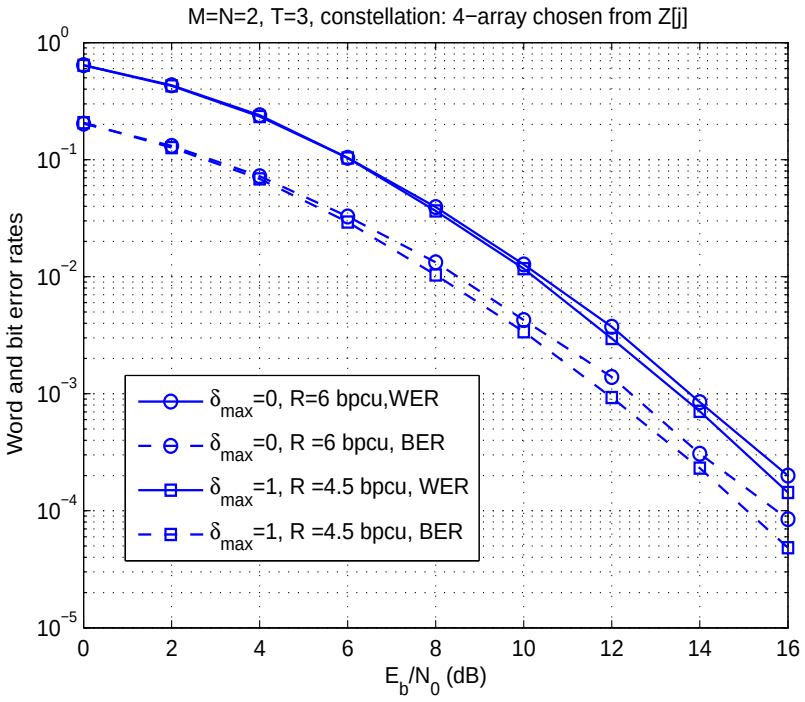

Figure 2.5: BER and WER performances of the proposed code when only two relays participate in signal transmission.

Chapter 3

Diversity Multiplexing Tradeoff of Asynchronous Relay Networks

3.1 Introduction

The diversity multiplexing tradeoff of a general two-hop *asynchronous* cooperative network is examined for various relaying protocols such as non-orthogonal selection decode-and-forward (NSDF), orthogonal selection decode-and-forward (OSDF), non-orthogonal amplify-and-forward (NAF), and orthogonal amplify-and-forward (OAF). The transmitter nodes send pulse amplitude modulation (PAM) signals asynchronously, in which information symbols are linearly modulated by a shaping waveform to be sent to the destination. We consider two different cases with respect to the type of the shaping waveforms used in the structure of the PAM signals. In the theoretical case where band-limited shaping waveforms with infinite time support are used, it is shown that asynchronism does not affect the DMT performance of the system and the same DMT as that of the corresponding synchronous network is obtained for all the aforementioned protocols. In the practical case where time-limited shaping waveforms are used, it is shown that better diversity gains may be achieved at the expense of a possible bandwidth expansion. In the decode-and-forward (DF) type protocols, the asynchronous network provide better diversity gains than those of the corresponding synchronous network throughout the range of the multiplexing gain. In the amplify-and-forward (AF) type protocols, the asynchronous network provides the same DMT as that of the corresponding synchronous counterpart under the OAF protocol; however, a better diversity gain is achieved under the NAF protocol throughout the range of the multiplexing gain. In particular, in the single relay asynchronous network, the NAF protocol provides the same DMT as that of the 2×1 multiple-input single-output (MISO) channel.

3.1.1 Diversity Multiplexing Tradeoff

Define $\{\mathcal{C}(\rho)\}$ as a family of variable rate codes each of them used at the corresponding signal to noise ratio, ρ. This family of codes is said to achieve the multiplexing gain r and the diversity gain $d(r)$ if

$$\lim_{\rho\to\infty} \frac{R(\rho)}{\log \rho} = r, \tag{3.1}$$

$$\lim_{\rho\to\infty} \frac{\log P_e(\rho)}{\log \rho} = -d(r), \tag{3.2}$$

where $R(\rho)$ is the transmission rate and $P_e(\rho)$ is the average error probability of the code $\mathcal{C}(\rho)$. DMT represents the tradeoff between r and $d(r)$ for the family of codes $\{\mathcal{C}(\rho)\}$. For each multiplexing gain r, it is shown that [34]

$$d(r) \leq d^*(r), \tag{3.3}$$

where $d^*(r)$ is the outage diversity which is defined as the negative exponent of ρ in the outage probability expression.

$$\lim_{\rho\to\infty} \frac{\log P_{\mathcal{O}}(R(\rho))}{\log \rho} = -d^*(r). \tag{3.4}$$

In this chapter, $\doteq$ is used to show the exponential equality. For example, $f(\rho) \doteq \rho^b$ if $\lim_{\rho\to\infty} \frac{\log f(\rho)}{\log \rho} = b$. $\dot{\leq}$ and $\dot{\geq}$ are defined similarly.

3.1.2 System Description

We consider a network containing one source node, one destination node, and M parallel relay nodes as shown in Fig. 3.1. h_i and g_i are fading coefficients representing the links from the i-th transmitting node to the destination and from the source to the i-th relay, respectively. All channel gains are assumed to be independent and identically distributed (i.i.d.) complex Gaussian random variables with zero mean and unit variance $\mathbb{C}\mathcal{N}(0,1)$. They are constant within the transmission of a frame and vary independently at the beginning of each frame.

We assume half-duplex signal transmission whereby each node can either transmit or receive but not both at any given time instant. Communication between the source and the destination is carried out in two phases. First, the source broadcasts its message to the relays and the destination in p channel uses. Second, the relays retransmit it to the destination in q channel uses based on the DF or the AF types relaying protocols. In the former, only those relays that are not in outage independently re-encode the source message and resend it to the destination; however in

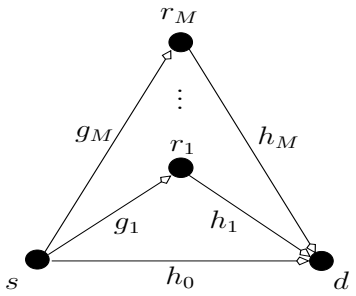

Figure 3.1: System structure

the latter, all relays perform linear transformations over the received signal and retransmit it to the destination. Assuming ℓ is the length of a cooperative frame, $\ell = p + q$. We consider both cases of non-orthogonal and orthogonal cooperating protocols where in the second phase of the former the source sends a new codeword of length q, while in the latter, the source becomes silent in the second phase. For each protocol, the case that the source transmits alone over a fix portion of a frame equal to p/ℓ for all multiplexing gains is considered first. Then, $\kappa \triangleq p/q$ is optimized to maximize the diversity gain at each multiplexing gain. Since the source may transmit over both phases, it may have two independent codebooks of proper codewords' length. The cooperation is avoided whenever it reduces the diversity gain compared to the case that the source transmits alone. Each node knows the channel state information (CSI) of its incoming links. The destination knows the CSI of all the links in AF type protocols and the CSI of the incoming links in DF type protocols, the number of the helping nodes, and their corresponding asynchronous delays.

Phase I

By assuming that the source uses an i.i.d. Gaussian codebook with codewords of length p in the first phase, its transmitted signal is given by

$$x'_0(t) = \sum_{k=0}^{p-1} x'_0(k)\psi_0(t - kT_s), \tag{3.5}$$

where $\underline{x}'_0 = [x'_0(0), x'_0(1), \ldots, x'_0(p-1)]^T$ is the transmitted codeword corresponding to the source message, T_s is the symbol interval, and $\psi_0(t)$ is a unit energy shaping waveform with support uT_s over $t \in [0, uT_s]$ for a positive integer value of u. $\psi_0(t)$ can simply be the shifted version of the truncation of a well-designed waveform in the interval $[-uT_s/2, uT_s/2]$ to the right by $uT_s/2$. The received signals in the first phase at the destination and at the i-th relay ($i = 1, \ldots, M$),

respectively, are modeled by

$$y'_d(t) = h_0 x'_0(t) + z'_d(t), \tag{3.6}$$

$$y_{r_i}(t) = g_i x'_0(t) + z_{r_i}(t), \tag{3.7}$$

where $z'_d(t)$ and $z_i(t)$ are additive white noises modeled by complex Gaussian random variables $\mathbb{CN}(0, \sigma_d^2)$ and $\mathbb{CN}(0, \sigma_r^2)$, respectively.

Phase II

Let $\mathcal{D}$ be a set containing index of the nodes participating in the second phase. Clearly, for the AF type protocols $\mathcal{D}$ contains index of all the relays; however, for the DF type protocols it contains only index of the relays that can fully decode the source message. $\mathcal{D}$ contains index of the source, which is zero in non-orthogonal protocols. In the DF type protocols, each relay is supported by an independent identically distributed (i.i.d.) random Gaussian codebook with codewords of length q. In the AF type protocols, the received signals at the relays are linearly processed and retransmitted to the destination. In both cases, the i-th relay uses a unit energy shaping waveform $\psi_i(t)$ with non-zero duration uT_s to transmit its message.

The i-th transmitted signal at the second phase is received at the destination by τ_i seconds asynchronous delay with reference to the earliest received signal. Without loss of generality, in non-orthogonal protocols, we assume that the source signal is the earliest received signal at the destination and the delays of the other received signals are measured with reference to this signal; hence, $\tau_0 = 0$. In orthogonal protocols, we assume that $\tau_1 = 0$. In any case, if m relays participate in the second phase, we index the nodes such that $\tau_0 < \tau_1 < \tau_2 < \ldots < \tau_m$. Since the relative delays are due to the random nature of the medium, the probability of the event that two of them are equal is zero. We assume that τ_i is less than a symbol interval. Generalizing the results to the case that asynchronous delays can be greater than a symbol interval is straightforward. Let $x_i(t)$ be the transmitted signal by the i-th transmitting node, $i \in \mathcal{D}$. The received signal at the destination in the second phase is modeled by

$$y_d(t) = \sum_{i \in \mathcal{D}} h_i x_i(t - \tau_i) + z_d(t). \tag{3.8}$$

3.1.3 Discrete Time Signal Model

Let E_m be the event of any m relays participate in the second phase of the process. E_0 corresponds to the case that only the source transmits in the second phase. Assume E_m occurs, $0 < m \leq M$.

$\mathcal{D} = \{0, 1, 2, \ldots, m\}$ is the index set pointing out to participating nodes in the second phase. Without loss of generality, we assume that $0 = \tau_0 < \tau_1 < \tau_2 < \ldots < \tau_m$. Note that for AF type protocols, $m = M$. To acquire the sufficient statistic of the received signal, it is passed through a set of parallel filters each of them matched to one of the incoming links [1]. The output of the i-th matched filter $i \in \{0, 1, \ldots, m\}$ sampled at $t = (k+1)T_s + \tau_i,\ k = 0, \ldots, q-1$, is given by

$$\begin{aligned} y_{d,i}(k) &= \int_{kT_s+\tau_i}^{(k+u)T_s+\tau_i} y_d(t)\psi_i^*(t - kT_s - \tau_i)dt \\ &= \sum_{j\in\mathcal{D}} h_{i,j} \sum_{n=-u}^{u} \gamma_{i,j}(n)x_j(k+n) + z_{d,i}(k), \end{aligned} \tag{3.9}$$

where $x_j(n) = 0,\ \forall\, n < 0$,

$$\begin{aligned} \gamma_{i,j}(n) &= \int_0^{uT_s} \psi_j(t - nT_s + \tau_{i,j})\psi_i^*(t)dt, \\ z_{d,i}(k) &= \int_{kT_s+\tau_i}^{(k+u)T_s+\tau_i} z_d(t)\psi_i^*(t - kT_s - \tau_i)dt, \end{aligned}$$

and the relative delay $\tau_{i,j}$ is defined as

$$\tau_{i,j} \triangleq \tau_i - \tau_j. \tag{3.10}$$

Since the shaping waveforms are of length u symbol intervals and the relays are asynchronous, every transmitted symbol of a relay is interfered by $2(u-1)$ symbols (if not zero) of the same transmitted stream and $2u-1$ symbols (if not zero) of every transmitted stream by other relays. This can be verified by checking that, $\gamma_{i,i}(u) = \gamma_{i,i}(-u) = 0, \forall\, i \in \mathcal{D}$. Moreover, for $j \neq i$ if $\tau_{i,j} < 0$, then $\gamma_{i,j}(u) = 0$. Else if $\tau_{i,j} > 0$, then $\gamma_{i,j}(-u) = 0$. The received signal vector at the output of the i-th matched filter is given by

$$\underline{y}_{d,i} = \sum_{j\in\mathcal{D}} h_j \mathbf{\Gamma}_{i,j}\underline{x}_j + \underline{z}_i, \tag{3.11}$$

where

$$\begin{aligned} \underline{y}_{d,i} &= [y_{d,i}(0), y_{d,i}(1), \ldots, y_{d,i}(q-1)]^T, \\ \underline{x}_j &= [x_j(0), x_j(1), \ldots, x_j(q-1)]^T, \\ \underline{z}_{d,i} &= [z_{d,i}(0), z_{d,i}(1), \ldots, z_{d,i}(q-1)]^T, \end{aligned}$$

and $\mathbf{\Gamma}_{i,j}$ in the general form is given in (3.12); however, $\gamma_{i,j}(-u)$ or $\gamma_{i,j}(u)$ might be zero depending on the asynchronous delays.

$\underline{z}_i$ is the colored noise vector with the covariance matrix given by

$$\mathbf{\Phi}_{i,j} = \sigma_d^2 \mathbf{\Gamma}_{i,j}. \tag{3.13}$$

$$\mathbf{\Gamma}_{i,j} = \begin{bmatrix} \gamma_{i,j}(0) & \gamma_{i,j}(-1)\cdots & \gamma_{i,j}(-u) & 0 & 0 & \dots & 0 & \dots & 0 \\ \gamma_{i,j}(1) & \cdots & \gamma_{i,j}(-u+1) & \gamma_{i,j}(-u) & 0 & \dots & 0 & \dots & 0 \\ \ddots & \ddots & \ddots & \ddots & \ddots & \ddots & \ddots & \ddots & \ddots \\ 0 & \dots & 0 & 0 & \gamma_{i,j}(u) & \cdots & \gamma_{i,j}(0) & \cdots & \gamma_{i,j}(-u) \\ \ddots & \ddots & \ddots & \ddots & \ddots & \ddots & \ddots & \ddots & \ddots \\ 0 & 0 & \cdots & 0 & \cdots & 0 & \gamma_{i,j}(u) & \cdots & \gamma_{i,j}(0) \end{bmatrix}. \tag{3.12}$$

The output vectors of the matched filters at the second phase can be written in a long vector form as

$$\underline{y} = \mathbf{H}\underline{x} + \underline{z}, \tag{3.14}$$

where

$$\begin{aligned} \underline{x} &= \left[\underline{x}_0^T, \underline{x}_1^T, \dots, \underline{x}_m^T\right]^T, \\ \underline{y} &= \left[\underline{y}_{d,0}^T, \underline{y}_{d,1}, \dots, \underline{y}_{d,m}\right]^T, \\ \underline{z} &= \left[\underline{z}_{d,0}^T, \underline{z}_{d,1}, \dots, \underline{z}_{d,m}\right]^T, \\ \mathbf{H} &= \mathbf{\Xi}(\mathbf{I}_q \otimes \hat{\mathbf{H}}), \end{aligned} \tag{3.15}$$

and

$$\begin{aligned} \hat{\mathbf{H}} &= \mathtt{diag}\{h_0, h_1, \dots, h_m\}, \\ \mathbf{\Xi} &= \begin{bmatrix} \mathbf{\Gamma}_{0,0} & \mathbf{\Gamma}_{0,1} & \mathbf{\Gamma}_{0,2} & \dots & \mathbf{\Gamma}_{0,m} \\ \mathbf{\Gamma}_{1,0} & \mathbf{\Gamma}_{1,1} & \mathbf{\Gamma}_{1,2} & \dots & \mathbf{\Gamma}_{1,m} \\ \vdots & \vdots & \vdots & & \vdots \\ \mathbf{\Gamma}_{m,0} & \mathbf{\Gamma}_{m,1} & \mathbf{\Gamma}_{m,2} & \dots & \mathbf{\Gamma}_{m,m} \end{bmatrix}. \end{aligned} \tag{3.16}$$

Equation (3.14) represents a simple MIMO channel model with correlated noise vector $\underline{z}$. The covariance matrix of $\underline{z}$ is given by

$$\mathbf{\Phi} = \sigma_d^2\, \mathbf{\Xi}. \tag{3.17}$$

One can check that $\gamma_{i,j}(n) = \gamma_{j,i}^*(-n)$, $n = 0, 1, \dots, q-1$. Hence, $\mathbf{\Gamma}_{i,j} = \mathbf{\Gamma}_{j,i}^\dagger$ and $\mathbf{\Xi}$ is a Hermitian matrix with banded Toeplitz blocks of order u.

3.1.4 Properties of Matrix $\boldsymbol{\Xi}$

For an absolutely summable infinite complex sequence $\{\gamma_{i,j}(k),\, k \in \mathbb{Z}\}$, where $\mathbb{Z}$ is the set of integers, the 2π-periodic Discrete-Time-Fourier-Transform (DTFT) is defined as [69]

$$\Gamma_{i,j}(\omega) \triangleq \sum_k \gamma_{i,j}(k) e^{-\xi\omega k},\ \omega \in [0, 2\pi], \tag{3.18}$$

where $\xi = \sqrt{-1}$. Define Matrix $\boldsymbol{\Gamma}(\omega)$ as

$$\boldsymbol{\Gamma}(\omega) \triangleq \begin{bmatrix} \Gamma_{0,0}(\omega) & \Gamma_{0,1}(\omega) & \cdots & \Gamma_{0,m}(\omega) \\ \Gamma_{1,0}(\omega) & \Gamma_{1,1}(\omega) & \cdots & \Gamma_{1,m}(\omega) \\ \vdots & \vdots & \cdots & \vdots \\ \Gamma_{m,0}(\omega) & \Gamma_{m,1}(\omega) & \cdots & \Gamma_{m,m}(\omega) \end{bmatrix}. \tag{3.19}$$

$\boldsymbol{\Gamma}(\omega)$ is a Hermitian matrix, i.e., $\boldsymbol{\Gamma}(\omega) = \boldsymbol{\Gamma}(\omega)^\dagger$. In the sequel, we will need the following theorem from [70].

Theorem 3.1. *Let λ_k, $k = 1, 2, \ldots, (m+1)q$, be the k-th eigenvalue of $\boldsymbol{\Xi}$. Let $\mu_k(\omega)$, $k = 1, 2, \ldots, m+1$, be the k-the eigenvalue of $\boldsymbol{\Gamma}(\omega)$. For all continuous functions, $F(\cdot)$, one has*

$$\lim_{q\to\infty} \frac{1}{q} \sum_{k=1}^{(m+1)q} F(\lambda_k) = \frac{1}{2\pi} \int_{-\pi}^{\pi} \sum_{k=1}^{m+1} F(\mu_k(\omega)) d\omega.$$

Moreover the eigenvalues of $\boldsymbol{\Xi}$ lie in $[\min_{k,\omega} \mu_k(\omega), \max_{k,\omega} \mu_k(\omega)]$ and if they are sorted in a descending order, then for every positive integer a, the lowest (largest) a eigenvalues of $\boldsymbol{\Xi}$ are convergent in q, i.e.,

$$\lim_{q\to\infty} \lambda_{(m+1)q-a+1} = \min_{k,\omega} \mu_k(\omega)$$
$$\lim_{q\to\infty} \lambda_a = \max_{k,\omega} \mu_k(\omega).$$

See [70] for the proof. The above theorem extends the results of the Szegö's Theorem in [71] to Hermitian block Toeplitz matrices.

Lemma 3.1. *Matrix $\boldsymbol{\Gamma}(\omega)$ can be expressed as*

$$\boldsymbol{\Gamma}(\omega) = \int_0^{T_s} \left(\sum_{i=0}^{u} \underline{\psi}(t + iT_s) e^{\xi\omega i} \right)^\dagger \sum_{i=0}^{u} \underline{\psi}(t + iT_s) e^{\xi\omega i} dt.$$

where $\underline{\psi}(t) \triangleq [\psi_0(t), \psi_1(t - \tau_{1,0}), \ldots, \psi_m(t - \tau_{m,0})]$.

Proof. Let $\underline{\psi}(t) \triangleq [\psi_0(t), \psi_1(t-\tau_{1,0}), \ldots, \psi_m(t-\tau_{m,0})]$ and $\underline{\psi}_\omega(t) = \sum_{v=-u}^{u} \underline{\psi}(t-vT_s)e^{-\xi\omega v}$. One can easily check that

$$\begin{aligned}\mathbf{\Gamma}(\omega) &= \int_{-\infty}^{\infty} \underline{\psi}^\dagger(t)\underline{\psi}_\omega(t)dt \\ &= \sum_{v=-u}^{u} \int_{-\infty}^{\infty} \underline{\psi}^\dagger(t)\underline{\psi}(t-vT_s)e^{-\xi\omega v}dt \\ &= \sum_{v=-u}^{-1} \mathbf{A}_v + \mathbf{A}_0 + \sum_{v=1}^{u} \mathbf{A}_v, \end{aligned} \tag{3.20}$$

where $\mathbf{A}_v = \int_{-\infty}^{\infty} \underline{\psi}^\dagger(t)\underline{\psi}(t-vT_s)e^{-\xi\omega v}dt$. We have,

$$\begin{aligned}\sum_{v=-u}^{-1} \mathbf{A}_v &= \sum_{v=-u}^{-1} \int_0^{(u+v+1)T_s} \underline{\psi}^\dagger(t)\underline{\psi}(t-vT_s)e^{-\xi\omega v}dt \\ &= \sum_{v=1}^{u}\sum_{n=0}^{u-v} \int_0^{T_s} \underline{\psi}^\dagger(t+nT_s)\underline{\psi}(t+(n+v)T_s)e^{\xi\omega v}dt \\ &= \sum_{n=0}^{u} \int_0^{T_s} \underline{\psi}^\dagger(t+nT_s) \sum_{v=1}^{u-n} \underline{\psi}(t+(n+v)T_s)e^{\xi\omega v}dt.\end{aligned}$$

$$\begin{aligned}\mathbf{A}_0 &= \int_0^{(u+1)T_S} \underline{\psi}^\dagger(t)\underline{\psi}(t)dt \\ &= \sum_{n=0}^{u} \int_0^{T_S} \underline{\psi}(t+nT_s)^\dagger\underline{\psi}(t+nT_s)dt.\end{aligned}$$

$$\begin{aligned}\sum_{v=1}^{u} \mathbf{A}_v &= \sum_{v=1}^{u} \int_{vT_s}^{(u+1)T_s} \underline{\psi}^\dagger(t)\underline{\psi}(t-vT_s)e^{-\xi\omega v}dt \\ &= \sum_{v=1}^{u}\sum_{n=v}^{u} \int_0^{T_s} \underline{\psi}^\dagger(t+nT_s)\underline{\psi}(t+(n-v)T_s)e^{-\xi\omega v}dt \\ &= \sum_{n=0}^{u} \int_0^{T_s} \underline{\psi}^\dagger(t+nT_s) \sum_{v=1}^{u} \underline{\psi}(t+(n-v)T_s)e^{-\xi\omega v}dt.\end{aligned}$$

$\mathbf{\Gamma}(\omega)$ can be rewritten as follows.

$$\begin{aligned}\mathbf{\Gamma}(\omega) = \sum_{n=0}^{u} \int_0^{T_s} \underline{\psi}^\dagger(t+nT_s)e^{-\xi\omega n}\Big[\underline{\psi}(t+nT_s)e^{\xi\omega n} + \sum_{v=1}^{u-n} \underline{\psi}(t+(v+n)T_s)e^{\xi\omega(v+n)} + \\ \sum_{v=1}^{n} \underline{\psi}(t+(n-v)T_s)e^{\xi\omega(n-v)}\Big]dt \\ = \int_0^{T_s} \left[\sum_{n=0}^{u} \underline{\psi}(t+nT_s)e^{\xi\omega q}\right]^\dagger \sum_{v=0}^{u} \underline{\psi}(t+vT_s)e^{\xi\omega v}dt.\end{aligned}$$

This concludes the proof. □

Proposition 3.1. $\mathbf{\Gamma}(\omega)$ *is a semi-positive definite matrix* $\forall\,\omega \in [0, 2\pi]$*, i.e.,* $\det \mathbf{\Gamma}(\omega) \geq 0$*. The equality holds if and only if* $\exists\ \underline{c} \in \mathbb{C}^{(m+1)\times 1}, \exists\ \omega \in [0, 2\pi]$ *such that*

$$\left(\sum_{i=0}^{u} \underline{\psi}(t + iTs)e^{\xi\omega i}\right)\underline{c} = 0, \quad \forall t \in [0, T_s], \tag{3.21}$$

where $\mathbb{C}$ *is the field of complex numbers.*

Proof. Proving that $\mathbf{\Gamma}(\omega)$ is a semi-positive definite matrix $\forall\,\omega$ is a direct result of Lemma 3.1. Hence,

$$\forall \underline{c} \in \mathbb{C}^{(m+1)\times 1}, \quad \underline{c}^{\dagger}\mathbf{\Gamma}(\omega)\underline{c} \geq 0.$$

Using Lemma 3.1, $\underline{c}^{\dagger}\mathbf{\Gamma}(\omega)\underline{c}$ is equal to

$$\underline{c}^{\dagger}\mathbf{\Gamma}(\omega)\underline{c} = \int_0^{T_s} \left[\left(\sum_{i=0}^{u} \underline{\psi}(t + iT_s)e^{\xi\omega i}\right)\underline{c}\right]^{\dagger} \left(\sum_{i=0}^{u} \underline{\psi}(t + iT_s)e^{\xi\omega i}\right)\underline{c}\, dt.$$

If $\underline{c}^{\dagger}\mathbf{\Gamma}(\omega)\underline{c} = 0$, there must exist $\underline{c} \in \mathbb{C}^{(m+1)\times 1}$ such that

$$\left(\sum_{i=0}^{u} \underline{\psi}(t + iT_s)e^{\xi\omega i}\right)\underline{c} = 0, \quad \forall t \in [0, T_s].$$

This concludes the proof. □

System model with time-limited waveforms

$\sum_{i=0}^{u} \underline{\psi}(t + iT_s)e^{\xi\omega i}$ is a vector containing the DTFT of the samples of the vector $\underline{\psi}(t')$ at $t' = t + iT_s$, $i \in \mathbb{Z}$, $\forall\, t \in [0, T_s]$. For a finite value of u, the spectrum of the waveforms has infinite support and occupies the whole frequency axis. Hence, the signal cannot be recovered from its samples and the DTFT of a set of samples (for a specific $t \in [0, T_s]$) is a function of the shift t and does not necessarily relate to the DTFT of another set of samples. Hence, equation (3.21) does not hold almost always when time-limited waveforms are used.

According to Proposition 3.1, if the shaping waveforms do not satisfy (3.21), $\mathbf{\Gamma}(\omega)$ is a positive definite matrix, and it has $(m + 1)$ non-zero positive real eigenvalues. Since all the $\{\gamma_{i,j}(k)\}$ sequences are assumed to be absolutely summable, $\sum_{i=1}^{(m+1)} \mu_i(\omega)$ which is equal to the trace of $\mathbf{\Gamma}(\omega)$ is a bounded value. Consequently, all eigenvalues of $\mathbf{\Gamma}(\omega)$ are also bounded. In this case, where according to Theorem 3.1, $\mathbf{\Xi}$ is a full-rank matrix with all bounded real eigenvalues, the discrete system model presented in (3.14) is used.

System model with band-limited waveforms

For an even value of u, define $\underline{\hat{\psi}}(t) \triangleq \underline{\psi}(t+\frac{u}{2}T_s)$. Hence, $\sum_{i=0}^{u} \underline{\psi}(t+iT_s)e^{\xi\omega i} = e^{\xi\omega u/2}\sum_{i=-u/2}^{u/2} \underline{\hat{\psi}}(t+iT_s)e^{\xi\omega i}$ and equation (3.21) can be rewritten based on $\underline{\hat{\psi}}(t)$ as follows.

$$\left(\sum_{i=-u/2}^{u/2} \underline{\hat{\psi}}(t+iT_s)e^{\xi\omega i}\right)\underline{c} = 0, \quad \forall t \in [0, T_s]. \tag{3.22}$$

Assume that the shaping waveforms are such that for $u \to \infty$ the communication is carried out over a strictly limited bandwidth W. Let $u \to \infty$. In this case $\lim_{u\to\infty}\sum_{i=-u/2}^{u/2}$ $\underline{\hat{\psi}}(t+iT_s)e^{\xi\omega i}$ is a vector containing the DTFT of the elements of the vector $\underline{\hat{\psi}}(t')$ sampled at $t' = t + iT_s$, $i \in \mathbb{Z}$, $\forall\, t \in [0, T_s]$. If the frequency bandwidth W is such that $W \leq \frac{1}{2T_s}$, then the shift property of the DTFT for non-integer delays is held (see Section 3.7.1) and equation (3.22) can be written as follows.

$$e^{-\xi\omega t}\sum_{i=0}^{m} c_i \hat{\Psi}_j(-\omega)e^{\xi\omega\tau_{i,0}} = 0, \quad \forall\, t \in [0, T_s], \tag{3.23}$$

where $\hat{\Psi}_j(\omega)$ is the DTFT of the samples of $\hat{\psi}_j(t') = \psi_j(t' + uT_s/2)$. It is obvious that for each $\omega \in [0, 2\pi]$, there are many choices for vector $\underline{c}$ which satisfy equation (3.23). This is because the exponential term containing the shift parameter t appears as the multiplicative factor of all the coefficients, c_i's, and does not affect the roots of this equation. Therefore, $\mathbf{\Gamma}(\omega)$ is not full rank which according to Theorem 3.1 implies that $\mathbf{\Xi}$ is not full-rank either (for large values of q).

To determine the rank order of $\mathbf{\Gamma}(\omega)$ in this case, one can see from Lemma 3.1 that

$$\begin{aligned}
\mathbf{\Gamma}(\omega) &= \int_0^{T_s}\left(\sum_{i=0}^{u}\underline{\psi}(t+iT_s)e^{\xi\omega i}\right)^{\dagger}\sum_{i=0}^{u}\underline{\psi}(t+iT_s)e^{\xi\omega i}dt \\
&= \int_0^{T_s}\left(\sum_{i=0}^{u}\underline{\hat{\psi}}(t+(i-u/2)T_s)e^{\xi\omega i}\right)^{\dagger}\sum_{i=0}^{u}\underline{\hat{\psi}}(t+(i-u/2)T_s)e^{\xi\omega i}dt \\
&= \int_0^{T_s}\left(\sum_{i=-u/2}^{u/2}\underline{\hat{\psi}}(t+iT_s)e^{\xi\omega(i+u/2)}\right)^{\dagger}\sum_{i=-u/2}^{u/2}\underline{\hat{\psi}}(t+iT_s)e^{\xi\omega(i+u/2)}dt.
\end{aligned}$$

When $u \to \infty$, we obtain

$$\mathbf{\Gamma}(\omega) = T_s\hat{\mathbf{\Psi}}^*(-\omega)\underline{e}\underline{e}^{\dagger}\hat{\mathbf{\Psi}}(-\omega), \tag{3.24}$$

where

$$\begin{aligned}
\hat{\mathbf{\Psi}}(\omega) &= \mathtt{diag}\{\hat{\Psi}_0(\omega), \hat{\Psi}_1(\omega), \ldots, \hat{\Psi}_m(\omega)\} \\
\underline{e} &= [1, e^{-\xi\omega\hat{\tau}_{1,0}}, \ldots, e^{-\xi\omega\hat{\tau}_{m,0}}]^T.
\end{aligned}$$

As can be seen, $\mathbf{\Gamma}_{i,j}$ has rank order equal to one. In this case, one matched filter is adequate to acquire the sufficient statistic. However, since the received signal is bandwidth limited, sampling with $f_s = 2W$ without matched filtering is enough for this purpose. The discrete model of the channel in this case, which is used throughout the chapter when band-limited waveforms are used, is given as follows.

$$\underline{y}_d = \sum_{j=0}^{m} h_j \mathbf{\Gamma}_j \underline{x}_j + \underline{z}_d, \tag{3.25}$$

where $\underline{z}_d$ is the white Gaussian noise vector with covariance matrix $\sigma_d^2 \mathbf{I}_q$. Assuming $\gamma_j(k) = \psi_j(kT_s - \tau_{j,0})$, $k = -q+1, \ldots, 0, \ldots, q-1$, is the k-th sample of the shaping waveform, $\mathbf{\Gamma}_j$ is given by

$$\mathbf{\Gamma}_j = \begin{bmatrix} \gamma_j(0) & \gamma_j(-1) & \cdots & \gamma_j(-q+1) \\ \gamma_j(1) & \gamma_j(0) & \cdots & \gamma_j(-q+2) \\ \ddots & \ddots & \cdots & \ddots \\ \gamma_j(q-1) & \gamma_j(q-2) & \cdots & \gamma_j(0) \end{bmatrix}. \tag{3.26}$$

Proposition 3.2. *For well-designed shaping waveforms with non-zero spectrum over the bandwidth W and the sampling frequency $f_s = 2W$, $\mathbf{\Gamma}_j$ is a full rank matrix $\forall\, q < \infty$ with all bounded eigenvalues.*

Proof. Define $\tilde{\mathbf{\Gamma}}_j$ of size $N \times N$, $N > 2q$ as in (3.27).

$$\tilde{\mathbf{\Gamma}}_j = \begin{bmatrix} \gamma_j(0) & \cdots & \gamma_j(-q+1) & 0 & 0 & \ldots & 0 & \gamma_j(q-1) & \ldots & \gamma_j(1) \\ \ddots & \ddots & \ddots & \ddots & \ddots & \ddots & \ddots & \ddots & \ddots & \ddots \\ \gamma_j(q-1) & \cdots & \gamma_j(0) & \cdots & \gamma_j(-q+1) & 0 & \ldots & 0 & \cdots & 0 \\ \ddots & \ddots & \ddots & \ddots & \ddots & \ddots & \ddots & \ddots & \ddots & \\ 0 & \cdots & 0 & \cdots & 0 & \gamma_j(q-1) & \cdots & \gamma_j(0) & \cdots & \gamma_j(-q+1) \\ \ddots & \ddots & \ddots & \ddots & \ddots & \ddots & \ddots & \ddots & \ddots & \\ \gamma_j(-1) & \cdots & \gamma_j(-q+1) & 0 & \cdots & \cdots & 0 & \gamma_j(q-1) & \cdots & \gamma_j(0) \end{bmatrix}. \tag{3.27}$$

$\tilde{\mathbf{\Gamma}}_j$ is the circular convolution matrix of the sequence $\underline{\hat{\gamma}}_j = [\gamma_j(0), \ldots, \gamma_j(q-1), 0, \ldots, 0, \gamma_j(-q+1), \ldots, \gamma_j(-1)]$ of length N. Hence, it can be decomposed as $\tilde{\mathbf{\Gamma}}_j = \mathbf{U}_N \mathbf{\Lambda}_j \mathbf{U}_N^{\dagger}$, where $\mathbf{U}_N$ is the discrete Fourier transform (DFT) matrix of dimension N defined as

$$\mathbf{U}_N(i,j) = \frac{1}{\sqrt{N}} e^{-\xi \frac{2\pi(i-1)(j-1)}{N}}, i, j = 1, 2, \ldots, N, \tag{3.28}$$

and $\mathbf{\Lambda}_j$ is a diagonal matrix containing the DFT elements of the vector $\underline{\hat{\gamma}}_j$ on its main diagonal. The k-th diagonal entry of this matrix is given by

$$\mathbf{\Lambda}_j(k,k) = \sum_{n=0}^{N-1} \hat{\gamma}_j(k) e^{-\xi \frac{2\pi}{N} kn}, \tag{3.29}$$

where $\hat{\gamma}_j(k)$ is the k-th entry of $\underline{\hat{\gamma}}_j$. If $\psi_j(t)$ has a non-zero spectrum over the bandwidth W and the sampling frequency $f_s = 2W$ is chosen, the DFT vector of $\underline{\hat{\gamma}}_j$ does not have any deterministic zero. Hence, $\mathbf{\Lambda}_j$ and accordingly $\tilde{\mathbf{\Gamma}}_j$ are full rank matrices. Sine $\mathbf{\Gamma}_j$ is the top left sub matrix of $\tilde{\mathbf{\Gamma}}_j$, it is also a full rank matrix.

Let M_f be the essential supremum $M_f = \texttt{ess sup} f$ of a real value function $f(x)$ which is defined as the smallest number a for which $f(x) \leq a$ except on a set of measure zero. Let m_f be the essential infimum $m_f = \texttt{ess inf} f$ of a real value function $f(x)$ which is defined as the largest number a for which $f(x) \geq a$ except on a set of measure zero. Let λ_k, $k = 1, 2, \ldots, q$ be the k-th eigenvalue of $\mathbf{\Gamma}_j$. It is proved in [72] that if $\mathbf{\Gamma}_j$ is Hermitian

$$m_f \leq \lambda_k \leq M_f,$$

whether or not

$$\max_k \lambda_k \leq 2M_{|f|},$$

where f here is the DTFT function of the samples of the shaping waveform $\psi_j(t)$. Since m_f, M_f, and $M_{|f|}$ are bounded values for well-designed shaping waveforms, therefore, $\mathbf{\Gamma}_j$ is a full rank matrix with non-zero bounded eigenvalues for all $j \in \{0, 1, \ldots, m\}$. This concludes the proof. □

3.2 Asynchronous NSDF Relaying Protocol

For our DF type protocols, the outage probability, $P_{\mathcal{O}}$, is calculated as follows.

$$P_{\mathcal{O}} = \sum_{m=0}^{M} Pr(I_{E_m} < R) Pr(E_m), \tag{3.30}$$

where I_{E_m} is the mutual information between the source and the destination when E_m occurs. Let $\mathcal{D}$ be the index set corresponding to the event E_m. For a transmission rate R, the probability

of the occurrence of the event E_m, $Pr(E_m)$, is given by

$$\begin{aligned}
Pr(E_m) &= \prod_{k\in\mathcal{D}} Pr(I_{s,r_k} \geq R) \prod_{k\notin\mathcal{D}} Pr(I_{s,r_k} < R) \\
&= \prod_{k\in\mathcal{D}} Pr\left(p\log(1+\rho|g_k|^2) \geq \ell R\right) \prod_{k\notin\mathcal{D}} Pr\left(p\log(1+\rho|g_k|^2) < \ell R\right) \\
&= \prod_{k\in\mathcal{D}} Pr\left(|g_k|^2 \geq \frac{2^{\frac{\ell R}{p}}-1}{\rho}\right) \prod_{k\notin\mathcal{D}} Pr\left(|g_k|^2 < \frac{2^{\frac{\ell R}{p}}-1}{\rho}\right) \\
&= \prod_{k\in\mathcal{D}} e^{-\frac{2^{\frac{\ell R}{p}}-1}{\rho}} \prod_{k\notin\mathcal{D}} \left(1-e^{-\frac{2^{\frac{\ell R}{p}}-1}{\rho}}\right),
\end{aligned}$$

where I_{s,r_k} is the mutual information between the source and the k-th relay in the first phase. The last equality comes from the fact that $|g_k|^2$ has exponential distribution with parameter $\lambda_k = 1$. By considering $R = r\log\rho$ for large values of ρ,

$$e^{-\frac{2^{\frac{\ell R}{p}}-1}{\rho}} = e^{-\frac{\rho^{\frac{\ell r}{p}}-1}{\rho}} \doteq \begin{cases} 1-\rho^{-\left(1-\frac{\ell r}{p}\right)}, & 0 \leq r \leq \frac{p}{\ell} \\ 0, & \frac{p}{\ell} < r. \end{cases}$$

Since the diversity gain is zero for $r > 1$, we only consider the case that $0 \leq r \leq 1$. Despite the relays which are in outage with probability one for $r > \frac{p}{\ell}$, the source node continues transmitting signal to the destination. Hence, $Pr(E_0) = 1$ when $\frac{p}{\ell} < r \leq 1$. Thus,

$$Pr(E_m) \doteq \begin{cases} \rho^{-(1-\frac{\ell r}{p})(M-m)}, & 0 \leq r \leq \frac{p}{\ell}, \\ 0, & \frac{p}{\ell} < r \leq 1,\ 1 \leq m \leq M \\ 1, & \frac{p}{\ell} < r \leq 1,\ m = 0. \end{cases} \tag{3.31}$$

3.2.1 Asynchronous NSDF with Band-Limited Waveforms

For the case that band-limited waveforms are used, the system is modeled by equation (3.25). By assuming a uniform power distribution among all the transmitting nodes, the mutual information between the source and the destination when E_m occurs is given by

$$I_{E_m} = \frac{p}{\ell}\log\left(1+\rho|h_0|^2\right) + \frac{1}{\ell}\log\det\left(\mathbf{I}_q + \rho\sum_{j=0}^{m}|h_j|^2\mathbf{\Gamma}_j\mathbf{\Gamma}_j^\dagger\right). \tag{3.32}$$

Since all Toeplitz matrices asymptotically commute, they are normal and are diagonalized on the same basis [72]. Moreover, according to Proposition 3.2, for proper designed shaping waveforms, $\mathbf{\Gamma}_j$ is a full rank Toeplitz matrix with all non-zero eigenvalues bounded. Hence, for large values of ρ, we obtain

$$I_{E_m} \doteq \frac{p}{\ell}\log\left(1+\rho|h_0|^2\right) + \frac{q}{\ell}\log\left(1+\rho\sum_{i=0}^{m}|h_i|^2\right). \tag{3.33}$$

As can be seen, I_{E_m} in this case is the same as that of the corresponding synchronous network given in [42]. Hence, the DMT performance of both networks is the same.

Define $\alpha_i = -\frac{\log|h_i|^2}{\log\rho}$. Let $\alpha = \min_{i\geq 1}\alpha_i$. We obtain,

$$I_{E_m} \doteq \left[\frac{p}{\ell}(1-\alpha_0)^+ + \frac{q}{\ell}(1-\alpha)^+\right]\log\rho, \tag{3.34}$$

where $(x)^+ = \max\{0, x\}$. By proceeding in the footsteps of [34], the outage probability at high values of SNR when E_m occurs is obtained as

$$\begin{aligned} P_{\mathcal{O}|E_m} &= Pr\left(I_{E_m} < R\right) \\ &= Pr\Big(p(1-\alpha_0)^+ + q(1-\alpha)^+ < \ell r\Big) \\ &= \int_{\mathcal{R}_{E_m}} p(\alpha_0,\ldots,\alpha_m)d\alpha_0\ldots d\alpha_m \\ &\doteq \int_{\mathcal{R}_{E_m}} \rho^{-\sum_{j=0}^{m}\alpha_j} d\alpha_0\ldots d\alpha_m \\ &\doteq \rho^{-d_{E_m}(r)}, \end{aligned} \tag{3.35}$$

where $p(\alpha_0,\ldots,\alpha_m)$ is the joint probability density function of the parameters $\alpha_0,\ldots,\alpha_m$; $\mathcal{R}_{E_m} = \{(\alpha_0,\alpha) \mid p(1-\alpha_0)^+ + q(1-\alpha)^+ < \ell r,\ \alpha_0,\alpha \geq 0\}$, and

$$d_{E_m}(r) = \inf_{p(1-\alpha_0)^+ + q(1-\alpha)^+ < \ell r} \alpha_0 + \alpha. \tag{3.36}$$

By solving the above optimization problem and using (3.30) and (3.31) we get

Theorem 3.2. *For band-limited waveforms, the DMT performance of the NSDF protocol over the underlying asynchronous relay network for a fixed value of $\kappa = \frac{p}{q}$ is given as follows.*
Let $\kappa_M = \frac{1+\sqrt{1+4M^2}}{2M}$. If $1 \leq \kappa \leq \kappa_M$,

$$d^*(r) = M\Big(1-\frac{\ell}{p}r\Big)^+ + (1-r), \quad 0 \leq r \leq 1,$$

else, for $\kappa \geq \kappa_M$,

$$d^*(r) = \begin{cases} (M+1)\big(1-\frac{M\ell}{(M+1)q}r\big), & 0 \leq r \leq \frac{q}{\ell} \\ \frac{\ell}{p}(1-r), & \frac{q}{\ell} \leq r \leq \frac{(M+1)p-\ell}{(M-1)\ell+p} \\ (M+1)\big(1-\frac{M\ell+p}{(M+1)p}r\big), & \frac{(M+1)p-\ell}{(M-1)\ell+p} \leq r \leq \frac{p}{\ell} \\ 1-r, & \frac{p}{\ell} \leq r \leq 1. \end{cases}$$

When κ varies to maximize the DMT at each multiplexing gain r, it is given by

$$d^*(r) = \begin{cases} (M+1)\left(1-\frac{M(1+\kappa_M)}{M+1}\right), & 0 \leq r < \frac{1}{1+\kappa_M} \\ \frac{(M+1-r)(1-r)}{(M-1)r+1}, & \frac{1}{1+\kappa_M} \leq r \leq 1. \end{cases}$$

The optimal value of κ for a gain r is given by

$$\kappa = \begin{cases} \kappa_M, & 0 \leq r \leq \frac{1}{1+\kappa_M} \\ \frac{1+(M-1)r}{M(1-r)}, & \frac{1}{1+\kappa_M} < r \leq 1. \end{cases}$$

The proof is given in [42] and is omitted here for brevity.

3.2.2 Asynchronous NSDF with Time-Limited Waveforms

For time-limited waveforms, the mutual information between the source and the destination when E_m occurs is given by

$$I_{E_m} = \frac{p}{\ell} \log(1 + \rho|h_0|^2) + \frac{1}{\ell} \log\det\left(\mathbf{I}_{(m+1)q} + \mathbf{\Phi}^{-1}\mathbf{H}\mathbf{\Sigma}_x\mathbf{H}^\dagger\right), \tag{3.37}$$

where the first and the second terms on the right hand side of the above equation are the resulted mutual information between the transmitting nodes and the destination, respectively, in the first and in the second phases. $\mathbf{\Sigma}_x$ is the autocorrelation matrix of the input vector $\underline{x}$. For simplicity, we consider a uniform power allocation for all the transmitting nodes in the second phase. Define $\mathcal{A} \triangleq \mathbf{I}_{(m+1)q} + \mathbf{\Phi}^{-1}\mathbf{H}\mathbf{\Sigma}_x\mathbf{H}^\dagger$. By substituting (3.15) and (3.17) into (3.37), we have

$$\det\mathcal{A} = \det\left(\mathbf{I}_{(m+1)q} + \rho(\mathbf{I}_q \otimes \hat{\mathbf{H}}\hat{\mathbf{H}}^\dagger)\mathbf{\Xi}\right).$$

$\mathbf{\Xi}$ is a Hermitian matrix and can be decomposed as $\mathbf{\Xi} = \mathbf{V}\mathbf{\Lambda}\mathbf{V}^\dagger$, where $\mathbf{V}$ is a unitary matrix and $\mathbf{\Lambda}$ is a diagonal matrix containing eigenvalues of $\mathbf{\Xi}$ on its main diagonal. According to proposition 3.1, for well-designed shaping waveforms, $\mathbf{\Xi}$ is a positive definite matrix with all eigenvalues real and bounded. By replacing all the eigenvalues by the smallest one, say λ, we get

$$\det\mathcal{A} \geq \det\left(\mathbf{I}_{(m+1)q} + \rho\lambda\mathbf{I}_q \otimes \hat{\mathbf{H}}\hat{\mathbf{H}}^\dagger\right).$$

Since λ is a bounded value, this lower bound is tight when $\rho \to \infty$. In this case, the mutual information between the source and the destination at high values of SNR is given by

$$\begin{aligned} I_{E_m} &\doteq \log(1 + \rho|h_0|^2) + \frac{q}{\ell}\sum_{i=1}^{m}\log(1 + \rho|h_i|^2) \\ &\doteq \left[(1-\alpha_0)^+ + \frac{q}{\ell}\sum_{i=1}^{m}(1-\alpha_i)^+\right]\log\rho. \end{aligned} \tag{3.38}$$

As can be seen, the resulted mutual information among the transmitting nodes and the destination is similar to that of a parallel channel with $(m+1)$ independent links. By proceeding in the footsteps of [34], $P_{\mathcal{O}|E_m}$ for a transmission rate $R = r\log\rho$ is calculated as follows.

$$P_{\mathcal{O}|E_m} = Pr\left(I_{E_m} < r\log\rho\right) \doteq \rho^{-d_{E_m}(r)} \tag{3.39}$$

where for $\alpha_i \geq 0$, $i = 0, \ldots, m$,

$$d_{E_m}(r) = \inf_{(1-\alpha_0)^+ + \frac{q}{\ell}\sum_{i=1}^{m}(1-\alpha_i)^+ < r} \sum_{i=0}^{m} \alpha_i. \tag{3.40}$$

By solving the above optimization problem for a fixed value of $\kappa = \frac{p}{q}$, we obtain

Lemma 3.2.

$$d_{E_m}(r) = \begin{cases} 1 + m - \frac{\ell}{q} r, & 0 \leq r \leq \frac{mq}{\ell}, \\ 1 + \frac{mq}{\ell} - r, & \frac{mq}{\ell} < r \leq 1. \end{cases}$$

Clearly, when $m \geq \kappa + 1$, then $\frac{mq}{\ell} \geq 1$. Hence,

$$d_{E_m}(r) = 1 + m - \frac{\ell}{q} r, \qquad 0 \leq r \leq 1.$$

Proof. Clearly, $\inf \sum_{i=1}^{m} \alpha_i$ occurs in the region $0 \leq \alpha_i \leq 1,\ i \in \{0, 1, \ldots, m\}$. Hence, we focus on this region to proceed the proof.

$$\begin{aligned} & (1-\alpha_0)^+ + \frac{q}{\ell}\sum_{i=1}^{m}(1-\alpha_i)^+ < r \\ \Rightarrow \quad & \alpha_0 + \frac{q}{\ell}\sum_{i=1}^{m}\alpha_i > 1 + \frac{mq}{\ell} - r \\ \Rightarrow \quad & \sum_{i=1}^{m}\alpha_i > \frac{\ell}{q}\left[(1-\alpha_0) + \frac{mq}{\ell} - r\right] \\ \Rightarrow \quad & \sum_{i=1}^{m}\alpha_i > m + \frac{\ell}{q}(1-\alpha_0) - \frac{\ell}{q} r. \end{aligned}$$

Hence

$$d_{E_m}(r) = \inf_{0 \leq \alpha_0 \leq 1} \alpha_0 + \max\left\{0, m + \frac{\ell}{q}(1-\alpha_0) - \frac{\ell}{q} r\right\}.$$

If $0 \leq r \leq \frac{mq}{\ell}$, then $(m + \frac{\ell}{q}(1-\alpha_0) - \frac{\ell}{q} r) \geq 0$ for all $0 \leq \alpha \leq 1$. Hence,

$$\begin{aligned} d_{E_m}(r) &= \inf_{0 \leq \alpha_0 \leq 1} \left(m + 1 + \frac{p}{q}(1-\alpha_0) - \frac{\ell}{q} r\right) \\ &= 1 + m - \frac{\ell}{q} r, \quad 0 \leq r \leq \frac{mq}{\ell}. \end{aligned}$$

For $r \geq \frac{mq}{\ell}$, if $\left(m + \frac{\ell}{q}(1-\alpha_0) - \frac{\ell}{q} r\right) \geq 0$, then $\alpha_0 \leq 1 + \frac{mq}{\ell} - r$. In this case, we have

$$\begin{aligned} d_{E_m}(r) &= \inf_{0 \leq \alpha_0 \leq 1 + \frac{mq}{\ell} - r} m + 1 + \frac{p}{q}(1-\alpha_0) - \frac{\ell}{q} r \\ &= 1 + \frac{mq}{\ell} - r, \quad \frac{mq}{\ell} \leq r \leq 1. \end{aligned}$$

In contrast, when $\alpha_0 > 1 + \frac{mq}{\ell} - r$, we have

$$\begin{aligned} d_{E_m}(r) &= \inf_{1+\frac{mq}{\ell}-r \le \alpha_0 \le 1} \alpha_0 \\ &= 1 + \frac{mq}{\ell} - r, \quad \frac{mq}{\ell} \le r \le 1. \end{aligned}$$

Hence, for $m \le \kappa + 1$

$$d_{E_m}(r) = \begin{cases} 1 + m - \frac{\ell}{q} r, & 0 \le r \le \frac{mq}{\ell} \\ 1 + \frac{mq}{\ell} - r, & \frac{mq}{\ell} < r \le 1. \end{cases}$$

For $m \ge \kappa + 1$, $\frac{mq}{\ell} \ge 1$. Thus

$$d_{E_m}(r) = 1 + m - \frac{\ell}{q} r, \quad 0 \le r \le 1.$$

This concludes the proof. □

The following theorem treats the case where there is only one relay in the network.

Proposition 3.3. *For time-limited waveforms, the DMT performance of the NSDF protocol over the single relay asynchronous cooperative network for a fixed value of $\kappa \ge 1$ is as follows.*
If $1 \le \kappa \le \hat{\kappa}$

$$d^*(r) = \begin{cases} (1 - \frac{\ell}{p} r) + (1 - r), & 0 \le r \le \frac{p}{\ell} \\ 1 - r, & \frac{p}{\ell} \le r \le 1, \end{cases}$$

else, for $\kappa \ge \hat{\kappa}$

$$d^*(r) = \begin{cases} 2(1 - \frac{\ell}{2q} r), & 0 \le r \le \frac{q}{\ell} \\ 1 + \frac{q}{\ell} - r, & \frac{q}{\ell} \le r \le \frac{p^2}{\ell^2} \\ (1 - \frac{\ell}{p} r) + (1 - r), & \frac{p^2}{\ell^2} \le r \le \frac{p}{\ell} \\ 1 - r, & \frac{p}{\ell} \le r \le 1, \end{cases}$$

where $\hat{\kappa} = \frac{1+\sqrt{5}}{2}$. If κ varies to maximize the diversity gain, we get

$$d^*(r) = \begin{cases} [1 - (1 + \frac{1}{\hat{\kappa}})r] + (1 - r), & 0 \le r \le \frac{1}{\hat{\kappa}+1} \\ (1 - \sqrt{r}) + (1 - r), & \frac{1}{\hat{\kappa}+1} \le r \le 1. \end{cases}$$

The optimum κ corresponding to each r is given by

$$\kappa = \begin{cases} \hat{\kappa}, & 0 \le r \le \frac{1}{\hat{\kappa}+1} \\ \frac{\sqrt{r}}{1-\sqrt{r}}, & \frac{1}{\hat{\kappa}+1} \le r \le 1. \end{cases}$$

The proof is given in Section 3.7.2. Since both $Pr(E_m)$ and $P_{\mathcal{O}|E_m}$ required in (3.30) are known, calculating DMT in a general network with $M > 1$ relays is straightforward. However, it is easier if we assume that the DMT performance of a simpler network containing $(M - 1)$ relays is known. Let $d^*_M(r)$ be the DMT of the NSDF protocol over an M relay asynchronous cooperative network. The following theorem concludes the results in the general case.

Theorem 3.3. *For time-limited waveforms, the DMT of the NSDF protocol over a general two-hop asynchronous cooperative network with M relays for a fixed $\kappa \geq 1$ is as follows.*
If $\kappa \leq \frac{M+\sqrt{M^2+4M}}{2}$,

$$d_M^*(r) = \left(1 - \frac{\ell}{p}r\right) + d_{M-1}^*(r), \quad 0 \leq r \leq \frac{p}{\ell}.$$

Else, for $\kappa \geq \frac{M+\sqrt{M^2+4M}}{2}$

$$d_M^*(r) = \begin{cases} (1 - \frac{\ell}{p}r) + d_{M-1}^*(r), & 0 \leq r \leq \frac{Mq}{\ell} \\ 1 + \frac{Mq}{\ell} - r, & \frac{Mq}{\ell} \leq r \leq \frac{p^2}{\ell^2} \\ M(1 - \frac{\ell}{p}r) + 1 - r, & \frac{p^2}{\ell^2} \leq r \leq \frac{p}{\ell}, \\ (1 - r), & \frac{p}{\ell} \leq r \leq 1, \end{cases}$$

When κ varies to maximize the diversity gain at each multiplexing gain r, we have

$$d(r) = \begin{cases} M[1 - (1 + \frac{1}{\hat{\kappa}})r] + (1 - r), & 0 \leq r \leq \frac{1}{1+\hat{\kappa}} \\ M(1 - \sqrt{r}) + (1 - r), & \frac{1}{1+\hat{\kappa}} \leq r \leq 1. \end{cases}$$

where $\hat{\kappa} = \frac{1+\sqrt{5}}{2}$. The optimum κ corresponding to each r is given by

$$\kappa = \begin{cases} \hat{\kappa}, & 0 \leq r \leq \frac{1}{1+\hat{\kappa}} \\ \frac{\sqrt{r}}{1-\sqrt{r}}, & \frac{1}{1+\hat{\kappa}} \leq r < 1. \end{cases}$$

The proof is given in Section 3.7.3. Fig. 3.2 illustrates the DMT performances of the NSDF protocol over the asynchronous single relay network for various values of κ and for both scenarios of using time-limited shaping waveforms (solid lines), and using band-limited shaping waveforms (dashed lines). Note that the DMT performance of the second scenario, when $u \to \infty$, is the same as that of the corresponding synchronous network. For the sake of comparison, the DMT performance of the 2×1 MISO channel is also shown (dotted line). As can be seen from this figure, for each r, there is a unique κ which provides the maximum diversity gain. Fig. 3.3 depicts the DMT curves for the two aforementioned cases when κ varies to maximize the diversity gain at each multiplexing gain r. It is observed that for $\kappa \leq \frac{1+\sqrt{5}}{2}$, the DMT performances of both scenarios are the same; however, for $\kappa > \frac{1+\sqrt{5}}{2}$, the asynchronous protocol with time-limited shaping waveforms provides higher diversity gain than that of the corresponding counterpart. Note that the extra diversity gain at high multiplexing region is at the expense of a possible bandwidth expansion at high values of SNR due to using time-limited waveforms.

3.3 Asynchronous OSDF Relaying Protocol

In the OSDF protocol, the source is silent in the second phase; however, the relays perform the same acts as those in the NSDF protocol. Hence, with some minor changes, the aforementioned

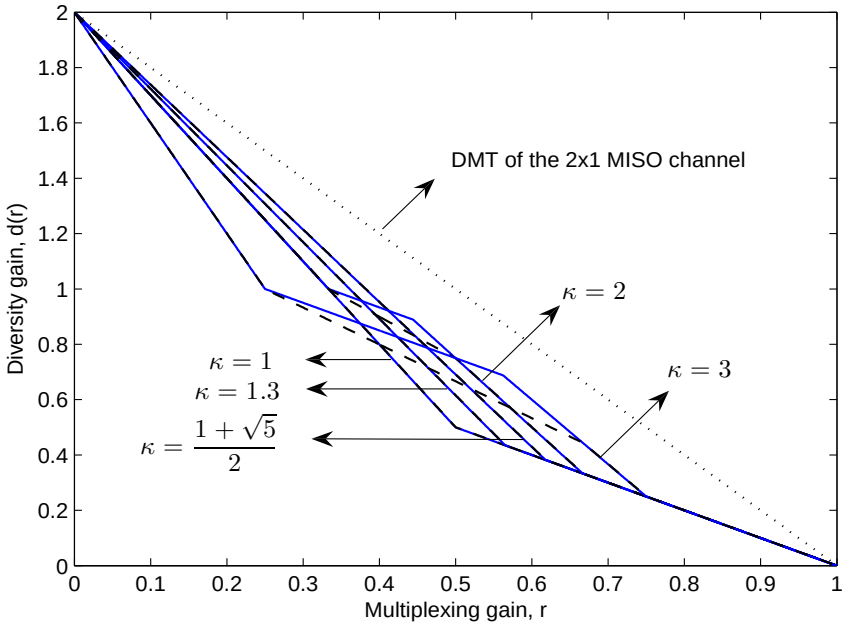

Figure 3.2: The DMT performances of the asynchronous NSDF protocol over a single relay network for both time-limited and band-limited shaping waveforms and for various values of $\kappa > 1$.

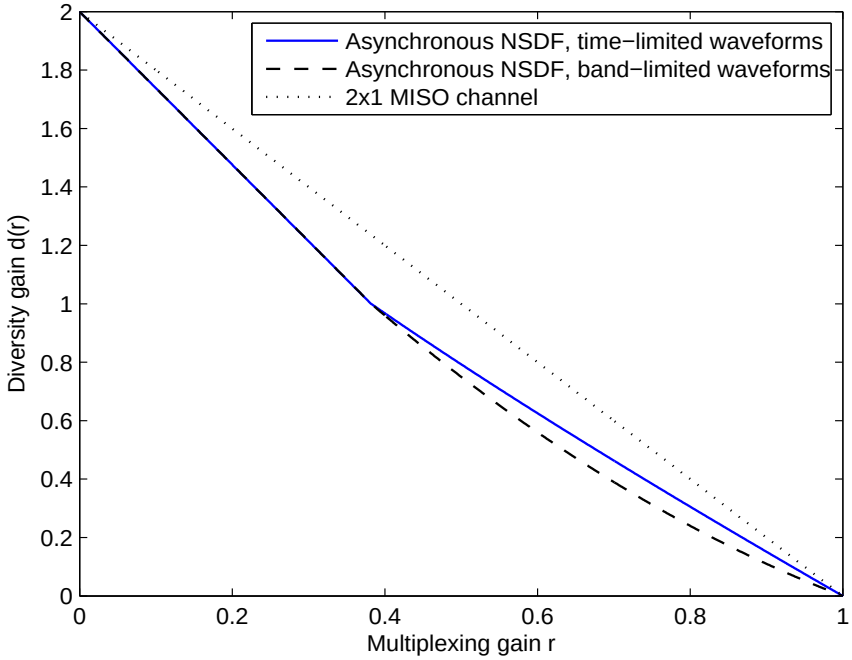

Figure 3.3: The DMT performances of the asynchronous NSDF protocol over a single relay network for both time-limited and band-limited shaping waveforms and optimum values of $\kappa > 1$.

mathematical analysis is applicable to this case. Here, asynchronism appears when at least two relays exist in the network.

3.3.1 Asynchronous OSDF with Band-Limited Waveforms

By pursuing the same procedure as that of the NSDF protocol in Section 3.2.1, the mutual information between the source and the destination when E_m occurs, $0 \leq m \leq M$, for large values of ρ is given by

$$I_{E_m} \doteq \frac{p}{\ell}\log(1+\rho|h_0|^2) + \frac{q}{\ell}\log\left(1+\rho\sum_{i=1}^{m}|h_i|^2\right). \tag{3.41}$$

As can be seen, I_{E_m} is the same as that of the corresponding synchronous network [42]. Hence, the DMT performances of the OSDF over both networks are the same.

Theorem 3.4. *For band-limited waveforms, the DMT performance of the OSDF protocol over the underlying asynchronous cooperative relay network for a fixed value of $\kappa \geq 1$ is given by*
If $1 \leq \kappa \leq \frac{M+1}{M}$,

$$d^*(r) = \begin{cases} (M+1)(1-\frac{\ell}{p}r), & 0 \leq r \leq \eta_1 \\ 1-r, & \eta_1 \leq r \leq 1, \end{cases}$$

else, for $\kappa \geq \frac{M+1}{M}$,

$$d^*(r) = \begin{cases} (M+1)(1-\frac{M\ell}{(M+1)q}r), & 0 \leq r \leq \eta_2 \\ \frac{\ell}{p}(1-r), & \eta_2 \leq r \leq \eta_3 \\ (M+1)(1-\frac{\ell}{p}r), & \eta_3 \leq r \leq \eta_1 \\ 1-r, & \eta_1 \leq r \leq 1. \end{cases}$$

where $\eta_1 = \frac{Mp}{(M+1)\ell-p}$, $\eta_2 = \frac{q}{\ell}$, and $\eta_3 = \frac{(M+1)p-\ell}{M\ell}$. When κ varies to maximize the diversity gain at each multiplexing gain r, we get

$$d^*(r) = \begin{cases} (M+1)\left(1-\frac{2M+1}{M+1}r\right), & 0 \leq r \leq \frac{M}{2M+1} \\ \frac{(M+1)(1-r)}{Mr+1}, & \frac{M}{2M+1} \leq r \leq 1. \end{cases}$$

where the optimum κ corresponding to each r is given by

$$\kappa = \begin{cases} \frac{M+1}{M}, & 0 \leq r \leq \frac{M}{2M+1} \\ \frac{1+Mr}{M(1-r)}, & \frac{M}{2M+1} \leq r \leq 1. \end{cases}$$

The proof is given in [42] and is omitted here for brevity.

3.3.2 Asynchronous OSDF with Time-Limited Waveforms

By pursuing the same procedure as that of the NSDF protocol in Section 3.2.2, one can show that at high SNR regime the mutual information between the source and the destination when $E_m, 0 \leq m \leq M$, occurs is given by

$$\begin{aligned} I_{E_m} &\doteq \frac{p}{\ell}\log(1+\rho|h_0|^2) + \frac{q}{\ell}\sum_{i=1}^{m}\log(1+\rho|h_i|^2) \\ &\doteq \left[\frac{p}{\ell}(1-\alpha_0)^+ + \frac{q}{\ell}\sum_{i=1}^{m}(1-\alpha_i)^+\right]\log\rho. \end{aligned} \tag{3.42}$$

Similarly, the outage probability in this case is obtained as

$$P_{\mathcal{O}|E_m} = Pr(I_{E_m} < r\log\rho) \doteq \rho^{-d_{E_m}(r)}, \tag{3.43}$$

where for $\alpha_i \geq 0$, $i = 0, \ldots, m$,

$$d_{E_m}(r) = \inf_{p(1-\alpha_0)^+ + q\sum_{i=1}^{m}(1-\alpha_i)^+ < \ell r} \sum_{i=0}^{m}\alpha_i. \tag{3.44}$$

By solving the above optimization problem, we get

Lemma 3.3.

$$d_{E_m}(r) = \begin{cases} 1+m-\frac{\ell}{q}r, & 0 \leq r \leq \frac{mq}{\ell} \\ 1+\frac{mq}{p}-\frac{\ell}{p}r, & \frac{mq}{\ell} < r \leq \frac{p}{\ell}. \end{cases}$$

Clearly, when $m \geq \kappa$, then $\frac{mq}{\ell} \geq \frac{p}{\ell}$. In this case,

$$d_{E_m}(r) = 1+m-\frac{\ell}{q}r, \quad 0 \leq r \leq \frac{p}{\ell}.$$

The proof is similar to that of the Lemma 3.2 and is omitted for brevity. Here $Pr(E_m)$ is given by

$$Pr(E_m) \doteq \begin{cases} \rho^{-(1-\frac{\ell r}{p})(M-m)}, & 0 \leq r \leq \frac{p}{\ell}, \\ 0, & \frac{p}{\ell} < r \leq 1. \end{cases} \tag{3.45}$$

The following theorem treats the simplest case where there are only two relays in the network.

Proposition 3.4. *For time-limited waveforms, the DMT performance of the OSDF protocol over the underlying asynchronous cooperative network with two relays and for a fixed $\kappa \geq 1$ is as follows.*
If $1 \leq \kappa < 2$,

$$d^*(r) = \begin{cases} 3(1-\frac{\ell}{p}r), & 0 \leq r \leq \frac{2p}{3\ell-p} \\ 1-r, & \frac{2p}{3\ell-p} \leq r \leq 1, \end{cases}$$

else if $2 \leq \kappa < 3$,

$$d^*(r) = \begin{cases} 3 - \frac{\ell^2}{pq} r, & 0 \leq r \leq \frac{q}{\ell} \\ 2(1 - \frac{\ell}{p} r) + \frac{q}{p}, & \frac{q}{\ell} \leq r \leq \frac{p-q}{\ell} \\ 3(1 - \frac{\ell}{p} r), & \frac{p-q}{\ell} \leq r \leq \frac{2p}{3\ell - p} \\ 1 - r, & \frac{2p}{3\ell - p} \leq r \leq 1, \end{cases}$$

else, for $\kappa \geq 3$,

$$d^*(r) = \begin{cases} 3 - \frac{\ell^2}{pq} r, & 0 \leq r \leq \frac{q}{\ell} \\ 2(1 - \frac{\ell}{p} r) + \frac{q}{p}, & \frac{q}{\ell} \leq r \leq \frac{q(p-q)}{\ell(p-2q)} \\ 3 - \frac{\ell}{q} r, & \frac{q(p-q)}{\ell(p-2q)} \leq r \leq \frac{2q}{\ell} \\ 1 - \frac{\ell}{p} r + \frac{2q}{p}, & \frac{2\ell}{q} \leq r \leq \frac{p-q}{\ell} \\ 3(1 - \frac{\ell}{p} r), & \frac{p-q}{\ell} \leq r \leq \frac{2p}{3\ell - p} \\ 1 - r, & \frac{2p}{3\ell - p} \leq r \leq 1. \end{cases}$$

When κ *varies to maximize the diversity gain at each multiplexing gain* r*, we have*

$$d^*(r) = \begin{cases} 3\left(1 - \frac{3}{2} r\right), & 0 \leq r \leq \frac{1}{3} \\ \frac{3(1-r)}{1+r}, & \frac{1}{3} \leq r \leq 1. \end{cases}$$

The optimum value of κ *corresponding to each multiplexing gain* r *is given by*

$$\kappa = \begin{cases} 2, & 0 \leq r \leq \frac{1}{3} \\ \frac{1+r}{1-r}, & \frac{1}{3} \leq r \leq 1. \end{cases}$$

The proof is given in Appendix 3.7.4. To extend the above results to the general case, let $d^*_M(r)$ be the DMT performance of the OSDF protocol over an M relay asynchronous cooperative network when the cooperation is not stopped throughout the range of the multiplexing gain. The following theorem concludes the results.

Theorem 3.5. *For time-limited waveforms, the DMT performance of the OSDF protocol over an asynchronous two-hop cooperative network with* M *relays for a fixed* κ *is given by*
If $\kappa \leq M + 1$,

$$d^*_M(r) = \begin{cases} (1 - \frac{\ell}{p} r) + d^*_{M-1}(r), & 0 \leq r \leq \frac{p}{\ell} \\ 0, & \frac{p}{\ell} \leq r \leq 1, \end{cases}$$

else, for $\kappa > M + 1$,

$$d^*_M(r) = \begin{cases} (1 - \frac{\ell}{p} r) + d^*_{M-1}(r), & 0 \leq r \leq \eta_1 \\ 1 + M - \frac{\ell}{q} r, & \eta_1 \leq r \leq \eta_2 \\ 1 + \frac{Mq}{p} - \frac{\ell}{p} r, & \eta_2 \leq r \leq \eta_3 \\ (M+1)(1 - \frac{\ell}{p} r), & \eta_3 \leq r \leq \eta_4 \\ 0, & \eta_4 \leq r \leq 1, \end{cases}$$

where $\eta_1 = \frac{(M-1)(p-q)q}{\ell(p-2q)}$, $\eta_2 = \frac{Mq}{\ell}$, $\eta_3 = \frac{p-q}{\ell}$, *and* $\eta_4 = \frac{p}{\ell}$. *The resulted DMT for each region of* κ *is compared to* $(1-r)$ *to decide when to stop the cooperation.*

When κ *varies to maximize the diversity gain at each multiplexing gain* r, *we obtain*

$$d^*(r) = \begin{cases} (M+1)\left(1-\frac{3}{2}r\right), & 0 \le r \le \frac{1}{3} \\ (M+1)\frac{1-r}{1+r}, & \frac{1}{3} \le r \le 1. \end{cases}$$

The optimum κ *for each* r *is given by*

$$\kappa = \begin{cases} 2, & 0 \le r \le \frac{1}{3} \\ \frac{1+r}{1-r}, & \frac{1}{3} \le r \le 1. \end{cases}$$

The proof is given in Section 3.7.5. Fig. 3.4 illustrates the DMT performances of the OSDF protocol over the asynchronous two relay network for various values of κ and for both scenarios of using time-limited shaping waveforms (solid lines), and using band-limited shaping waveforms (dashed lines). Note that the DMT performance in the second scenario, when band-limited waveforms are used, is the same as that of the corresponding synchronous network. For comparison, the DMT of the 3×1 MISO channel is also shown (dotted line). As can be seen from this figure, for each r, there is a unique κ which provides the maximum diversity gain. Fig. 3.5 depicts the DMT curves for the two aforementioned cases when κ varies to maximize the diversity gain at each multiplexing gain r. It is observed that the asynchronous protocol with time-limited shaping waveforms provides higher diversity gain than the corresponding counterpart throughout the range of the multiplexing gain. It is worth noting that the extra diversity gain is at the expense of a possible bandwidth expansion at high values of SNR.

3.4 Asynchronous NAF Relaying Protocol

In the second phase of the AF type protocols, the relays perform linear processing (not decoding) on the received signals and retransmit them to the destination. If $\underline{y}_{r_i}$ is the received signal vector at the i-th relay in the first phase, the transmitted vector $\underline{x}_i$ from this node is modeled by

$$\underline{x}_i = \mathbf{A}_i \underline{y}_{r_i}, \tag{3.46}$$

where $\mathbf{A}_i$ is a $q \times p$ matrix of rank $q \le p$. In the NAF protocol, the source sends a new codeword of length q to the destination in the second phase.

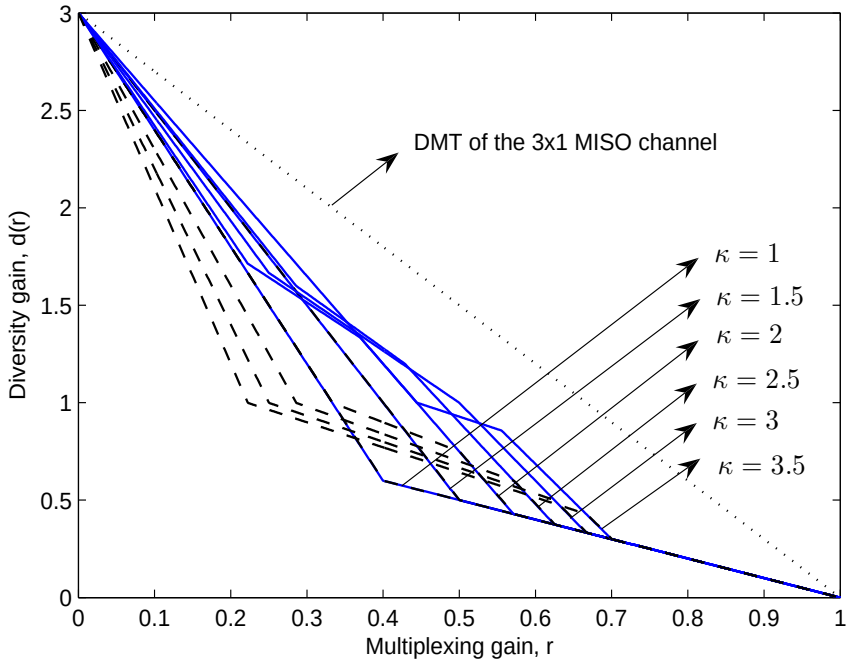

Figure 3.4: The DMT performances of the asynchronous OSDF protocol over a two relay network for both time-limited and band-limited shaping waveforms and for various values of $\kappa > 1$.

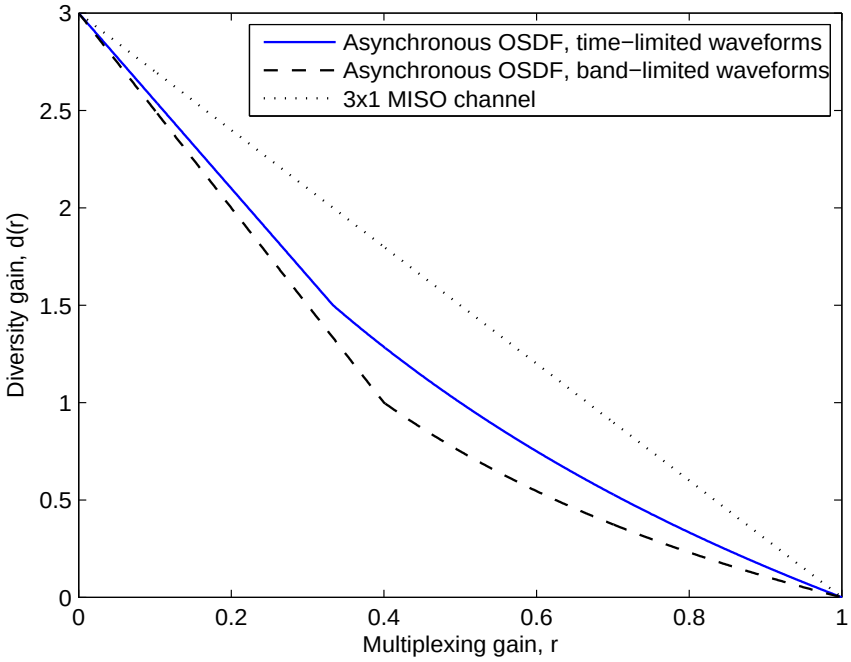

Figure 3.5: The DMT performances of the asynchronous OSDF protocol over a two relay network for both time-limited and band-limited shaping waveforms and optimum values of $\kappa > 1$.

3.4.1 Asynchronous NAF with Band-Limited Waveforms

If $\underline{x}'_0$ is the source's transmitted codeword in the first phase, the received signal vectors at the i-th relay and the destination are given by

$$\underline{y}_{r_i} = g_i \underline{x}'_0 + \underline{z}_{r_i}, \tag{3.47}$$

$$\underline{y}'_d = h_0 \underline{x}'_0 + \underline{z}'_d, \tag{3.48}$$

where all vectors are of length p. $\underline{z}_{r_i}$ and $\underline{z}'_d$ are the additive white Gaussian noise vectors at the i-th relay and at the destination in the first phase.

The received signals at the relays are linearly processed and retransmitted to the destination. At the destination, the received signal vector in the second phase according to (3.25) is given by

$$\underline{y}_d = \sum_{j=0}^{M} h_j \mathbf{\Gamma}_j \underline{x}_j + \underline{z}_d, \tag{3.49}$$

where $\mathbf{\Gamma}_j$ is given in (3.26). By replacing $\underline{x}_j = \mathbf{A}_j(g_j \underline{x}'_0 + \underline{z}_{r_j})$ for $j = 1, 2, \ldots, M$, we obtain

$$\underline{y}_d = h_0 \underline{x}_0 + \Big(\sum_{j=1}^{M} h_j g_j \mathbf{\Gamma}_j \mathbf{A}_j \Big) \underline{x}'_0 + \sum_{j=1}^{M} h_j \mathbf{\Gamma}_j \mathbf{A}_j \underline{z}_{r_j} + \underline{z}_d,$$

The system model for both phases is given by

$$\underline{y} = \mathbf{H} \underline{x} + \underline{z}, \tag{3.50}$$

where

$$\underline{y} = \left[\left(\underline{y}'_d\right)^T, \underline{y}_d^T \right]^T,$$

$$\underline{z} = \left[\left(\underline{z}'_d\right)^T, \underline{c}^T + \underline{z}_d^T \right]^T,$$

$$\underline{x} = \left[\left(\underline{x}'_0\right)^T, \underline{x}_0^T \right]^T,$$

$$\mathbf{H} = \begin{bmatrix} h_0 \mathbf{I}_p & \mathbf{0}_{p \times q} \\ \mathbf{G} & h_0 \mathbf{I}_q \end{bmatrix},$$

$\underline{c} = \sum_{j=1}^{M} h_j \mathbf{\Gamma}_j \mathbf{A}_j \underline{z}_{r_j}$, and $\mathbf{G} = \sum_{j=1}^{M} h_j g_j \mathbf{\Gamma}_j \mathbf{A}_j$. The covariance matrix of the noise vector $\underline{z}$ is given by

$$\mathbf{\Phi} = \sigma_d^2 \begin{bmatrix} \mathbf{I}_p & \mathbf{0}_{p \times q} \\ \mathbf{0}_{q \times p} & \mathbf{C} \end{bmatrix}, \tag{3.51}$$

where $\mathbf{C} = \mathbf{I}_q + \frac{\sigma_r^2}{\sigma_d^2}\sum_{j=1}^{M}|h_j|^2\mathbf{\Gamma}_j\mathbf{A}_j\mathbf{A}_j^\dagger\mathbf{\Gamma}_j^\dagger$. If the codebooks are Gaussian, the mutual information between the source and the destination is given by

$$\begin{aligned} I(\underline{x};\underline{y}) &= \log\det(\mathbf{I}_\ell + \mathbf{H}\mathbf{\Sigma}_x\mathbf{H}^\dagger\mathbf{\Phi}^{-1}) \\ &= (1+\rho|h_0|^2)^p \det(\mathbf{C}^{-1})\det\Big[\mathbf{C} + \rho|h_0|^2\mathbf{I}_q + \frac{\rho}{1+\rho|h_0|^2}\mathbf{G}\mathbf{G}^\dagger\Big], \end{aligned} \tag{3.52}$$

where $\mathbf{\Sigma}_x$ is the autocorrelation matrix of the input vector $\underline{x}$ which is assumed to be equal to $\mathcal{E}\mathbf{I}_\ell$, where $\mathcal{E}$ is the average transmitted energy per symbol. It is shown in [42] that

$$\mathbf{G}\mathbf{G}^\dagger \preceq M\sum_{j=1}^{M}|h_jg_j|^2\mathbf{\Gamma}_j\mathbf{A}_j\mathbf{A}_j^\dagger\mathbf{\Gamma}_j^\dagger.$$

Moreover, since $\mathbf{C} \succeq \mathbf{I}_q$, we have $\det\mathbf{C}^{-1} \leq 1$. Let $\mathcal{A} \doteq \mathbf{I}_\ell + \mathbf{H}\mathbf{\Sigma}_x\mathbf{H}^\dagger\mathbf{\Phi}^{-1}$. By proceeding in the footsteps of [42], we get

$$\det\mathcal{A} \dot{\leq} (1+\rho|h_0|^2)^p\left(1+\rho|h_0|^2+\sum_{j=1}^{M}|h_j|^2+\frac{\rho|h_jg_j|^2}{1+\rho|h_0|^2}\right)^q \tag{3.53}$$

It is shown in [42] that by proper choice of the $\mathbf{A}_j$ matrices, this bound is achievable and is in fact tight. Define $\alpha_j \doteq -\frac{\log|h_j|^2}{\log\rho}$, and $\beta_j \doteq \frac{\log|h_jg_j|^2}{\log\rho}$. Let $\beta = \min_{j\geq1}\beta_j$ and $\alpha = \min_{j\geq1}\alpha_j$. We get

$$I(\underline{x};\underline{y}) \doteq \big[(p-q)(1-\alpha_0)^+ + q\max\{-\alpha, 2(1-\alpha_0), (1-\alpha-\alpha_0), (1-\beta)\}^+\big]\log\rho. \tag{3.54}$$

By proceeding in the footsteps of [34], the outage probability at high values of SNR is given by

$$P_{\mathcal{O}} = Pr(I(\underline{x};\underline{y}) < \ell r\log\rho) \doteq \rho^{-d^*(r)}, \tag{3.55}$$

where

$$d^*(r) = \inf_{\mathcal{R}}\alpha_0 + M\alpha + M\beta, \tag{3.56}$$

and $\mathcal{R} = \{(p-q)(1-\alpha_0)^+ + q\max\{-\alpha, 2(1-\alpha_0), (1-\alpha-\alpha_0), (1-\beta)\}^+ < \ell r,\ \alpha_0, \alpha, \beta \geq 0\}$. Clearly, it is sufficient to consider $0 \leq \alpha_0, \beta \leq 1$. Moreover, since $\alpha \geq 0$, we simply set it to zero to get

$$d^*(r) = \inf_{(p-q)\alpha_0 + q\min\{2\alpha_0-1,\beta\} > p-\ell r}\alpha_0 + M\beta. \tag{3.57}$$

By solving the above optimization problem, we obtain

Theorem 3.6. *For band-limited waveforms, the DMT performance of the NAF protocol over the underlying asynchronous cooperative network for a fixed value of $\kappa \geq 1$ is as follows.*
If $1 \leq \kappa \leq \frac{M+1}{M}$.

$$d^*(r) = M(1-2r)^+ + (1-r), \quad 0 \leq r \leq 1.$$

Else, for $\kappa \geq \frac{M+1}{M}$

$$d^*(r) = \begin{cases} \left(1 - \frac{M(p-q)}{q} r\right) + M(1-2r), & 0 \leq r \leq \frac{q}{\ell} \\ (1-r) + \frac{q}{p-q}(1-2r), & \frac{q}{\ell} \leq r \leq \frac{1}{2} \\ 1-r, & \frac{1}{2} \leq r \leq 1. \end{cases}$$

The best DMT is achieved when $1 \leq \kappa \leq \frac{M+1}{M}$.

The proof is given in Appendix 3.7.6. It is seen that the best DMT performance of the NAF protocol over the underlying asynchronous network is the same as the DMT of this protocol over the corresponding synchronous network. Hence, the asynchronism does not diminish the DMT performance of the underlying network.

3.4.2 Asynchronous NAF with Time-Limited Waveforms

If $\underline{x}'_0$ is the source's transmitted codeword in the first phase, the received signal vectors at the i-th relay and the destination are given by

$$\underline{y}_{r_i} = g_i \mathbf{\Gamma}'_{0,0} \underline{x}'_0 + \underline{z}_{r_i}, \tag{3.58}$$

$$\underline{y}'_{d,0} = h_0 \mathbf{\Gamma}'_{0,0} \underline{x}'_0 + \underline{z}'_{d,0}, \tag{3.59}$$

where all vectors are of length p. $\mathbf{\Gamma}'_{0,0}$ of size $p \times p$ represents the effect of the ISI among the source's transmitted symbols at phase one. $\underline{z}_{r_i}$ and $\underline{z}'_{d,0}$ are the additive Gaussian noise vectors at the i-th relay and at the destination in the first phase with the covariance matrices $\sigma_r^2 \mathbf{\Gamma}'_{0,0}$, $\sigma_d^2 \mathbf{\Gamma}'_{0,0}$, respectively.

The received signals at the relays are linearly processed and retransmitted to the destination. The output matched filters are indexed from 0 to M where the 0-th filter is matched to the link between the source and the destination. The received signal vector at the output of the i-th matched filter in the second phase according to (3.11) is given by

$$\underline{y}_{d,i} = \sum_{j=0}^{M} h_j \mathbf{\Gamma}_{i,j} \underline{x}_j + \underline{z}_i, \quad i = 0, 1, \ldots, M. \tag{3.60}$$

By replacing $\underline{x}_j = \mathbf{A}_j (g_j \mathbf{\Gamma}'_{0,0} \underline{x}'_0 + \underline{z}_{r_j})$ for $j = 1, 2, \ldots, M$, we obtain

$$\underline{y}_{d,i} = h_0 \mathbf{\Gamma}_{0,0} \underline{x}_0 + \Big(\sum_{j=1}^{M} h_j g_j \mathbf{\Gamma}_{i,j} \mathbf{A}_j \mathbf{\Gamma}'_{0,0} \Big) \underline{x}'_0 + \sum_{j=1}^{M} h_j g_j \mathbf{\Gamma}_{i,j} \mathbf{A}_j \underline{z}_{r_j} + \underline{z}_i. \tag{3.61}$$

The system model for both phases is given by

$$\underline{y} = \mathbf{H}\underline{x} + \underline{z}, \tag{3.62}$$

where

$$\begin{aligned}
\underline{y} &= \left[(\underline{y}'_{d,0})^T, \underline{y}_{d,0}^T, \underline{y}_{d,1}^T, \ldots, \underline{y}_{d,M}^T\right]^T, \\
\underline{z} &= \left[(\underline{z}'_{d,0})^T, \underline{c}_0^T + \underline{z}_{d,0}^T, \underline{c}_1^T + \underline{z}_{d,1}^T, \ldots, \underline{c}_M^T + \underline{z}_{d,M}^T\right]^T, \\
\underline{x} &= \left[\left(\underline{x}'_0\right)^T, \underline{x}_0^T\right]^T, \\
\mathbf{H} &= \begin{bmatrix} h_0\mathbf{\Gamma}'_{0,0} & \mathbf{0}_{p\times q} \\ \mathbf{G} & h_0\mathbf{\Gamma} \end{bmatrix}.
\end{aligned}$$

$\mathbf{G} = [\mathbf{G}_0^T, \mathbf{G}_1^T, \ldots, \mathbf{G}_M^T]^T$ and $\mathbf{\Gamma} = [\mathbf{\Gamma}_{0,0}^T, \mathbf{\Gamma}_{1,0}^T, \ldots, \mathbf{\Gamma}_{M,0}^T]^T$, where for $i = 0, 1, \ldots, M$,

$$\begin{aligned}
\mathbf{G}_i &= \sum_{j=1}^{M} h_j g_j \mathbf{\Gamma}_{i,j}\mathbf{A}_j\mathbf{\Gamma}'_{0,0}, \\
\underline{c}_i &= \sum_{j=1}^{M} h_j \mathbf{\Gamma}_{i,j}\mathbf{A}_j\underline{z}_{r_j}.
\end{aligned}$$

The covariance matrix of the noise is calculated as

$$\mathbf{\Phi} = \sigma_d^2 \begin{bmatrix} \mathbf{\Gamma}'_{0,0} & \mathbf{0}_{p\times(M+1)q} \\ \mathbf{0}_{(M+1)q\times p} & \mathbf{C} \end{bmatrix}, \tag{3.63}$$

where $\mathbf{C} = \left[\mathbf{C}_{i,j}\right]$, $i, j = 0, 1, \ldots, M$, and

$$\mathbf{C}_{i,j} = \mathbf{\Gamma}_{i,j} + \frac{\sigma_r^2}{\sigma_d^2}\sum_{k=1}^{M} |h_k|^2 \mathbf{\Gamma}_{i,k}\mathbf{A}_k\mathbf{\Gamma}'_{0,0}\mathbf{A}_k^\dagger\mathbf{\Gamma}_{j,k}^\dagger.$$

Define

$$\mathbf{\Xi} \triangleq \begin{bmatrix} \mathbf{\Gamma}_{0,0} & \mathbf{\Gamma}_{0,1} & \ldots & \mathbf{\Gamma}_{0,M} \\ \mathbf{\Gamma}_{1,0} & \mathbf{\Gamma}_{1,1} & \ldots & \mathbf{\Gamma}_{1,M} \\ \vdots & \vdots & & \vdots \\ \mathbf{\Gamma}_{M,0} & \mathbf{\Gamma}_{M,1} & \ldots & \mathbf{\Gamma}_{M,M} \end{bmatrix}, \tag{3.64}$$

$$\mathbf{\Sigma} \triangleq \left[h_1 g_1 \mathbf{A}_1^T, h_2 g_2 \mathbf{A}_2^T, \ldots, h_M g_M \mathbf{A}_M^T\right]^T. \tag{3.65}$$

One can check that

$$\mathbf{G} = \mathbf{\Xi}[\mathbf{0}_{p\times q}, (\mathbf{\Sigma}\mathbf{\Gamma}'_{0,0})^\dagger]^\dagger, \tag{3.66}$$

$$\mathbf{\Gamma}\mathbf{\Gamma}^\dagger = \mathbf{\Xi}\mathtt{diag}\{\mathbf{I}_q, \mathbf{0}_{Mq\times Mq}\}\mathbf{\Xi} \tag{3.67}$$

$$\mathbf{C} = (\mathbf{\Xi}\mathtt{diag}\{\mathbf{0}, \hat{\mathbf{A}}_1, \ldots, \hat{\mathbf{A}}_M\} + \mathbf{I}_{(M+1)q})\mathbf{\Xi}, \tag{3.68}$$

where $\hat{\mathbf{A}}_i = \frac{\sigma_x^2}{\sigma_d^2}|h_i|^2\mathbf{A}_i\mathbf{\Gamma}'_{0,0}\mathbf{A}_i^\dagger$. Hence, $\mathbf{C}^{-1}$ exists if and only if $\mathbf{\Xi}^{-1}$ exists. According to Proposition 3.1, if the shaping waveforms $\psi_i(t), i = 0, \ldots, M$, are designed properly, $\mathbf{\Xi}$ is a positive definite matrix and $\mathbf{\Xi}^{-1}$ exists. Assuming $\psi_0(t)$ is a well designed waveform with non-zero spectrum over its bandwidth, $\mathbf{\Gamma}'_{0,0}$ is also a full rank matrix with bounded positive real eigenvalues (see [72]). Therefore, $\mathbf{\Phi}^{-1}$ is given by

$$\mathbf{\Phi}^{-1} = \frac{1}{\sigma_d^2}\,\mathtt{diag}\{(\mathbf{\Gamma}'_{0,0})^{-1}, \mathbf{C}^{-1}\}. \tag{3.69}$$

Let $\mathcal{A} \triangleq \mathbf{I}_{p+(M+1)q} + \mathbf{H}\mathbf{\Sigma}_x\mathbf{H}^\dagger\mathbf{\Phi}^{-1}$. The mutual information between the source and the destination is given by

$$I(\underline{x};\underline{y}) = \log\det\mathcal{A}. \tag{3.70}$$

$\mathcal{A}$ is given by

$$\mathcal{A} = \begin{bmatrix} \mathbf{I}_p + \rho|h_0|^2\mathbf{\Gamma}'_{0,0} & \rho h_0\mathbf{\Gamma}'_{0,0}\mathbf{G}^\dagger\mathbf{C}^{-1} \\ \rho h_0^*\mathbf{G} & \mathbf{I}_{(M+1)q} + \rho(\mathbf{G}\mathbf{G}^\dagger + |h_0|^2\mathbf{\Gamma}\mathbf{\Gamma}^\dagger)\mathbf{C}^{-1} \end{bmatrix}.$$

The determinant of $\mathcal{A}$ is given by

$$\det\mathcal{A} = \det\left(\mathbf{I}_p + \rho|h_0|^2\mathbf{\Gamma}'_{0,0}\right)\det\left(\mathbf{I}_{(M+1)q} + \rho|h_0|^2\mathbf{\Gamma}\mathbf{\Gamma}^\dagger\mathbf{C}^{-1} + \rho\mathbf{G}\mathbf{B}\mathbf{G}^\dagger\mathbf{C}^{-1}\right)$$

where $\mathbf{B} = \left(\mathbf{I}_p + \rho|h_0|^2\mathbf{\Gamma}'_{0,0}\right)^{-1}$. It can be checked that

$$\begin{aligned}\mathbf{G}\mathbf{B}\mathbf{G}^\dagger\mathbf{C}^{-1} &= \mathbf{\Xi}\;\mathtt{diag}\{\mathbf{0}_{q\times q}, \mathbf{\Sigma}\mathbf{\Gamma}'_{0,0}\mathbf{B}(\mathbf{\Gamma}'_{0,0})^\dagger\Sigma^\dagger\}\mathbf{\Psi},\\ \mathbf{\Gamma}\mathbf{\Gamma}^\dagger\mathbf{C}^{-1} &= \mathbf{\Xi}\mathtt{diag}\{\mathbf{I}_q, \mathbf{0}_{Mq\times Mq}\}\mathbf{\Psi},\end{aligned}$$

where $\mathbf{\Psi} = \left(\mathbf{\Xi}\mathtt{diag}\{0, \hat{\mathbf{A}}_1, \ldots, \hat{\mathbf{A}}_M\} + \mathbf{I}_{(M+1)q}\right)^{-1}$. Hence,

$$\det\mathcal{A} = \det\left(\mathbf{I}_p + \rho|h_0|^2\mathbf{\Gamma}'_{0,0}\right)\det\left(\mathbf{I}_{(M+1)q} + \rho\mathbf{\Xi}\mathtt{diag}\{|h_0|^2\mathbf{I}_q, \mathbf{\Sigma}\mathbf{\Gamma}'_{0,0}\mathbf{B}(\mathbf{\Gamma}'_{0,0})^\dagger\Sigma^\dagger\}\mathbf{\Psi}\right).$$

Since $\mathbf{\Xi}$, $\mathbf{\Psi}$, and $\mathbf{\Gamma}'_{0,0}$ are positive definite matrices with all bounded eigenvalues, they do not affect the mutual information when $\rho \to \infty$. We obtain,

$$\begin{aligned}\det\mathcal{A} \doteq& (1+\rho|h_0|^2)^{p+q}\det(\mathbf{I}_q + \rho\mathbf{\Sigma}^\dagger\mathbf{\Sigma}\mathbf{B})\\ \doteq& (1+\rho|h_0|^2)^p\Big(1+\rho|h_0|^2 + \rho\sum_{j=1}^{M}|h_jg_j|^2\Big)^q\end{aligned} \tag{3.71}$$

Let $\alpha_0 \triangleq -\frac{\log|h_0|^2}{\log\rho}$, $\beta_i \triangleq -\frac{\log|h_ig_i|^2}{\log\rho}$, and $\beta \triangleq \min_{i\geq 1}\beta_i$. We obtain,

$$I(\underline{x};\underline{y}) \doteq \left[p(1-\alpha_0)^+ + q\max\{1-\alpha_0, 1-\beta\}^+\right]\log\rho. \tag{3.72}$$

By proceeding in the footsteps of [34], the outage probability is given by

$$P_{\mathcal{O}}(R) = Pr(I(\underline{x};\underline{y}) < \ell R) \doteq \rho^{-d^*(r)},$$

where for $\alpha_i, \beta_i \geq 0$, $\forall i \in \{0, 1, \ldots, M\}$,

$$d^*(r) = \inf_{p(1-\alpha_0)^+ + q\max\{1-\alpha_0, 1-\beta\}^+ < \ell r} \alpha_0 + M\beta. \tag{3.73}$$

Clearly, $\inf(\alpha_0 + M\beta)$ occurs when $0 \leq \alpha_0, \beta \leq 1$. Hence,

$$d^*(r) = \inf_{p\alpha_0 + q\min\{\alpha_0, \beta\} > \ell(1-r)} \alpha_0 + M\beta. \tag{3.74}$$

By solving the above optimization problem, we get

Theorem 3.7. *For time-limited waveforms, the DMT performance of the NAF protocol over the underlying asynchronous cooperative network with M relays for a fixed $\kappa \geq 1$ is given by*

$$d^*(r) = \begin{cases} (M+1)(1 - \frac{M\ell}{(M+1)q}r), & 0 \leq r \leq \frac{q}{\ell} \\ 1 + \frac{q}{p} - \frac{\ell}{p}r, & \frac{q}{\ell} \leq r \leq 1. \end{cases}$$

The best DMT is achieved when $\kappa = 1$. In this case, we get

$$d^*(r) = \begin{cases} (M+1)(1 - \frac{2M}{(M+1)}r), & 0 \leq r \leq \frac{1}{2} \\ 2(1-r), & \frac{1}{2} \leq r \leq 1. \end{cases}$$

Proof. If $\min\{\alpha_0, \beta\} = \alpha_0$, then

$$\begin{aligned} d^*(r) &= \inf_{\alpha_0 > 1-r} (M+1)\alpha_0 \\ &= (M+1)(1-r). \end{aligned}$$

If $\min\{\alpha_0, \beta\} = \beta$, in this case $\hat{\alpha}_0 = \hat{\beta} = 1 - r$ is a feasible solution. The objective value for this feasible solution is $d(r) = (M+1)(1-r)$.

Let $\tilde{\alpha}_0 \triangleq \hat{\alpha}_0 + \delta$, where δ is a positive real number. In this case $\tilde{\alpha}_0$ and $\tilde{\beta} = \hat{\beta} - \frac{p}{q}\delta$ is another feasible solution. The objective value for the new variables is

$$d^*(r) = (M+1)(1-r) - \left(\frac{Mp}{q} - 1\right)\delta. \tag{3.75}$$

As $0 \leq \beta \leq \alpha_0 \leq 1$, δ should be chosen such that $\tilde{\alpha}_0 \leq 1$, and $\tilde{\beta} \geq 0$. We get

$$\begin{aligned} \tilde{\alpha}_0 \leq 1 \quad &\rightarrow \quad \delta \leq r \\ \tilde{\beta} \geq 0 \quad &\rightarrow \quad \delta \leq \frac{q}{p}(1-r). \end{aligned}$$

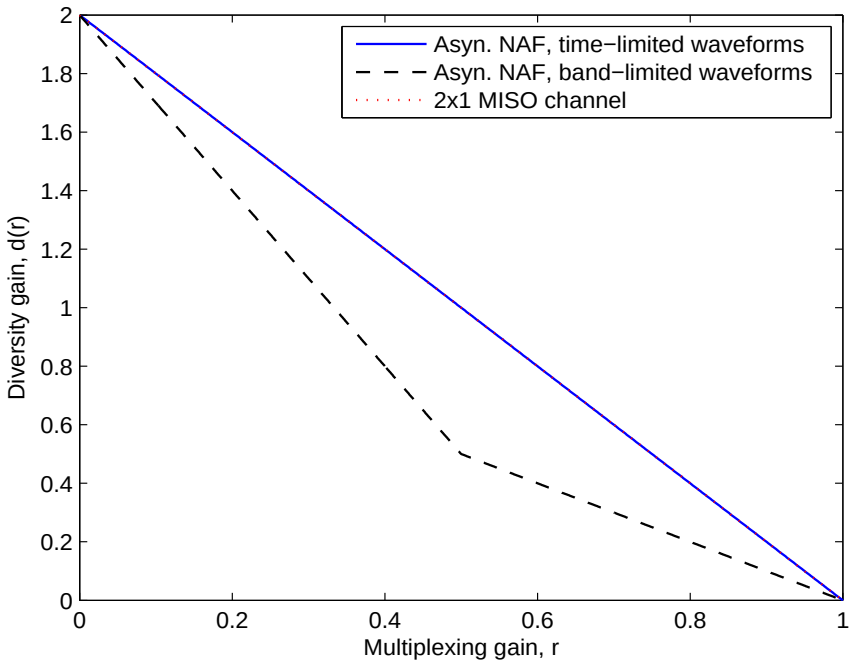

Figure 3.6: The DMT performances of the asynchronous NAF protocol for both time-limited and band-limited shaping waveforms and optimum values of $\kappa = 1$.

As both conditions should be satisfied, we have

$$\delta = \begin{cases} r, & 0 \le r \le \frac{q}{\ell} \\ \frac{q}{p}(1-r), & \frac{q}{\ell} \le r \le 1. \end{cases}$$

By replacing δ into (3.75), we obtain

$$d^*(r) = \begin{cases} (M+1)(1-\frac{M\ell}{(M+1)n}r), & 0 \le r \le \frac{q}{\ell} \\ 1+\frac{q}{p}-\frac{\ell}{p}r, & \frac{q}{\ell} \le r \le 1. \end{cases}$$

One can see that the best DMT is achieved when $\kappa = 1$. This concludes the proof. □

Fig. 3.6 depicts the DMT curves of the NAF protocol over a single relay asynchronous cooperative network for both cases of using time-limited shaping waveforms (solid line), and using band-limited shaping waveforms (dashed line) for the optimum value of $\kappa = 1$. Note that the DMT performance in the latter case is the same as that of the corresponding synchronous network. As can be seen, the asynchronous network with time-limited shaping waveforms provides the same DMT performance as that of a 2×1 MISO channel. Obviously, the extra gain is achieved at the expense of a possible bandwidth expansion at high values of SNR.

3.5 Asynchronous OAF Relaying Protocol

In the OAF protocol, the source becomes silent in the second phase; however, the relays perform the same acts as those of the NAF protocol. Hence, with some minor changes, the mathematical analysis presented in Section 3.4 can be used here. Since the protocol is orthogonal, asynchronism appears when at least two relays are in the network.

3.5.1 Asynchronous OAF with Band-Limited Waveforms

By pursuing the same procedure as that of the NAF protocol presented in Section 3.4.1, the mutual information between the source and the destination for large values of SNR is given by

$$I(\underline{x};\underline{y}) \dot{\leq} \log(1+\rho|h_0|^2)^p \left(1+\sum_{j=1}^{M}|h_j|^2+\frac{\rho|h_j g_j|^2}{1+\rho|h_0|^2}\right)^q. \tag{3.76}$$

It is shown in [42] that this upper bound is achievable and in fact is tight. Define $\alpha_j \doteq -\frac{\log|h_j|^2}{\log\rho}$, and $\beta_j \doteq \frac{\log|h_j g_j|^2}{\log\rho}$. Let $\beta = \min_{j\geq 1}\beta_j$ and $\alpha = \min_{j\geq 1}\alpha_j$. We get

$$I(\underline{x};\underline{y}) \doteq \left[(p-q)(1-\alpha_0)^+ + q\max\{-\alpha,(1-\alpha_0),(1-\alpha-\alpha_0),(1-\beta)\}^+\right]\log\rho. \tag{3.77}$$

By proceeding in the footsteps of [34], the outage probability at high values of SNR is given by

$$P_{\mathcal{O}} = Pr(I(\underline{x};\underline{y}) < \ell r\log\rho) \doteq \rho^{-d^*(r)}, \tag{3.78}$$

where by considering $0 \leq \alpha_0, \beta \leq 1$ and $\alpha = 0$,

$$d^*(r) = \inf_{(p-q)\alpha_0+q\min\{\alpha_0,\beta\}\geq p-\ell r} \alpha_0 + M\beta. \tag{3.79}$$

One can see that $I(\underline{x};\underline{y})$ of the underlying asynchronous network under the OAF protocol is the same as that of the corresponding synchronous network under the same protocol given in [42]. Hence, both networks provide the same DMT performances.

Theorem 3.8. *For band-limited waveforms, the DMT performance of the OAF protocol over the underlying asynchronous network for a fixed $\kappa \geq 1$ is as follows.*
If $\kappa \leq \frac{M+1}{M}$

$$d^*(r) = \begin{cases} (M+1)(1-\frac{\ell}{p}r), & 0 \leq r \leq \frac{p}{\ell} \\ 0, & \frac{p}{\ell} \leq r \leq 1, \end{cases}$$

else if $\kappa \geq \frac{M+1}{M}$

$$d^*(r) = \begin{cases} (M+1)(1-\frac{M\ell}{(M+1)q}r), & 0 \leq r \leq \frac{q}{\ell} \\ \frac{p}{p-q}(1-\frac{\ell}{p}r), & \frac{q}{\ell} \leq r \leq \frac{p}{\ell} \\ 0, & \frac{p}{\ell} \leq r \leq 1. \end{cases}$$

The best DMT for $0 \leq r \leq \frac{1}{2}$ *is achieved when* $\kappa = \frac{M+1}{M}$. *For* $\frac{1}{2} \leq r \leq 1$, *the best DMT is achieved when the source transmits alone. Hence,*

$$\begin{aligned} d^*(r) &= \begin{cases} (M+1)(1-\frac{2M+1}{M+1}r), & 0 \leq r \leq \frac{1}{2} \\ 1-r, & \frac{1}{2} \leq r \leq 1. \end{cases} \\ &= M(1-2r)^+ + (1-r)^+. \end{aligned}$$

The proof is given in [42] and is omitted here for brevity. Note that the result is the same as the DMT performance of the NAF protocol when band-limited waveforms are used.

3.5.2 Asynchronous OAF with Time-Limited Waveforms

By pursuing the same procedure as we presented for the NAF protocol in Section 3.4.2, the received signal model in both phases is given by

$$\underline{y} = \mathbf{H}\underline{x} + \underline{z}, \tag{3.80}$$

where

$$\begin{aligned} \underline{x} &= \underline{x}'_0, \\ \underline{y} &= \left[\left(\underline{y}'_{d,0}\right)^T, \underline{y}_{d,1}^T, \underline{y}_{d,2}^T, \ldots, \underline{y}_{d,M}^T \right]^T, \\ \underline{z} &= \left[\left(\underline{z}'_{d,0}\right)^T, \underline{c}_1^T + \underline{z}_{d,1}^T, \underline{c}_2^T + \underline{z}_{d,2}^T, \ldots, \underline{c}_M^T + \underline{z}_{d,M}^T \right]^T, \\ \mathbf{H} &= \left[h_0 (\mathbf{\Gamma}'_{0,0})^T, \mathbf{G}^T \right]^T. \end{aligned}$$

In the above equation $\mathbf{G} = [\mathbf{G}_1^T, \ldots, \mathbf{G}_M^T]^T$, where

$$\begin{aligned} \mathbf{G}_i &= \sum_{j=1}^{M} h_j g_j \mathbf{\Gamma}_{i,j} \mathbf{A}_j \mathbf{\Gamma}'_{0,0} \\ \underline{c}_i &= \sum_{j=1}^{M} h_j \mathbf{\Gamma}_{i,j} \mathbf{A}_j \underline{z}_{r_j}. \end{aligned}$$

The covariance matrix of the noise vector $\underline{z}$ is calculated as

$$\mathbf{\Phi} = \sigma_d^2 \begin{bmatrix} \mathbf{\Gamma}'_{0,0} & \mathbf{0}_{p \times Mq} \\ \mathbf{0}_{Mq \times p} & \mathbf{C} \end{bmatrix}, \tag{3.81}$$

where $\mathbf{C} = [\mathbf{C}_{i,j}]$, $i, j = 1, 2, \ldots, M$, and

$$\mathbf{C}_{i,j} = \mathbf{\Gamma}_{i,j} + \frac{\sigma_r^2}{\sigma_d^2} \sum_{k=1}^{M} |h_k|^2 \mathbf{\Gamma}_{i,k} \mathbf{A}_k \mathbf{\Gamma}'_{0,0} \mathbf{A}_k^\dagger \mathbf{\Gamma}_{j,k}^\dagger.$$

Define

$$\mathbf{\Xi} \triangleq \begin{bmatrix} \mathbf{\Gamma}_{1,1} & \mathbf{\Gamma}_{1,2} & \ldots & \mathbf{\Gamma}_{1,M} \\ \mathbf{\Gamma}_{2,1} & \mathbf{\Gamma}_{2,2} & \ldots & \mathbf{\Gamma}_{2,M} \\ \vdots & \vdots & \ldots & \vdots \\ \mathbf{\Gamma}_{M,1}^\dagger & \mathbf{\Gamma}_{M,2}^\dagger & \ldots & \mathbf{\Gamma}_{M,M} \end{bmatrix}, \tag{3.82}$$

$$\mathbf{\Sigma} \triangleq \left[h_1 g_1 \mathbf{A}_1^T, h_2 g_2 \mathbf{A}_2^T, \ldots, h_M g_M \mathbf{A}_M^T \right]^T. \tag{3.83}$$

One can check that

$$\mathbf{G} = \mathbf{\Xi} \mathbf{\Sigma} \mathbf{\Gamma}'_{0,0} \tag{3.84}$$

$$\mathbf{C} = \left(\mathbf{\Xi} \mathtt{diag}\{\hat{\mathbf{A}}_1, \ldots, \hat{\mathbf{A}}_M\} + \mathbf{I}_{Mq} \right) \mathbf{\Xi}, \tag{3.85}$$

where $\hat{\mathbf{A}}_i = \frac{\sigma_r^2}{\sigma_d^2} |h_i|^2 \mathbf{A}_i \mathbf{\Gamma}'_{0,0} \mathbf{A}_i^\dagger$. Hence, $\mathbf{C}^{-1}$ exists if and only if $\mathbf{\Xi}^{-1}$ exists. According to Proposition 3.1, if the shaping waveforms $\psi_i(t), i = 0, \ldots, M$, are designed properly, $\mathbf{\Xi}$ is positive definite and $\mathbf{\Xi}^{-1}$ exists. $\mathbf{\Gamma}'_{0,0}$ is also a full rank matrix with bounded positive real eigenvalues (see [72]). Therefore, $\mathbf{\Phi}^{-1}$ is given by

$$\mathbf{\Phi}^{-1} = \frac{1}{\sigma_d^2} \, \mathtt{diag}\{(\mathbf{\Gamma}'_{0,0})^{-1}, \mathbf{C}^{-1}\}. \tag{3.86}$$

By pursuing the same procedure as that of the NAF protocol, for high values of SNR, the mutual information between the source and the destination is obtained as

$$\begin{aligned} I(\underline{x}; \underline{y}) &\doteq \log(1 + \rho |h_0|^2)^{p-q} \left(1 + \rho |h_0|^2 + \sum_{i=1}^{M} |h_i g_i|^2 \right)^q \\ &\doteq \left[(p-q)(1-\alpha_0)^+ + q \max\{1 - \alpha_0, 1 - \beta\}^+ \right] \log \rho. \end{aligned} \tag{3.87}$$

where $\alpha_0 \triangleq -\frac{\log |h_0|^2}{\log \rho}$, $\beta_i \triangleq -\frac{\log |h_i g_i|^2}{\log \rho}$, and $\beta = \min_{i \geq 1} \beta_i$. For the rate $R = r \log \rho$, the outage probability is given by

$$P_{\mathcal{O}}(r \log \rho) = Pr(I(\underline{x}; \underline{y}) < \ell r \log \rho) \doteq \rho^{-d^*(r)},$$

where for $\alpha_i, \beta_i \geq 0$, $\forall i \in \{0, 1, \ldots, M\}$

$$d^*(r) = \inf_{(p-q)(1-\alpha_0)^+ + q \max\{1-\alpha_0, 1-\beta\}^+ < \ell r} \alpha_0 + M\beta. \tag{3.88}$$

Clearly, $\inf(\alpha_0 + M\beta)$ occurs when $0 \leq \alpha_0, \beta \leq 1$. Hence,

$$d^*(r) = \inf_{(p-q)\alpha_0 + q\min\{\alpha_0,\beta\} > p-\ell r} \alpha_0 + M\beta. \tag{3.89}$$

As can be seen the optimum diversity gain in this case is the same as that of the OAF protocol when band-limited waveforms are used given in (3.79). We simply give the final result for the optimum value of κ at each multiplexing gain in the following theorem.

Theorem 3.9. *For time-limited waveforms, the DMT performance of the OAF protocol over the underlying asynchronous network when κ varies to maximize the diversity gain is given by.*

$$d(r) = M(1-2r)^+ + (1-r)^+.$$

The best DMT for $0 \leq r \leq \frac{1}{2}$ is achieved when $\kappa = \frac{M+1}{M}$. For $\frac{1}{2} \leq r \leq 1$, the best DMT is achieved when the source transmits alone.

The proof is similar to the proof of Theorem 3.8 which is given in [42] and is omitted here for brevity. Note that the result is similar to the DMT result of the asynchronous network with band-limited shaping waveforms presented in Section 3.5.1 and equivalently similar to the DMT result of the corresponding synchronous network. Fig. 3.7 illustrates the DMT curves of the OAF protocol over the two relay asynchronous cooperative network for both cases of using time-limited shaping waveforms and using band-limited shaping waveforms when κ is chosen to maximize the diversity gain at each multiplexing gain r. As can be seen, the OAF protocol over the underlying network performs the same as the corresponding synchronous protocol for both scenarios.

3.6 Discussion and Conclusion

We examined the DMT performances of the NSDF, OSDF, NAF, and OAF relaying protocols over a general two-hop *asynchronous* cooperative relay network containing one source node, one destination node, and M parallel relay nodes. To model the asynchronism, we assumed the nodes send PAM signals asynchronously wherein information symbols are linearly modulated by a shaping waveform. We analyze the DMT of the system from both theoretical and practical points of views. In the former, we consider the case that all transmitters use band-limited shaping waveforms with infinite time support. We showed that asynchronism in this case preserves the DMT performances of the system for all the aforementioned protocols. In the latter where time-limited shaping waveforms (as in practice) are used, the communication is carried out over a spectral mask which is not strictly limited in the frequency domain and its tails go to infinity

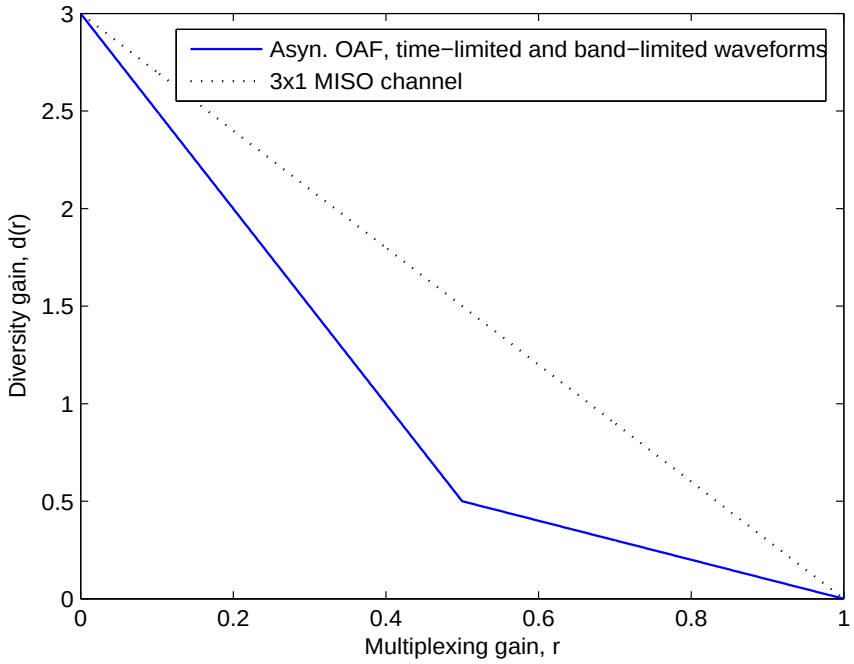

Figure 3.7: The DMT performances of the asynchronous NSDF protocol for both time-limited and band-limited shaping waveforms and optimum values of κ.

from both sides. We showed that in this case the asynchronism helps to improve the DMT performance in the NSDF, OSDF, and NAF protocols, while preserves the DMT in the OAF protocol.

3.6.1 Comparison of the DMT Performances of the Protocols

Figures 3.8 and 3.9 demonstrate the DMT performances of the discussed relaying protocols over the single relay and the two relay cooperative networks for both cases of using time-limited and using band-limited shaping waveforms. Note that for all protocols, the DMT performance of the underlying asynchronous network with band-limited shaping waveforms is the same as that of the corresponding synchronous network. As shown, except in OAF where both scenarios show the same DMT performances, in all other protocols, asynchronous protocols with time-limited shaping waveforms outperform the corresponding counterparts. In the single relay network, the asynchronous NAF with time-limited waveforms achieves the same DMT performance as that of the 2×1 MISO channel. However, it only shows the best DMT performance in low multiplexing gain regime over the two relay network. In the high multiplexing gain regime, the asynchronous NSDF with time-limited waveforms yields the best performance. One can check that by increasing the number of helping nodes ($M \geq 3$), this protocol becomes superior throughout the range of the multiplexing gain, while asynchronous NAF settles at the third place after the asynchronous OSDF protocol both with time-limited waveforms. Note that the extra diversity gain when the shaping waveforms are of limited time support is at the expense of a bandwidth expansion at high values of SNR.

3.6.2 Where Do the Gains Come From?

The main objective of this work is to show that the asynchronism does not diminish the DMT performance of a general two-hop cooperative network under the aforementioned relaying protocols. Moreover, when a practical cooperative network is considered wherein PAM signals with time-limited shaping waveforms are used, even better diversity gains can be achieved at the presence of the asynchronism. This gain is due to the fact that the communication in this case is carried out over a spectral mask with tails spanning over the entire frequency axis. This causes the mutual information between the source and the destination to behave similar to that of a parallel channel with the number of parallel branches equal to the number of links that carry independent codewords. For example, in DF type protocols where all links carry independent Gaussian codewords, the number of parallel links is equal to the number of transmitting nodes.

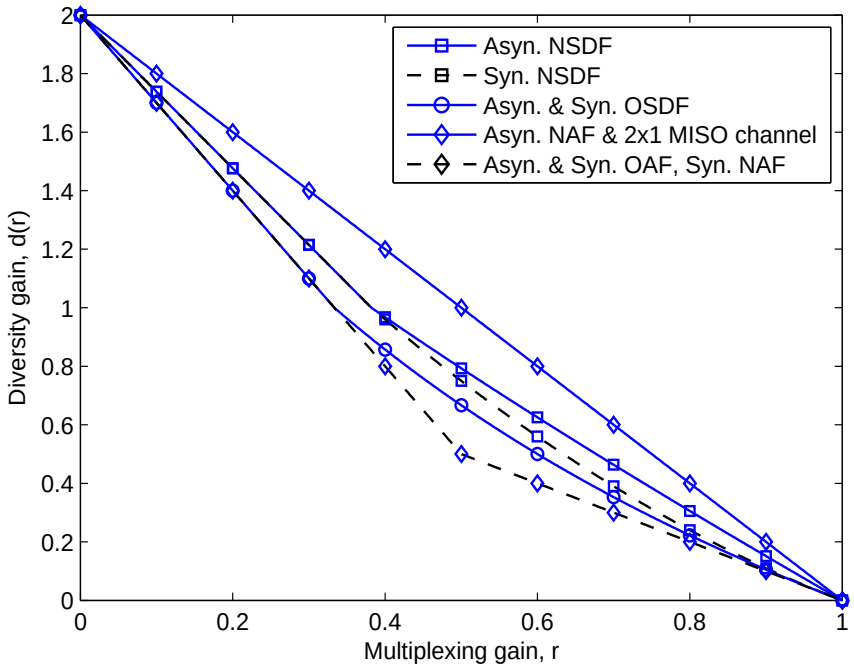

Figure 3.8: The DMT performances of the asynchronous protocols and the corresponding synchronous counterparts in a single relay network.

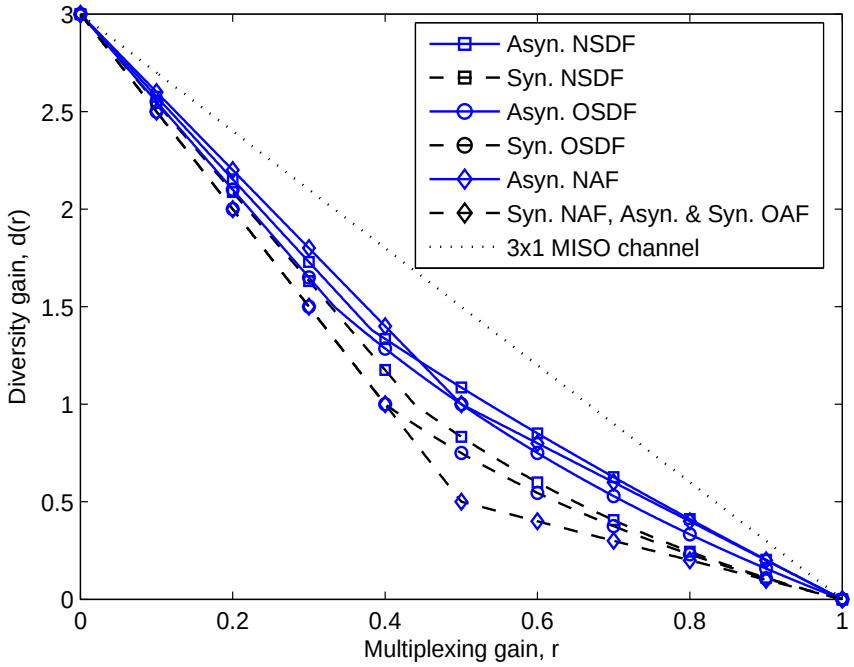

Figure 3.9: DMT performance of the asynchronous protocols and the corresponding synchronous counterparts in a two relay network.

In contrast, in the OAF protocol where all nodes carry correlated signals, the resulting mutual information of the asynchronous channel is the same as that of the corresponding synchronous channel and no parallel links appear. Note that the asynchronism is a critical factor to extract this gain from such channels. One can easily check that if the system is fully synchronous and the same time-limited shaping waveform is used , this gain is not revealed. This clears the advantage of asynchronous signaling over such channels.

3.6.3 Shaping Waveforms

The results of this work are applied to regular shaping waveforms used in theoretical analysis (e.g., the "sinc" and the "raised-cosine" waveforms). The truncated versions of such waveforms are extensively used in practice. One can easily see that the required condition in equation (3.21) is held when all nodes use band-limited shaping waveforms. On the other hand, all time-limited waveforms are used, this condition barely holds when the nodes are randomly asynchronous.

3.6.4 Practical Implementation

In practice, we propose using OFDM (inverse discrete Fourier Transform (DFT) at the transmitters and DFT at the receivers) to implement the asynchronous protocols. It can be shown that the same DMT performances can be achieved in the limit of the codeword's length. In this case, a DMT achieving space-times code designed for synchronous cooperative networks [42] also achieve the DMT of the corresponding asynchronous network.

Although it was assumed that the asynchronous delays are less than a symbol interval, the results are still held in the limit of the codewords' length when the delays are arbitrary finite random variables. In this case, one can discard a few samples from both sides of a received frame or increase the length of the cyclic prefix symbols if OFDM is used to adjust the remaining asynchronism among the nodes to be less than a symbol interval. Since the number of the discarded symbols is finite, they do not affect the maximum multiplexing gain for large length codewords.

3.7 Some Proofs of This Chapter

3.7.1 Shift Property of the DTFT for Non-Integer Delays

Lemma 3.4. *let $x(t)$ be a signal with a limited bandwidth W. $x(n)$ and $\hat{x}(n)$, $n \in \mathbb{Z}$ are two sequences of samples of this signal at $t = nT_s$ and $t = nT_s + \tau$, respectively. $X(\omega)$ and $\hat{X}(\omega)$ are defined as the DTFT of these two sequences. If the sampling frequency is chosen according to the Nyquist sampling Theorem, i.e., $W \leq \frac{1}{2T_s}$, the shift property of the DTFT is held for any real value of τ and we get*

$$\hat{X}(\omega) = X(\omega)e^{\xi\omega\hat{\tau}},$$

where $\hat{\tau} = \frac{\tau}{T_s}$.

Proof. Since $x(t)$ is bandlimited, it can be reconstructed from its samples if $W \leq \frac{1}{2T_s}$ as follows.

$$x(t) = \sum_n x(n)\mathtt{sinc}\left(\frac{t - nT_s}{T_s}\right),$$

where $\mathtt{sinc}(x) = \frac{\sin \pi x}{\pi x}$. We have

$$\begin{aligned}
\hat{X}(\omega) &= \sum_k \hat{x}(k)e^{-\xi\omega k} \\
&= \sum_k \sum_n x(n)\mathtt{sinc}\left(\frac{(k-n)T_s + \tau}{T_s}\right)e^{-\xi\omega k} \\
&= \sum_n x(n) \sum_k \mathtt{sinc}\left(k - n + \hat{\tau}\right)e^{-\xi\omega k} \\
&= e^{\xi\omega\hat{\tau}} \sum_n x(n)e^{-\xi\omega n} \\
&= e^{\xi\omega\hat{\tau}}X(\omega),
\end{aligned}$$

where the second last equality is due to the fact that the DTFT of $\mathtt{sinc}(n + a)$ is equal to $e^{\xi\omega a}$ for all real a. This concludes the proof. □

3.7.2 Proof of Proposition 3.3

The outage probability is calculated as

$$\begin{aligned}
P_{\mathcal{O}}(R) &= Pr(E_0)P_{\mathcal{O}|E_0} + Pr(E_1)P_{\mathcal{O}|E_1} \\
&\doteq \begin{cases} \rho^{-[(1-\frac{\ell}{p}r)+(1-r)]} + \rho^{-(2-\frac{\ell}{q}r)}, & 0 \leq r \leq \frac{q}{\ell} \\ \rho^{-[(1-\frac{\ell}{p}r)+(1-r)]} + \rho^{-(1+\frac{q}{\ell}-r)}, & \frac{q}{\ell} \leq r \leq \frac{p}{\ell} \\ \rho^{-(1-r)}, & \frac{p}{\ell} \leq r \leq 1. \end{cases}
\end{aligned}$$

In each region, the term with the largest exponent of ρ is dominant. We consider three distinct regions $0 \le r \le \frac{q}{\ell}$, $\frac{q}{\ell} \le r \le \frac{p}{\ell}$, and $\frac{p}{\ell} \le r \le 1$ and evaluate the diversity gain in each region. For $0 \le r \le \frac{q}{\ell}$,

$$\begin{aligned} \text{If } \left[\left(1-\frac{\ell}{p}r\right)+(1-r)\right] \le \left(2-\frac{\ell}{q}r\right) &\Rightarrow \frac{\ell}{p}+1 \ge \frac{\ell}{q} \\ &\Rightarrow \kappa^2-\kappa-1 \le 0. \end{aligned}$$

Hence assuming $\kappa \ge 1$, for $0 \le r \le \frac{q}{\ell}$ we have

$$d^*(r) = \begin{cases} \left(1-\frac{\ell}{p}r\right)+(1-r), & 1 \le \kappa \le \hat{\kappa} \\ 2\left(1-\frac{\ell}{2q}r\right), & \kappa \ge \hat{\kappa} \end{cases} \tag{3.90}$$

where $\hat{\kappa} = \frac{1+\sqrt{5}}{2}$.

For $\frac{q}{\ell} \le r \le \frac{p}{\ell}$,

$$\begin{aligned} \text{If } \left[\left(1-\frac{\ell}{p}r\right)+(1-r)\right] \le \left(1+\frac{q}{\ell}-r\right) &\Rightarrow 1-\frac{\ell}{p}r \le \frac{q}{\ell} \\ &\Rightarrow r \ge \frac{p^2}{\ell^2}. \end{aligned}$$

Clearly $\frac{p^2}{\ell^2} \le \frac{p}{\ell}$. Moreover,

$$\text{if } \frac{p^2}{\ell^2} \ge \frac{q}{\ell} \Rightarrow p^2 \ge q\ell \Rightarrow \kappa^2-\kappa-1 \ge 0.$$

Hence, if $1 \le \kappa \le \hat{\kappa}$, then $\frac{p^2}{\ell^2} \le \frac{q}{\ell}$ and we have

$$d^*(r) = \left(1-\frac{\ell}{p}r\right)+(1-r), \quad \frac{q}{\ell} \le r \le \frac{p}{\ell}.$$

However, if $\kappa \ge \hat{\kappa}$, then $\frac{p^2}{\ell^2} \ge \frac{q}{\ell}$ and therefore

$$d^*(r) = \begin{cases} 1+\frac{q}{\ell}-r, & \frac{q}{\ell} < r \le \frac{p^2}{\ell^2} \\ \left(1-\frac{\ell}{p}r\right)+(1-r), & \frac{p^2}{\ell^2} < r \le \frac{p}{\ell}. \end{cases}$$

For $\frac{p}{\ell} \le r \le 1$, it is clear that

$$d^*(r) = 1-r.$$

By combining the results of all the regions, we have

$$d^*(r) = \left(1-\frac{\ell}{p}r\right)^+ + (1-r), \quad 0 \le r \le 1,$$

when $1 \leq \kappa \leq \hat{\kappa}$ and

$$d^*(r) = \begin{cases} 2(1-\frac{\ell}{2q}r), & 0 \leq r \leq \frac{q}{\ell} \\ 1+\frac{q}{\ell}-r, & \frac{q}{\ell} < r \leq \frac{p^2}{\ell^2} \\ (1-\frac{\ell}{p}r)+(1-r), & \frac{p^2}{\ell^2} < r \leq \frac{p}{\ell} \\ 1-r, & \frac{p}{\ell} \leq r \leq 1, \end{cases}$$

when $\kappa \geq \hat{\kappa}$. This concludes the proof of the first part of the Theorem.

For $r \leq \frac{q}{\ell}$, the maximum diversity gain is achieved when $\kappa = \hat{\kappa} = \frac{1+\sqrt{5}}{2}$. If the optimum value of κ is chosen for this region, we have

$$r \leq \frac{q}{\ell} = \frac{1}{1+\hat{\kappa}}.$$

The corresponding diversity gain in this region is given by

$$\begin{aligned} d^*(r) &= \left(1-\frac{\ell}{p}r\right)+(1-r) \\ &= 2-\frac{2\hat{\kappa}+1}{\hat{\kappa}}r, \quad 0 \leq r \leq \frac{1}{1+\hat{\kappa}}. \end{aligned} \tag{3.91}$$

For a specific $r > \frac{1}{1+\hat{\kappa}}$, the maximum diversity gain is achieved when $r = \frac{p^2}{\ell^2}$. In this case,

$$r = \frac{p^2}{\ell^2} = \frac{\kappa^2}{(1+\kappa)^2}.$$

Hence, for $r > \frac{1}{1+\hat{\kappa}}$ and $\kappa > 1$

$$\kappa(r) = \frac{\sqrt{r}}{1-\sqrt{r}}. \tag{3.92}$$

The corresponding diversity gain is given by

$$\begin{aligned} d(r) &= 1+\frac{q}{\ell}-r \\ &= 1+\frac{1}{\kappa(r)+1}-r \\ &= 2-\sqrt{r}-r. \end{aligned} \tag{3.93}$$

By combining the results of all the regions we have

$$d^*(r) = \begin{cases} 1-(1+\frac{1}{\hat{\kappa}})r+(1-r), & 0 \leq r \leq \frac{1}{1+\hat{\kappa}} \\ (1-\sqrt{r})+(1-r), & \frac{1}{1+\hat{\kappa}} \leq r \leq 1. \end{cases}$$

The optimum κ corresponding to each r is given by

$$\kappa(r) = \begin{cases} \hat{\kappa}, & 0 \leq r \leq \frac{1}{1+\hat{\kappa}} \\ \frac{\sqrt{r}}{1-\sqrt{r}}, & \frac{1}{1+\hat{\kappa}} \leq r \leq 1. \end{cases}$$

This concludes the proof. □

3.7.3 Proof of Theorem 3.3

In asynchronous NSDF protocol, if $M \leq \kappa + 1$

$$d_{E_M}(r) = \begin{cases} 1 + M - \frac{\ell}{q}r, & 0 \leq r \leq \frac{Mq}{\ell} \\ 1 + \frac{Mq}{\ell} - r, & \frac{Mq}{\ell} \leq r \leq 1, \end{cases}$$

else if $M \geq \kappa + 1$

$$d_{E_M}(r) = 1 + M - \frac{\ell}{q}r, \quad 0 \leq r \leq 1.$$

In addition,

$$Pr(E_M) = \begin{cases} 1, & 0 \leq r \leq \frac{p}{\ell} \\ 0, & \frac{p}{\ell} < r \leq 1, \end{cases}$$

Let $b_m(r),\ m = 0, \ldots, M$ be the negative exponent of ρ in the expression $Pr(E_m)\rho^{-d_{Em}}$ when $\rho \to \infty$, i.e., $Pr(E_m)\rho^{-d_{Em}} \doteq \rho^{-b_m(r)}$. The outage probability at high values of SNR is given by

$$P_{\mathcal{O}} \doteq \sum_{i=0}^{M} \rho^{-b_m(r)}.$$

If $d^*_{M-1}(r)$ is the DMT performance of the NSDF protocol over a cooperative network containing $M-1$ relays, $d^*_M(r)$ can be expressed as follows.

$$d^*_M(r) = \min\Big\{\Big(1 - \frac{\ell}{p}r\Big) + d^*_{M-1}(r), b_M(r)\Big\},$$

which is simplified as follows.

If $\kappa \leq M - 1$, then $d^*_M(r)$ is given by

$$d^*_M(r) = \min\Big\{\Big(1 - \frac{\ell}{p}r\Big) + d^*_{M-1}(r), 1 + M - \frac{\ell}{q}r\Big\}, \quad 0 \leq r \leq \frac{p}{\ell}.$$

Else for $\kappa \geq M - 1$, $d^*_M(r)$ is given by

$$d^*_M(r) = \begin{cases} \min\{(1 - \frac{\ell}{p}r) + d^*_{M-1}(r), 1 + M - \frac{\ell}{q}r\}, & 0 \leq r \leq \frac{Mq}{\ell} \\ \min\{(1 - \frac{\ell}{p}r) + d^*_{M-1}(r), 1 + \frac{Mq}{\ell} - r\}, & \frac{Mq}{\ell} \leq r \leq \frac{p}{\ell}. \end{cases}$$

For $\frac{p}{\ell} \leq r \leq 1$, the source node transmits alone and

$$d^*_M(r) = 1 - r.$$

It can be seen that

$$\begin{aligned} \text{If} \quad 1 + M - \frac{\ell}{q}r \leq b_0(r) \ &\Rightarrow\ 1 + M - \frac{\ell}{q}r \leq M\Big(1 - \frac{\ell}{p}r\Big) + (1 - r) \\ &\Rightarrow\ \kappa^2 - M\kappa - M \geq 0, \end{aligned}$$

Thus, for $\kappa \leq \frac{M+\sqrt{M^2+4M}}{2}$, $b_M(r) \geq b_0(r)$ and the event E_M does not determine the DMT performance of the system. Hence for $\kappa \leq M-1$,

$$d_M^*(r) = \Big(1 - \frac{\ell}{p}r\Big) + d_{M-1}^*(r), \quad 0 \leq r \leq \frac{p}{\ell}. \tag{3.94}$$

For $\kappa \geq M-1$, if $0 \leq r \leq \frac{Mq}{\ell}$,

$$d_M^*(r) = \Big(1 - \frac{\ell}{p}r\Big) + d_{M-1}^*(r), \quad 0 \leq r \leq \frac{Mq}{\ell}. \tag{3.95}$$

In this region of κ, For $\frac{Mq}{\ell} \leq r \leq \frac{p}{\ell}$ we have

$$\begin{aligned}
b_0(r) &= M\Big(1 - \frac{\ell}{p}r\Big) + 1 - r, \\
b_1(r) &= (M-1)\Big(1 - \frac{\ell}{p}r\Big) + 1 + \frac{q}{\ell} - r, \\
b_2(r) &= (M-2)\Big(1 - \frac{\ell}{p}r\Big) + 1 + \frac{2q}{\ell} - r, \\
&\vdots \\
b_{M-1}(r) &= \Big(1 - \frac{\ell}{p}r\Big) + 1 + \frac{(M-1)q}{\ell} - r, \\
b_M(r) &= 1 + \frac{Mq}{\ell} - r.
\end{aligned}$$

It can be seen that if $r \leq \frac{p^2}{\ell^2}$, then $b_M(r) \leq b_{M-1}(r) \leq b_{M-2}(r) \leq \ldots \leq b_0(r)$. Otherwise, $b_M(r) \geq b_{M-1}(r) \geq b_{M-2}(r) \geq \ldots \geq b_0(r)$. One can check that if $\kappa \geq \frac{M+\sqrt{M^2+4M}}{2}$, then $\frac{p^2}{\ell^2} \geq \frac{Mq}{\ell}$. Hence, for $\kappa \geq \frac{M+\sqrt{M^2+4M}}{2}$ we have

$$d_M^*(r) = \begin{cases} 1 + \frac{Mq}{\ell} - r, & \frac{Mq}{\ell} \leq r \leq \frac{p^2}{\ell^2} \\ M(1 - \frac{\ell}{p}r) + 1 - r, & \frac{p^2}{\ell^2} \leq r \leq \frac{p}{\ell}. \end{cases} \tag{3.96}$$

For $\kappa \leq \frac{M+\sqrt{M^2+4M}}{2}$, $\frac{p^2}{\ell^2} \leq \frac{Mq}{\ell}$ and the event E_M does not affect the DMT performance. By combining the results we have

$$d_M^*(r) = \Big(1 - \frac{\ell}{p}r\Big) + d_{M-1}^*(r), \quad 0 \leq r \leq \frac{p}{\ell}.$$

when $\kappa \leq \frac{M+\sqrt{M^2+4M}}{2}$, and

$$d_M^*(r) = \begin{cases} \Big(1 - \frac{\ell}{p}r\Big) + d_{M-1}^*(r), & 0 \leq r \leq \frac{Mq}{\ell} \\ 1 + \frac{Mq}{\ell} - r, & \frac{Mq}{\ell} \leq r \leq \frac{p^2}{\ell^2} \\ M(1 - \frac{\ell}{p}r) + 1 - r, & \frac{p^2}{\ell^2} \leq r \leq \frac{p}{\ell}, \\ (1-r), & \frac{p}{\ell} \leq r \leq \frac{p+n}{\ell}. \end{cases}$$

when $\kappa \geq \frac{M+\sqrt{M^2+4M}}{2}$. This concludes the proof of the first part of the Theorem. The proof of the second part is similar to the proof of the second part of Proposition 3.3. □

3.7.4 Proof of Proposition 3.4

For $M = 2$, if $1 \leq \kappa < 2$, we have

$$d_{E_0(r)} = \begin{cases} 1 - \frac{\ell}{p}r, & 0 \leq r \leq \frac{p}{\ell} \\ 0, & \frac{p}{\ell} < r, \end{cases}$$

$$d_{E_1(r)} = \begin{cases} 2 - \frac{\ell}{q}r, & 0 \leq r \leq \frac{q}{\ell} \\ 1 + \frac{q}{p} - \frac{\ell}{p}r, & \frac{q}{\ell} \leq r \leq \frac{p}{\ell} \\ 0, & \frac{p}{\ell} < r, \end{cases}$$

$$d_{E_2(r)} = \begin{cases} 3 - \frac{\ell}{q}r, & 0 \leq r \leq \frac{p}{\ell} \\ 0, & \frac{p}{\ell} < r, \end{cases}$$

The outage probability in this region, $1 \leq \kappa \leq 2$, is given by

$$P_{\mathcal{O}} = \sum_{i=0}^{2} P_{\mathcal{O}|E_i} Pr(E_i) \doteq \begin{cases} \rho^{-d_1(r)}, & 0 \leq r \leq \frac{q}{\ell} \\ \rho^{-d_2(r)}, & \frac{q}{\ell} \leq r \leq \frac{p}{\ell} \\ 1, & \frac{p}{\ell} < r. \end{cases}$$

where $d_1(r) = \min\{3(1 - \frac{\ell}{p}r), 3 - \frac{\ell^2}{pq}r, 3 - \frac{\ell}{q}r\}$, and $d_2(r) = \min\{3(1 - \frac{\ell}{p}r), 2(1 - \frac{\ell}{p}r) + \frac{q}{p}, 3 - \frac{\ell}{q}r\}$.

Assume $0 \leq r \leq \frac{q}{\ell}$. Clearly $3 - \frac{\ell^2}{pq}r < 3 - \frac{\ell}{q}r$. Moreover, if $3(1 - \frac{\ell}{p}r) < 3 - \frac{\ell^2}{pq}r$, then $\kappa < 2$. Hence,

$$d^*(r) = 3\Big(1 - \frac{\ell}{p}r\Big), \quad 0 \leq r \leq \frac{q}{\ell}, \;\; 1 \leq \kappa < 2$$

Now consider $\frac{q}{\ell} < r \leq \frac{p}{\ell}$. It can be seen that $3\left(1 - \frac{\ell}{p}r\right) \;\begin{matrix} \leqq \\ > \end{matrix}\; 3 - \frac{\ell}{q}r$ if and only if $k \;\begin{matrix} \leqq \\ > \end{matrix}\; 3$. Furthermore, if $3\left(1 - \frac{\ell}{p}\right) < 2\left(1 - \frac{\ell}{p}\right) + \frac{q}{p}$, then $r < \frac{p-q}{\ell}$. One can check that, if $\kappa < 2$, then $\frac{p-q}{\ell} < \frac{q}{\ell}$. Hence,

$$d^*(r) = 3\left(1 - \frac{\ell}{p}r\right), \quad \frac{q}{\ell} \leq r \leq \frac{p}{\ell}, \;\; 1 \leq \kappa < 2.$$

The cooperation is avoided whenever it is beneficial to do so.

$$\text{if} \quad 1 - r \geq 3\left(1 - \frac{\ell}{p}r\right) \;\Rightarrow\; r \geq \frac{2p}{3\ell - p}.$$

Thus for $1 \leq \kappa < 2$,

$$d^*(r) = \begin{cases} 3(1 - \frac{\ell}{p}r), & 0 \leq r \leq \frac{2p}{3\ell - p} \\ 1 - r, & \frac{2p}{3\ell - p} \leq r \leq 1. \end{cases} \tag{3.97}$$

For $\kappa \geq 2$, $d_{E_0(r)}$ and $d_{E_1(r)}$ are the same as before. However, $d_{E_2(r)}$ is given by

$$d_{E_2(r)} = \begin{cases} 3 - \frac{\ell}{q}r, & 0 \leq r \leq \frac{2q}{\ell} \\ 1 + \frac{2q}{p} - \frac{\ell}{p}r, & \frac{2q}{\ell} < r \leq \frac{p}{\ell} \\ 0, & \frac{p}{\ell} < r. \end{cases}$$

The outage probability is given by

$$P_{\mathcal{O}} = \begin{cases} \rho^{-d_1(r)}, & 0 \le r \le \frac{q}{\ell} \\ \rho^{-d_2(r)}, & \frac{q}{\ell} \le r \le \frac{2q}{\ell} \\ \rho^{-d_3(r)}, & \frac{2q}{\ell} \le r \le \frac{p}{\ell} \\ 1, & \frac{p}{\ell} < r. \end{cases}$$

where $d_1(r) = \min\{3(1-\frac{\ell}{p}r), 3-\frac{\ell^2}{pq}r, 3-\frac{\ell}{q}r\}$, $d_2(r) = \min\{3(1-\frac{\ell}{p}r), 2(1-\frac{\ell}{p}r)+\frac{q}{p}, 3-\frac{\ell}{q}r\}$, and $d_3(r) = \min\{3(1-\frac{\ell}{p}r), 2(1-\frac{\ell}{p}r)+\frac{q}{p}, 1+\frac{2q}{p}-\frac{\ell}{p}r\}$. We focus on each of the above regions for r to calculate the diversity gain.

Assume $0 \le r \le \frac{q}{\ell}$. Clearly, $3-\frac{\ell^2}{pq}r < 3-\frac{\ell}{q}r$. Moreover, if $\kappa \ge 2$, then $3-\frac{\ell^2}{pq}r \le 3(1-\frac{\ell}{p}r)$. Hence,

$$d^*(r) = 3 - \frac{\ell^2}{pq}r, \quad 0 \le r \le \frac{q}{\ell}, \quad \kappa \ge 2. \tag{3.98}$$

Now consider $\frac{q}{\ell} \le r \le \frac{2q}{\ell}$. One can see that $3(1-\frac{\ell}{p}) \lesseqgtr 3-\frac{\ell}{q}r \iff \kappa \lesseqgtr 3$. On the other hand, if $3(1-\frac{\ell}{p}r) < 2(1-\frac{\ell}{p}r)+\frac{q}{p}$, then $1-\frac{\ell}{p}r < \frac{n}{p}$ which results in $r > \frac{p-q}{\ell}$. It is clear that if $\kappa \ge 2 \Rightarrow \frac{p-q}{\ell} \ge \frac{q}{\ell}$. Therefor, for $2 \le \kappa \le 3$,

$$d^*(r) = \begin{cases} 2(1-\frac{\ell}{p}r)+\frac{q}{p}, & \frac{q}{\ell} < r \le \frac{p-q}{\ell} \\ 3(1-\frac{\ell}{p}r), & \frac{p-q}{\ell} < r \le \frac{2q}{\ell}. \end{cases} \tag{3.99}$$

For $\kappa \ge 3$, one can check that $3-\frac{\ell}{q}r \le 3\left(1-\frac{\ell}{p}r\right)$. Furthermore, if $3-\frac{\ell}{q}r < 2\left(1-\frac{\ell}{p}r\right)+\frac{q}{p}$, then $1-\frac{q}{p} < \frac{(p-2q)\ell}{pq}r$ which results in $r > \frac{(p-q)q}{(p-2q)\ell}$. One can see that $\frac{(p-q)q}{(p-2q)\ell} \ge \frac{q}{\ell}$. Thus for $\kappa \ge 3$

$$d^*(r) = \begin{cases} 2(1-\frac{\ell}{p}r)+\frac{q}{p}, & \frac{q}{\ell} < r \le \frac{(p-q)q}{(p-2q)\ell} \\ 3-\frac{\ell}{q}r, & \frac{(p-q)q}{(p-2q)\ell} < r \le \frac{2q}{\ell}. \end{cases} \tag{3.100}$$

Now consider $\frac{2q}{p} < r \le \frac{p}{\ell}$. In this region $d(r) = \min\{3(1-\frac{\ell}{p}r), 2(1-\frac{\ell}{p}r)+\frac{q}{p}, 1+\frac{2q}{p}-\frac{\ell}{p}r\}$. One can check that if $3\left(1-\frac{\ell}{p}r\right) < 2\left(1-\frac{\ell}{p}r\right)+\frac{q}{p}$, then $r > \frac{p-q}{\ell}$. Moreover,

$$\text{if} \quad 3\left(1-\frac{\ell}{p}r\right) < 1-\frac{\ell}{p}r+\frac{2q}{p} \Rightarrow r > \frac{p-q}{\ell}.$$

One can check that $\frac{p-q}{\ell} \le \frac{2q}{p}$ if and only if $\kappa \le 3$. Considering the fact that the cooperation is avoided whenever it is beneficial to do so, for $2 \le \kappa \le 3$ we have

$$d^*(r) = \begin{cases} 3(1-\frac{\ell}{p}r), & \frac{2q}{p} < r \le \frac{2p}{3\ell-p} \\ 1-r, & \frac{2p}{3\ell-p} \le r \le 1. \end{cases} \tag{3.101}$$

For $\kappa \geq 3$ and for $\frac{2q}{\ell} < r \leq \frac{p-q}{\ell}$, $3\left(1-\frac{\ell}{p}r\right) > 2\left(1-\frac{\ell}{p}r\right)+\frac{q}{p}$, and $3\left(1-\frac{\ell}{p}r\right) > 1+\frac{2q}{p}-\frac{\ell}{p}r$. In this region

$$\text{if} \quad 2\left(1-\frac{\ell}{p}r\right)+\frac{q}{p} \leq 1+\frac{2q}{p}-\frac{\ell}{p}r \;\Rightarrow\; r \geq \frac{p-q}{\ell}.$$

Considering the fact that the cooperation is avoided whenever it is beneficial, for $\kappa \geq 3$ we have

$$d^*(r) = \begin{cases} 1+\frac{2q}{p}-\frac{\ell}{p}r, & \frac{2q}{\ell} \leq r \leq \frac{p-q}{\ell} \\ 3(1-\frac{\ell}{p}r), & \frac{p-q}{\ell} \leq r \leq \frac{2p}{3\ell-p} \\ 1-r, & \frac{2p}{3\ell-p} \leq r \leq 1. \end{cases} \tag{3.102}$$

By summarizing the above results, the proof of the first part is concluded. For the proof of the second part, it is seen that $\kappa = 2$ provides the best diversity gain for

$$r \leq \frac{q}{\ell} = \frac{q}{p+q} = \frac{1}{3}.$$

The corresponding diversity gain in this region is given by

$$d^*(r) = 3\Big(1-\frac{\ell}{p}r\Big) = 3\Big(1-\frac{3}{2}r\Big), \; 0 \leq r \leq \frac{1}{3}. \tag{3.103}$$

For other values of r the maximum diversity gain is achieved when $r = \frac{p-q}{\ell}$. In this case,

$$r = \frac{p-q}{\ell} = \frac{\kappa-1}{1+\kappa}.$$

Thus,

$$\kappa = \frac{1+r}{1-r}.$$

For $\frac{1}{3} \leq r \leq \frac{1}{2}$, we obtain

$$d^*(r) = 2\left(1-\frac{\ell}{p}r\right)+\frac{q}{p} = \frac{3(1-r)}{1+r}.$$

For $\frac{1}{2} \leq r \leq 1$, we obtain

$$d^*(r) = 1-\frac{\ell}{p}r+\frac{2n}{p} = \frac{3(1-r)}{1+r}.$$

By combining the results,we have

$$d^*(r) = \begin{cases} 3\left(1-\frac{3}{2}r\right), & 0 \leq r \leq \frac{1}{3} \\ \frac{3(1-r)}{1+r}, & \frac{1}{3} \leq r \leq 1. \end{cases} \tag{3.104}$$

The corresponding κ is given by

$$\kappa = \begin{cases} 2, & 0 \leq r \leq \frac{1}{3} \\ \frac{1+r}{1-r}, & \frac{1}{3} \leq r \leq 1. \end{cases} \tag{3.105}$$

This concludes the proof. □

3.7.5 Proof of Theorem 3.5

It is known that if $\kappa \leq M$

$$d_{E_M}(r) = 1 + M - \frac{\ell}{q}r, \quad 0 \leq r \leq \frac{p}{\ell},$$

else if $\kappa \geq M$

$$d_{E_M}(r) = \begin{cases} 1 + M - \frac{\ell}{q}r, & 0 \leq r \leq \frac{Mq}{\ell} \\ 1 + \frac{Mq}{p} - \frac{\ell}{p}r, & \frac{Mq}{\ell} \leq r \leq \frac{p}{\ell}. \end{cases}$$

In addition,

$$Pr(E_M) = \begin{cases} 1, & 0 \leq r \leq \frac{p}{\ell} \\ 0, & \frac{p}{\ell} < r \leq 1. \end{cases}$$

Let $b_m(r),\ m = 0, \ldots, M$, be the negative exponent of ρ in $Pr(E_m)\rho^{-d_{E_m}}$ when $\rho \to \infty$. The resulted DMT can be expressed as

$$d_M^*(r) = \min\left\{\left(1 - \frac{\ell}{p}r\right) + d_{M-1}^*(r), b_M(r)\right\},$$

which is simplified as follows.

If $\kappa \leq M$

$$d_M^*(r) = \min\left\{\left(1 - \frac{\ell}{p}r\right) + d_{M-1}^*(r), 1 + M - \frac{\ell}{q}r\right\},\ 0 \leq r \leq \frac{p}{\ell},$$

else, for $\kappa \geq M$,

$$d_M^*(r) = \begin{cases} \min\left\{(1 - \frac{\ell}{p}r) + d_{M-1}^*(r), 1 + M - \frac{\ell}{q}r\right\}, & 0 \leq r \leq \frac{Mq}{\ell} \\ \min\left\{(1 - \frac{\ell}{p}r) + d_{M-1}^*(r), 1 + \frac{Mq}{p} - \frac{\ell}{p}r\right\}, & \frac{Mq}{\ell} \leq r \leq \frac{p}{\ell}. \end{cases}$$

One can check

$$\begin{aligned} \text{If } \ 1 + M - \frac{\ell}{q}r \leq b_0(r) \Rightarrow \ & 1 + M - \frac{\ell}{q}r \leq (M+1)\Big(1 - \frac{\ell}{p}r\Big) \\ \Rightarrow \ & \kappa \geq M + 1. \end{aligned}$$

In addition,

$$\begin{aligned} \text{If } \ 1 + \frac{Mq}{p} - \frac{\ell}{p}r \leq (M+1)\Big(1 - \frac{\ell}{p}r\Big) \\ \Rightarrow r \leq \frac{p-q}{\ell} \end{aligned}$$

Clearly, for $\kappa \leq M+1$, $\frac{p-q}{\ell} \leq \frac{Mq}{\ell}$.Hence, for $1 \leq \kappa \leq M+1$

$$d_M^*(r) = \left(1 - \frac{\ell}{p}r\right) + d_{M-1}^*(r), \quad 0 \leq r \leq \frac{p}{\ell}. \tag{3.106}$$

For $\kappa \geq M+1$, when $0 \leq r \leq \frac{(M-1)q}{\ell}$ we have

$$\begin{aligned} b_{M-1}(r) &= \Big(1 - \frac{\ell}{p}r\Big) + M - \frac{\ell}{q}r \\ &\leq 1 + M - \frac{\ell}{q}r = b_M(r). \end{aligned}$$

Hence, for $\kappa \geq M+1$,

$$d_M^*(r) = \Big(1 - \frac{\ell}{p}r\Big) + d_{M-1}^*(r), \quad 0 \leq r \leq \frac{(M-1)q}{\ell}.$$

For $\frac{(M-1)q}{\ell} \leq r \leq \frac{Mq}{\ell}$, we have

$$\begin{aligned} b_0(r) &= (M+1)\Big(1 - \frac{\ell}{p}r\Big), \\ b_1(r) &= M\Big(1 - \frac{\ell}{p}r\Big) + \frac{q}{\ell}, \\ b_2(r) &= (M-1)\Big(1 - \frac{\ell}{p}r\Big) + \frac{2q}{\ell}, \\ &\vdots \\ b_{M-1}(r) &= 2\Big(1 - \frac{\ell}{p}r\Big) + \frac{(M-1)q}{\ell}, \\ b_M(r) &= 1 + M - \frac{\ell}{q}r. \end{aligned}$$

It can easily see that if $r \leq \frac{p-q}{\ell}$, then $b_{M-1}(r) \leq b_{M-2}(r) \leq \ldots \leq b_0(r)$ and vice versa. On the other hand, for $\kappa \geq M+1$, $\frac{p-q}{\ell} \geq \frac{Mq}{\ell}$. Hence, to determine the diversity gain when $\frac{(M-1)q}{\ell} \leq r \leq \frac{Mq}{\ell}$, only $b_M(r)$ and $b_{M-1}(r)$ need to be compared.

$$\begin{aligned} &\text{If} \quad b_{M-1}(r) \leq b_M(r) \\ &\Rightarrow \quad 2\Big(1 - \frac{\ell}{p}r\Big) + \frac{(M-1)q}{\ell} \leq 1 + M - \frac{\ell}{q}r \\ &\Rightarrow \quad r \leq \frac{(M-1)p^2q}{\ell^2(p-2q)} \end{aligned} \tag{3.107}$$

Assuming $\eta_1 = \frac{(M-1)p^2q}{\ell^2(p-2q)}$, for $\kappa \geq M+1$, $\frac{(M-1)q}{\ell} \leq \eta_1 \leq \frac{Mq}{\ell}$. Hence,

$$\begin{aligned} &d_M^*(r) = \\ &\begin{cases} 2(1 - \frac{\ell}{p}r) + \frac{(M-1)q}{p}, & \frac{(M-1)q}{\ell} \leq r \leq \eta_1 \\ 1 + M - \frac{\ell}{q}r, & \eta_1 \leq r \leq \frac{Mq}{\ell}. \end{cases} \end{aligned} \tag{3.108}$$

For $\frac{Mq}{\ell} \leq r \leq \frac{p}{\ell}$, we have

$$d_M^*(r) = \begin{cases} 1 + \frac{Mq}{\ell} - \frac{\ell}{p}r, & \frac{Mq}{\ell} \leq r \leq \frac{p-q}{\ell} \\ (M+1)(1 - \frac{\ell}{p}r), & \frac{p-q}{\ell} \leq r \leq \frac{p}{\ell}. \end{cases} \tag{3.109}$$

For $\frac{p}{\ell} \leq r \leq 1$, $d_M^*(r) = 0$. The resulted DMT in each region is compared to $(1-r)$ to determine wether or not avoiding the cooperation. Proof of the second part of the Theorem is similar to the proof of the second part of Proposition 3.4. □

3.7.6 Proof of Theorem 3.6

The goal is to find $d^*(r)$ which is characterized by the following optimization problem.

$$d^*(r) = \inf_{(p-q)\alpha_0 + q\min\{2\alpha_0-1,\beta\} > p-\ell r} \alpha_0 + M\beta.$$

If $\min\{2\alpha_0 - 1, \beta\} = 2\alpha_0 - 1$, then $\beta \geq \max\{0, 2\alpha_0 - 1\}$ and we get

$$\begin{aligned} d^*(r) &= \inf_{\alpha_0 \geq 1-r} \alpha_0 + M\max\{0, 2\alpha_0 - 1\} \\ &= \begin{cases} 1-r & 0 \leq \alpha_0 \leq \frac{1}{2} \\ (1-r) + M(1-2r) & \frac{1}{2} \leq \alpha_0 \leq 1. \end{cases} \\ &= \begin{cases} (1-r) + M(1-2r) & 0 \leq r \leq \frac{1}{2} \\ 1-r & \frac{1}{2} \leq r \leq 1. \end{cases} \end{aligned}$$

If $\min\{2\alpha_0 - 1, \beta\} = \beta$, then $1 \geq \alpha_0 \geq \frac{1+\beta}{2}$ and we get

$$d^*(r) = \inf_{(p-q)\alpha_0 + q\beta > p-\ell r} \alpha_0 + M\beta$$

If $r \geq p/\ell$, then $p - \ell r \leq 0$. In this case, $\alpha_0 = 1/2, \beta = 0$ is the optimal solution. One can check that $\alpha_0 = 1/2, \beta = 0$ is also the optimal solution for $1/2 \leq r \leq p/\ell$. Hence,

$$d^*(r) = \frac{1}{2}, \quad \frac{1}{2} \leq r \leq 1.$$

For $0 \leq r \leq 1/2$, if $p = q$, we obtain

$$\begin{aligned} d^*(r) &= \inf_{\beta \geq \max\{0, 1-2r\}} \frac{1+\beta}{2} + M\beta \\ &= (1-r) + M(1-2r) \qquad\qquad 0 \leq r \leq \frac{1}{2}. \end{aligned}$$

For $0 \leq r \leq 1/2$ and $p \neq q$, the cross point of the two linear conditions, $\alpha_0 = 1-r, \beta = 1-2r$, is a feasible solution. The objective value for this solution is

$$d(r) = (1-r) + M(1-2r), \quad 0 \leq r \leq \frac{1}{2}.$$

One can check that $\alpha_0' = 1 - r + \delta$ and $\beta' = 1 - 2r - \frac{p-q}{q}\delta$, for a positive value of δ, is also a feasible solution if

$$\begin{aligned}\delta &\leq \min\left\{r, \frac{q}{p-q}(1-2r)\right\} \\ &= \begin{cases} r, & 0 \leq r \leq \frac{q}{\ell} \\ \frac{q}{p-q}(1-2r), & \frac{q}{\ell} \leq r \leq \frac{1}{2}. \end{cases}\end{aligned}$$

The above condition comes from the fact that $\alpha_0' \leq 1$ and $\beta' \geq 0$. The objective value for the new feasible solution is

$$d(r) = (1-r) + M(1-2r) + \delta\Big(1 - \frac{M(p-q)}{q}\Big), \quad 0 \leq r \leq \frac{1}{2}$$

It is seen that for $\kappa \leq \frac{M+1}{M}$, the term $\big(1 - \frac{M(p-q)}{q}\big)$ is positive and it increases the objective value for any positive value of δ. Hence, $\alpha_0 = 1 - r, \beta = 1 - 2r$ is in fact the optimum solution for $1 < \kappa \leq \frac{M+1}{M}$ and we get

$$d^*(r) = \begin{cases} (1-r) + M(1-2r), & 0 \leq r \leq \frac{1}{2} \\ \frac{1}{2}, & \frac{1}{2} \leq r \leq 1. \end{cases}$$

For $\kappa \geq \frac{M+1}{M}$, the term $\big(1 - \frac{M(p-q)}{q}\big)$ is negative and it decreases the objective value for any positive value of δ. The optimal solution which is achieved for the maximum value of δ in each region is given by

$$d^*(r) = \begin{cases} 1 - \frac{M(p-q)}{q}r + M(1-2r), & 0 \leq r \leq \frac{q}{\ell} \\ (1-r) + \frac{q}{p-q}(1-2r), & \frac{q}{\ell} \leq r \leq \frac{1}{2} \\ \frac{1}{2}, & \frac{1}{2} \leq r \leq 1. \end{cases}$$

By comparing the results for different values of κ, it is seen that the best DMT is obtained when $1 \leq \kappa \leq \frac{M+1}{M}$ and is given by

$$d^*(r) = (1-r) + M(1-2r)^+, \quad 0 \leq r \leq 1.$$

This concludes the proof. □

Chapter 4

Asynchronous Interference Channels

4.1 Introduction

A constant K-user interference channel wherein users are not symbol synchronous is considered and the effect of the asynchronism existing among the users on the total DOF of this channel is investigated. It is shown that the asynchronism does not affect the total DOF of the system; however, it facilitates aligning interfering signals at each receiver node. As an achieving scheme for the total DOF equal to $K/2$, a novel interference alignment algorithm is proposed for this channel by taking advantage of asynchronous delays which inherently exist among the received signals at each receiver node. The asynchronism causes inter-symbol-interference (ISI) among transmitted symbols by different transmitters. In this case, the underlying quasi-static links are converted to ISI and accordingly into time varying channels solving the lack of channel variation required for the interference alignment in quasi-static scenarios. For simplicity and ease of understanding, we present the scheme first for the three-user interference channel with single antenna nodes. The results are then extended to a general single antenna nodes' interference channel with arbitrary number of users. Later, it is argued that the same scheme can be used in a K-user asynchronous interference channel with terminals each equipped with M antennas to achieve the total $MK/2$ DOF of the medium provided that each pair of transmitters-receivers experiences the same asynchronous delay for all the corresponding antennas. In contrast to previously proposed alignment schemes, the channel state information of the links does not need to be known at the transmitter nodes. Instead, the relative delays among the received signals at each receiver node are globally known to the entire network.

4.1.1 System Description

We consider a K-user interference channel consisting of K pairs of transmitters and receivers. Each node is equipped with a single antenna. We assume that the fading coefficients are constant non-zero random variables drawn from a probability distribution. The channel coefficient between the j-th transmitter and the i-th receiver is denoted by $h_{i,j}$, $i, j \in \{1, \ldots, K\}$. The transmitters, using a shared medium, send their individual messages to the corresponding receivers. Due to the broadcast nature of the wireless channel, the desired signal at each receiver is interfered by other transmitted signals.

Let $R_i(\rho),\ i = 1, 2, \ldots, K$, be the transmission rate of the i-th user at SNR, ρ, and $\mathcal{C}(\rho)$ be the capacity region of this channel, i.e., the set of all achievable rates, $\mathcal{R}(\rho) = \big(R_1(\rho), R_2(\rho), \ldots, R_K(\rho)\big)$, at this SNR. The region of degrees of freedom, $\mathcal{D}$, for this channel is defined as the set of all K-tuples $(d_1, d_2, \ldots, d_K) \in \mathbb{R}^+$ such that $\forall(\alpha_1, \alpha_2, \ldots, \alpha_K) \in \mathbb{R}_+^K$,

$$\sum_{i=1}^{K} \alpha_i d_i \leq \limsup_{\rho \to \infty} \left[\sup_{\mathcal{R}(\rho) \in \mathcal{C}(\rho)} \frac{1}{\log \rho} \sum_{i=1}^{K} \alpha_i R_i(\rho) \right], \tag{4.1}$$

where $\mathbb{R}_+^K$ is the set of vectors of size K with positive real entries [52]. For example, in a three-user fully synchronous interference channel with varying fading coefficients, this region is given in a closed form as [52]

$$\mathcal{D} = \{(d_1, d_2, d_3) :\ d_i + d_j \leq 1,\ \forall\, i, j \in \{1, 2, 3\}\}. \tag{4.2}$$

Since the nodes are located at different places and due to the effect of multi path and propagation delay, the received signals at each receiver node are not synchronous. We assume that the signals are frame synchronous; however, they are not symbol synchronous, i.e., the beginning and the end of each frame align up to a delay of length less than a symbol interval, T_s. To be more accurate, let $\tau_{i,j}$ denote the propagation delay of the received signal from the j-th transmitter to the i-th receiver. It is a continuous time random variable which depends on the propagation medium. We assume that $\tau_{i,j}$'s are constant during transmission of a frame. Since the nodes are frame synchronous and not symbol synchronous, one has $0 \leq \tau_{i,j} < T_s,\ \forall\, i, j \in \{1, 2, \ldots, K\}$. Let

$$\tau_{m,j}^{[i]} \triangleq \tau_{i,m} - \tau_{i,j}, \quad \forall\, i, j, m \in \{1, 2, \ldots, K\}, \tag{4.3}$$

be the relative delay between the transmitted signals from the m-th and the j-th transmitters measured at the i-th receiver node. Since the asynchronous delays are continuous independent random variables over a symbol interval, $\tau_{m,j}^{[i]}$'s are distinct $\forall\, i, j, m \in \{1, 2, \ldots, K\}$, $(m \neq j)$, with probability one and $-T_s < \tau_{m,j}^{[i]} < T_s$.

Each transmitter uses a unit energy shaping waveform $\psi_j(t)$, $j \in \{1, \ldots, K\}$, to linearly modulate its information symbols in a PAM like signal. The transmitted signal of the j-th transmitter is given by

$$x_j(t) = \sum_k x_j(k)\psi_j(t - kT_s), \tag{4.4}$$

where $x_j(k)$ is the transmitted symbol by the j-th transmitter at the k-th symbol interval. These signals are received asynchronously at the receiver nodes. The received signal at the i-th receiver is modeled as follows [1].

$$y_i(t) = \sum_{j=1}^{K} h_{i,j}x_j(t - \tau_{i,j}) + z_i(t),\ i \in \{1, \ldots, K\}, \tag{4.5}$$

where $z_i(t)$ is the noise signal at the i-th receiver node.

4.1.2 Main Results

Theorem 4.1. *The total number of degrees of freedom of the underlying constant K-user symbol-asynchronous interference channel with single antenna nodes is $K/2$ with probability one.*

We consider a constant K-user asynchronous interference channel and argue that the total DOF of this channel is the same as that of the corresponding synchronous channel. For this purpose, we will first show that the total DOF of this channel is upper bounded by $K/2$. Then, we propose a novel interference alignment scheme which deploys the asynchronous delays among the users to achieve the total $K/2$ DOF of the channel. Our scheme is similar to the vector alignment scheme invented in [52] for varying fading channels; however, it is proposed for the constant interference channels. For simplicity and ease of understanding, the proposed scheme is first presented for the three-user single antenna nodes interference channel. The results are then generalized to the K-user asynchronous interference channel. As a corollary, it is argued that the DOF region of the constant three-user asynchronous interference channel is the same as that of the corresponding synchronous channel with varying fading coefficients. When all terminals are equipped with M antenna nodes, we will argue that the same interference alignment scheme proposed for the single antenna nodes' K-user interference channel is sufficient to achieve the total $MK/2$ DOF of the medium provided that each pair of transmitters-receivers experiences the same asynchronous delay for all the corresponding antennas. This results in performing the alignment task in a smaller number of symbol extensions.

4.1.3 Proof of Converse

Assume all the transmitters use $\psi(t)$ (e.g., the "sinc" function, $\texttt{sinc}(x) = \frac{\sin \pi x}{\pi x}$) with bandwidth $W = \frac{1}{2T_s}$ as the shaping waveform. Since the transmitted signals are independent, the frequency bandwidth of the received signal at each receiver node is also W. By taking the Fourier Transform of both sides of equation (4.5), we obtain

$$\begin{aligned} Y_i(f) &= \int_{-\infty}^{\infty} \left(\sum_{j=1}^{K} h_{i,j} x_j(t - \tau_{i,j}) + z_i(t) \right) e^{-\xi 2\pi f t} dt \\ &= \sum_{j=1}^{K} h_{i,j} e^{-\xi 2\pi f \tau_{i,j}} \int_{-\infty}^{\infty} \sum_{k} x_j(k) \psi(t - kT_s) e^{-\xi 2\pi f t} dt + Z_i(f) \\ &= \sum_{j=1}^{K} h_{i,j} \Psi(f) e^{-\xi 2\pi f \tau_{i,j}} \sum_{k} x_j(k) e^{-\xi 2\pi f k T_s} + Z_i(f) \\ &= \sum_{j=1}^{K} h_{i,j} \Psi(f) e^{-\xi 2\pi f \tau_{i,j}} X_j(f) + Z_i(f) \\ &= \sum_{j=1}^{K} h'_{i,j}(f) X_j(f) + Z_i(f), \end{aligned} \tag{4.6}$$

where $Z_i(f)$ is the FT of $z_i(t)$, $h'_{i,j}(f) = h_{i,j}\Psi(f)e^{-\xi 2\pi f \tau_{i,j}}$, $\xi = \sqrt{-1}$, and $X_j(f)$ is the 2π-periodic Discrete-Time-Fourier-Transform (DTFT) of the transmitted sequence by the j-th transmitter given by

$$\begin{aligned} X_j(f) &= \sum_{k} x_j(k) e^{-\xi 2\pi f T_s k} \\ &= \sum_{k} x_j(k) e^{-\xi \omega k} \triangleq X_j(\omega), \end{aligned} \tag{4.7}$$

and $\omega = 2\pi f T_s$. Equation (4.6), represents the mathematical model of a synchronous K-user interference channel with varying fading coefficients in the frequency domain. Since $\psi(t)$ has bandwidth W, $\Psi(f) = 0$, $\forall |f| > W$. Hence, there are W complex frequency degrees of freedom per second in the underlying system. For each of them, equation (4.6) models a constant synchronous interference channel. According to [56], the total number of spatial DOF of this channel per frequency DOF is upper bounded by $K/2$. This concludes the proof of the converse. □

4.2 System Model and Signaling Scheme

We assume that all shaping waveforms are the same, i.e., $\psi_j(t) = \psi(t)$, $\forall j$. Theoretically, $\psi(t)$ is a well-designed waveform with a strictly limited bandwidth W resulting in infinite time support

(e.g., the sinc function). In practice, however, using shaping waveforms with infinite time support is not feasible. Hence, either a truncated version of common waveforms or a new designed waveform with finite time support, say equal to uT_s, is used. We consider both scenarios and present a unified channel model for both cases.

4.2.1 When $\psi(t)$ is a Time-Limited Waveform

Assume that $\psi(t)$ has a time support equal to uT_s, i.e., $\psi(t) = 0, \forall\, t \notin [0, uT_s]$. In our proposed signaling scheme, at the j-th transmitter, a codeword of length N, $\underline{x}_j = [x_j(0), x_j(1), \ldots, x_j(N-1)]^T$ is supported by cyclic prefix and cyclic suffix symbols (CPS) each of length $u+1$ such that the first and the last $u+1$ symbols of $\underline{x}_j$ are respectively repeated at the end and at the beginning of this vector. The resulting vector $\underline{x}_j^{cps} = [x_j(N-u-1), x_j(N-u), \ldots, x_j(N-1), x_j(0), x_j(1), \ldots, x_j(N-1), x_j(0), x_j(1), \ldots, x_j(u)]^T$ of length $\ell = N + 2(u+1)$ is transmitted over the channel. The received signal model at the i-th receiver node is given by

$$y_i(t) = \sum_{j=1}^{K} h_{i,j} \sum_{k=0}^{\ell-1} x_j^{cps}(k)\psi(t - kT_s - \tau_{i,j}) + z_i(t), \tag{4.8}$$

where $x_j^{cps}(k)$ is the k-th entry of $\underline{x}_j^{cps}$. This signal is passed through a filter matched to the desired link. The output of the matched filter sampled at $t = (k+1)T_s + \tau_{i,i},\ k = 0, \ldots, \ell-1$, is given by

$$\begin{aligned} y_i(k) &= \int_{kT_s+\tau_{i,i}}^{(k+u)T_s+\tau_{i,i}} y_i(t)\psi^*(t - kT_s - \tau_{i,i})dt \\ &= \sum_{j=1}^{K} h_{i,j} \sum_{q=-u}^{u} \gamma_{i,j}(q) x_j^{cps}(k+q) + z_i(k), \end{aligned} \tag{4.9}$$

where $x_j^{cps}(q) = 0,\ \forall q < 0$,

$$\begin{aligned} \gamma_{i,j}(q) &= \int_0^{uT_s} \psi(t - qT_s + \tau_{i,j}^{[i]})\psi^*(t)dt, \\ z_i(k) &= \int_{kT_s+\tau_{i,i}}^{(k+u)T_s+\tau_{i,i}} z_i(t)\psi^*(t - kT_s - \tau_{i,i})dt, \end{aligned} \tag{4.10}$$

and $\tau_{i,j}^{[i]} = \tau_{i,i} - \tau_{i,j}$ is the relative delay between transmitted signals by the i-th and the j-th transmitter nodes measured at the i-the receiver node.

We assume that the shaping waveform has a length equal to $u \geq 1$ symbol intervals. Hence, each transmitted symbol of a stream is interfered by $(u-1)$ previous and $(u-1)$ future symbols (if not zero) of the same stream. It is also interfered by $2u-1$ symbols (if not zero) of each of the

other transmitted streams. If the interfering stream is ahead of the desired stream, $u-1$ previous and u future symbols of that stream interfere with the current symbol of the desired stream. However, if the interfering stream is behind the desired stream, u previous and $u-1$ future symbols of that interfere with the current symbol of the desired stream. These can be verified by checking that $\gamma_{i,i}(u) = \gamma_{i,i}(-u) = 0$ and for $i \neq j$, $\gamma_{i,j}(u) = 0$ if $\tau_{i,j}^{[i]} < 0$, and $\gamma_{i,j}(-u) = 0$ if $\tau_{i,j}^{[i]} > 0$.

By discarding CPS symbols at the output of the matched filter, we obtain

$$\underline{y}_i = \sum_{j=1}^{K} h_{i,j} \mathbf{\Gamma}_{i,j} \underline{x}_j + \underline{z}_i, \tag{4.11}$$

where

$$\begin{aligned}
\underline{x}_j &= [x_j(0), x_j(1), \ldots, x_j(N-1)]^T, \\
\underline{y}_i &= [y_i(u+1), y_i(u+2), \ldots, y_i(u+N)]^T, \\
\underline{z}_i &= [z_i(u+1), z_i(u+2), \ldots, z_i(u+N)]^T,
\end{aligned}$$

and $\mathbf{\Gamma}_{i,j}$ is the circulant convolution matrix of the generator sequence $\hat{\underline{\gamma}}_{i,j} = [\gamma_{i,j}(0), \gamma_{i,j}(1), \ldots, \gamma_{i,j}(u), 0, \ldots, 0, \gamma_{i,j}(-u), \ldots, \gamma_{i,j}(-1)]^T$ of length N. In the general form, $\mathbf{\Gamma}_{i,j}$ is given in equation (4.12) for all i, j. However, depending on the values of the relative asynchronous delays, $\gamma_{i,j}(-u)$ or $\gamma_{i,j}(u)$ might be zero. Clearly, N should be large enough such that $N \geq 2u$.

$$\mathbf{\Gamma}_{i,j} = \tag{4.12}$$

$$\begin{bmatrix}
\gamma_{i,j}(0) & \cdots & \gamma_{i,j}(-u) & 0 & 0 & \ldots & 0 & \gamma_{i,j}(u) & \gamma_{i,j}(u-1) & \ldots & \gamma_{i,j}(1) \\
\gamma_{i,j}(1) & \cdots & \gamma_{i,j}(-u+1) & \gamma_{i,j}(-u) & 0 & \ldots & 0 & 0 & \gamma_{i,j}(u) & \ldots & \gamma_{i,j}(2) \\
\ddots & \ddots & \ddots & \ddots & \ddots & \ddots & \ddots & \ddots & \ddots & \ddots & \ddots \\
0 & \cdots & 0 & \cdots & 0 & \gamma_{i,j}(u) & \cdots & \gamma_{i,j}(1) & \gamma_{i,j}(0) & \gamma_{i,j}(-1) \cdots & \gamma_{i,j}(-u) \\
\ddots & \ddots & \ddots & \ddots & \ddots & \ddots & \ddots & \ddots & \ddots & \ddots & \ddots \\
\gamma_{i,j}(-1) & \cdots & \gamma_{i,j}(-u) & 0 & \cdots & \cdots & 0 & \gamma_{i,j}(u) & \cdots & \gamma_{i,j}(1) & \gamma_{i,j}(0)
\end{bmatrix}.$$

$\underline{z}_i$ is the colored noise vector at the i-th receiver with the covariance matrix given by

$$\mathbf{\Phi}_i = \sigma_i^2 \tilde{\mathbf{\Gamma}}_0 \tag{4.13}$$

where σ_i^2 is the variance of the additive white Gaussian noise at the i-th receiver and $\tilde{\mathbf{\Gamma}}_0$ is given

in (4.14).

$$\tilde{\mathbf{\Gamma}}_0 = \begin{bmatrix} \gamma_{i,i}(0) & \gamma_{i,i}(-1)\cdots & \gamma_{i,i}(-u+1) & 0 & 0 & \dots & 0 & \dots & 0 \\ \gamma_{i,i}(1) & \cdots & \gamma_{i,i}(-u+2) & \gamma_{i,i}(-u+1) & 0 & \dots & 0 & \dots & 0 \\ \ddots & \ddots & \ddots & \ddots & \ddots & \ddots & \ddots & \ddots & \ddots \\ 0 & \dots & 0 & 0 & \gamma_{i,i}(u-1) & \cdots & \gamma_{i,i}(0) & \cdots & \gamma_{i,i}(-u+1) \\ \ddots & \ddots & \ddots & \ddots & \ddots & \ddots & \ddots & \ddots & \ddots \\ 0 & 0 & \cdots & 0 & \cdots & 0 & \gamma_{i,i}(u-1) & \cdots & \gamma_{i,i}(0) \end{bmatrix}. \tag{4.14}$$

$\tilde{\mathbf{\Gamma}}_0$ is a Hermitian banded Toeplitz matrix of order u. This matrix is shown to be asymptotically equivalent to $\mathbf{\Gamma}_{i,i}$ given in (4.12) [72]. Since these matrices are Hermitian, their eigenvalues are all non-negative real numbers. Using properties of asymptotically equivalent Hermitian matrices in [72], it can be shown that the eigenvalues of $\tilde{\mathbf{\Gamma}}_0$ are all bounded[1].

As can be seen from (4.11), due to the effect of the asynchronism among the users, the original quasi-static links with constant coefficients over a block as $h_{i,j}\mathbf{I}_N,\ i,j \in \{1,2,\dots,K\}$, are converted into frequency selective links with correlated coefficients over time and with gains given by $h_{i,j}\mathbf{\Gamma}_{i,j}$.

Remark 4.1. *In our signaling scheme, we use both the cyclic prefix and the cyclic suffix symbols to manage the asynchronism among the nodes, because both the previous and the future transmitted symbols of all the streams affect the current transmitted symbol of every single stream. Since, we are interested in having a circulant $\mathbf{\Gamma}_{i,j}$ matrices for all i,j, it is necessary to add both the cyclic prefix and the cyclic suffix symbols to every transmitted frame.*

Properties of $\mathbf{\Gamma}_{i,j}$ Matrices

Remark 4.2. *$\mathbf{\Gamma}_{i,j}$ is a circulant matrix. Hence, its eigenvalue decomposition is given by [72]*

$$\mathbf{\Gamma}_{i,j} = \mathbf{U}^{\dagger}\mathbf{\Lambda}_{i,j}\mathbf{U}, \tag{4.15}$$

where $\mathbf{U}$ is the DFT matrix of dimension N given as

$$\mathbf{U}(q,s) = \frac{1}{\sqrt{N}} e^{-\xi\frac{2\pi(q-1)(s-1)}{N}},\ q,s = 1,2,\dots,N, \tag{4.16}$$

[1]The correlated noise vector can be whitened by passing the received signal vector through a whitening filter. However, it is not necessary for our purpose, because the bounded eigenvalues of $\tilde{\mathbf{\Gamma}}_i$ do not affect the total number of degrees of freedom of the underlying channel.

and $\mathbf{\Lambda}_{i,j}$ *is a diagonal matrix containing the elements of the DFT of the generator sequence of* $\mathbf{\Gamma}_{i,j}$*. i.e.,* $\mathbf{\Lambda}_{i,j} = \texttt{diag}\{\lambda_{i,j}(0), \lambda_{i,j}(1), \ldots, \lambda_{i,j}(N-1)\}$*, where*

$$\lambda_{i,j}(k) = \sum_{q=0}^{N-1} \hat{\gamma}_{i,j}(q) e^{-\xi \frac{2\pi}{N} qk}, \quad k = 0. \ldots, N-1, \tag{4.17}$$

and $\hat{\gamma}_{i,j}(q)$ *is the* q*-th element of* $\underline{\hat{\gamma}}_{i,j}$*.*

Proposition 4.1. *For a well-designed shaping waveform with non-zero spectrum over its bandwidth,* $\mathbf{\Gamma}_{i,j}$ *is a full rank matrix* $\forall\, i, j \in \{1, 2, \ldots, K\}$*. In addition, its eigenvalues (the diagonal entries of* $\mathbf{\Lambda}_{i,j}$*) are bounded.*

Proof. Define $\gamma(\tau)$, the auto correlation function of the shaping waveform $\psi(t)$, as follows

$$\gamma(\tau) \triangleq \int_{-\infty}^{\infty} \psi(t-\tau)\psi^*(t)dt. \tag{4.18}$$

We assume that the shaping waveform has a low-pass frequency support W. If u is finite, $W \to \infty$. $\gamma(\tau)$ has the same frequency support as that of the shaping waveform because it is readily shown that $\Gamma(f) = |\Psi(-f)|^2$, where $\Gamma(f), \Psi(f)$ are the Fourier Transforms of $\gamma(\tau), \psi(t)$, respectively. Let W_0 be the frequency bandwidth of $\psi(t)$ when $u \to \infty$. W_0 is a finite value and in general $W_0 \leq W$. To take best advantage of the frequency degrees of freedom, the sampling frequency $f_s = \frac{1}{T_s}$ is chosen as the Nyquist sampling rate equal to $2W_0$. Let $\gamma^p(\tau) = \sum_{k=-\infty}^{\infty} \gamma(\tau + kT)$ be a periodic expansion of $\gamma(\tau)$ with period $T = NT_s$. Since the shaping waveform has a time support equal to uT_s, the auto correlation function has a time support smaller than or equal to $2uT_s$. We assume that $N \geq 2u$. $\underline{\hat{\gamma}}_{i,j} = [\gamma_{i,j}(0), \gamma_{i,j}(1), \ldots, \gamma_{i,j}(u), 0, \ldots, 0, \gamma_{i,j}(-u), \gamma_{i,j}(-u+1), \ldots, \gamma_{i,j}(-1)]$, which is the generator sequence of the matrix $\mathbf{\Gamma}_{i,j}$, represents the samples of $\gamma^p(\tau)$ over one period at $\tau = qT_s - \tau_{i,j}^{[i]},\ q = 0, \ldots, N-1$, and sampling frequency equal to $f_s = 2W_0$. Since for any value of u, $W \geq W_0$, the DFT coefficients of the samples of $\gamma^p(\tau)$ over one period does not have any deterministic zero if the shaping waveform has a non-zero spectrum over its bandwidth. These coefficients appear as the diagonal entries of $\mathbf{\Lambda}_{i,j}$. Hence $\mathbf{\Lambda}_{i,j}$ and equivalently $\mathbf{\Gamma}_{i,j}$ are full rank matrices. In addition, since the sequence $\underline{\hat{\gamma}}_{i,j}$ is absolutely summable, diagonal entries of $\mathbf{\Lambda}_{i,j}$ are bounded. This concludes the proof. □

By decomposing the circulant $\mathbf{\Gamma}_{i,j}$ matrices on the DFT basis, we get

$$\underline{y}'_i = \sum_{j=1}^{K} h_{i,j} \mathbf{\Lambda}_{i,j} \underline{x}'_j + \underline{z}'_i, \tag{4.19}$$

where $\underline{y}'_i, \underline{x}'_j, \underline{z}'_i$ are respectively the linear transformations of $\underline{y}_i, \underline{x}_j, \underline{z}_i$ by the DFT matrix, $\mathbf{U}$. According to Proposition 4.1, $\mathbf{\Lambda}_{i,j}$'s are diagonal matrices with non-zero bounded diagonal entries.

Hence, one can interpret equation (4.19) as the model of a received signal at the i-th receiver of a K-user synchronous interference channel with varying fading coefficients. Hence, the total number of DOF of this channel is upper bounded by $K/2$ [52]. Although in the proposed asynchronous signaling scheme, in a portion of the time equal to $\frac{2(u+1)}{N+2(u+1)}$ no useful information is conveyed from the source nodes to the destination nodes due to the existence of CPS symbols, this portion is negligible for large length codewords, i.e. when $N \gg 2(u+1)$, and does not affect the total DOF of the system.

Matrix $\mathbf{\Lambda}_{i,j}$ contains the samples of the DFT of $\hat{\gamma}_{i,j}$ or equivalently the samples of the DTFT of the sequence $\{\gamma_{i,j}(k), \forall k \in \mathbb{Z}\}$ given in (4.10) on its main diagonal. When $u \to \infty$ ($N \geq 2u$), $\gamma_{i,j}(k)$'s are the samples of a strictly limited bandwidth process of bandwidth $W = 1/2T_s$ (see the proof of Propoition 4.1). In this case, the shift theorem of the DTFT is held and we get

$$\mathbf{\Lambda}_{i,j} = \mathbf{\Lambda}_0 \mathbf{E}\big(\hat{\tau}_{i,j}^{[i]}\big), \tag{4.20}$$

where $\hat{\tau}_{i,j}^{[i]} = \frac{\tau_{i,j}^{[i]}}{T_s}$, $\mathbf{\Lambda}_0$ is defined similar to $\mathbf{\Lambda}_{i,j}$ when $\hat{\tau}_{i,j}^{[i]} = 0$, and

$$\mathbf{E}(\hat{\tau}_{i,j}^{[i]}) = \mathtt{diag}\left\{1, e^{-\xi\frac{2\pi}{N}\hat{\tau}_{i,j}^{[i]}}, \ldots, e^{-\xi\frac{2\pi(N-1)}{N}\hat{\tau}_{i,j}^{[i]}}\right\}. \tag{4.21}$$

Equation (4.20) holds when $u \to \infty$.

Lemma 4.1. *If the shaping waveform has a sub-linear decaying rate in time (i.e, $|\psi(t)| \leq a/|t/T_s|^{\eta}$, where a is a constant value and $\eta > 1$), for a finite value of u, the equality* (4.20) *is still held up to a bounded approximation error which goes to zero as u increases. i.e,*

$$\mathbf{\Lambda}_{i,j} = \mathbf{\Lambda}_0 \mathbf{E}\big(\hat{\tau}_{i,j}^{[i]}\big) + \epsilon, \tag{4.22}$$

where $|\epsilon| \to 0$ as $u \to \infty$.

Proof. Let $x(t)$ be a signal with a strictly limited bandwidth W. We assume that $x(t)$ is a decaying function of $|t/T_s|$ such that $|x(t)| \leq \frac{a}{|t/T_s|^{\eta}}$ for large enough values of t and $\eta > 0$. This translates into having the most part of the energy of $x(t)$ near the origin. Let $\{\hat{x}(k),\, k \in \mathbb{Z}\}$ be the sequence of samples of this signal at $t = kT_s$, where $T_s \leq \frac{1}{2W}$. Let $\{x(k),\, k \in \mathbb{Z}\}$ be the sequence of samples of $x(t)$ at $t = kT_s - \tau$, $0 < \tau < T_s$. According to the shift property of the DTFT, we get

$$X(\omega) = \hat{X}(\omega)e^{-\xi\omega\tau},$$

where $\hat{X}(\omega) = \sum_k \hat{x}(k)e^{-\xi\omega k}$ and $X(\omega) = \sum_k x(k)e^{-\xi\omega k}$ are the DTFT of the sequences $\{\hat{x}(k),\, k \in \mathbb{Z}\}$ and $\{x(k),\, k \in \mathbb{Z}\}$, respectively. Define $A_k \triangleq x(k)e^{-\xi\omega k}$, $B_k \triangleq \hat{x}(k)e^{-\xi\omega(k+\tau)}$, and $\epsilon =$

$\sum_{k=-\infty}^{-u-1}(B_k - A_k) + \sum_{k=u+1}^{\infty}(B_k - A_k)$. We get

$$\sum_{k=-u}^{u} A_k = \sum_{k=-u}^{u} B_k + \epsilon$$

$|\epsilon|$ is upper bounded as follows.

$$\begin{aligned}
|\epsilon| &= |\sum_{k=-\infty}^{-u-1}(B_k - A_k) + \sum_{k=u+1}^{\infty}(B_k - A_k)| \\
&\leq |\sum_{k=-\infty}^{-u-1}(B_k - A_k)| + |\sum_{k=u+1}^{\infty}(B_k - A_k)| \\
&\leq \sum_{k=-\infty}^{-u-1}(|B_k| + |A_k|) + \sum_{k=u+1}^{\infty}(|B_k| + |A_k|) \\
&\leq \sum_{k=u+1}^{\infty}\frac{2a}{k^{\eta}} + \frac{a}{(k-\hat{\tau})^{\eta}} + \frac{a}{(k+\hat{\tau})^{\eta}} \\
&\leq 4a\sum_{k=u}^{\infty}\frac{1}{k^{\eta}},
\end{aligned}$$

where $\hat{\tau} = \tau/T_s$. One can see that if $\eta > 1$, $|\epsilon|$ is bounded and it goes to zero when $u \to \infty$. Hence, for a sufficiently large value of u and $\eta > 1$, $|\epsilon|$ is negligible and we have

$$\sum_{k=-u}^{u} x(k)e^{-\xi\omega k} = \Big(\sum_{k=-u}^{u}\hat{x}(k)e^{-\xi\omega k}\Big)e^{-\xi\omega\tau}.$$

This concludes the proof. □

In the sequel, whenever a time-limited shaping waveform is used, we assume that it satisfies equation (4.22) with a bounded approximation error and u is large enough such that ϵ is negligible. In this case, the received signal model at the i-th receiver node is simplified to

$$\underline{y}'_i = \mathbf{\Lambda}_0 \sum_{j=1}^{K} h_{i,j}\mathbf{E}\big(\hat{\tau}_{i,j}^{[i]}\big)\underline{x}'_j + \underline{z}'_i, \tag{4.23}$$

4.2.2 When $\psi(t)$ is a Band-Limited Waveform

When $\psi(t)$ is a band-limited waveform, for codewords of length N, the received signal at the i-th receiver sampled at $t = kT_s + \tau_{i,i},\ k = 0, 1, \ldots, N-1$, is given by

$$y_i(k) = \sum_{j=1}^{K} h_{i,j}\sum_{q=0}^{N-1}\gamma_{i,j}(k-q)x_j(q) + z_i(k), \tag{4.24}$$

where $\gamma_{i,j}(k) \triangleq \psi\left(kT_s + \tau_{i,j}^{[i]}\right)$, $z_i(k)$ is the sample of the noise signal $z_i(t)$ at $t = kT_s + \tau_{i,i}$, and $\tau_{i,j}^{[i]} = \tau_{i,i} - \tau_{i,j}$. The received samples can be written in a vector form as follows.

$$\underline{y}_i = \sum_{j=1}^{K} h_{i,j} \hat{\mathbf{\Gamma}}_{i,j} \underline{x}_j + \underline{z}_i, \tag{4.25}$$

where

$$\begin{aligned}
\underline{y}_i &= [y_i(0), y_i(1), \ldots, y_i(N-1)], \\
\underline{x}_j &= [x_j(0), x_j(1), \ldots, x_j(N-1)], \\
\underline{z}_i &= [z_i(0), z_i(1), \ldots, z_i(N-1)], \\
\hat{\mathbf{\Gamma}}_{i,j} &= \\
&\begin{bmatrix}
\gamma_{i,j}(0) & \gamma_{i,j}(-1) & \gamma_{i,j}(-2) & \cdots & \gamma_{i,j}(-N+1) \\
\gamma_{i,j}(1) & \gamma_{i,j}(0) & \gamma_{i,j}(-1) & \cdots & \gamma_{i,j}(-N+2) \\
\gamma_{i,j}(2) & \gamma_{i,j}(1) & \gamma_{i,j}(0) & \cdots & \gamma_{i,j}(-N+3) \\
\vdots & \vdots & \vdots & \cdots & \vdots \\
\gamma_{i,j}(N-1) & \gamma_{i,j}(N-2) & \gamma_{i,j}(N-3) & \cdots & \gamma_{i,j}(0)
\end{bmatrix}.
\end{aligned} \tag{4.26}$$

As can be seen, due to the existence of the asynchronism among the users, one has inter-symbol-interference (ISI) among the transmitted symbols by the different users. This ISI is represented by the matrix $\hat{\mathbf{\Gamma}}_{i,j}$.

When $\psi(t)$ is a band-limited waveform, it is not possible to make the corresponding channel matrices circulant by inserting CPS symbols. Here, we approximate them with their asymptotically equivalent circulant matrices and show that the approximation error goes to zero for large length codewords.

Definition 4.1. *Two matrix sequences $\{\mathbf{A}_N\}$ and $\{\mathbf{B}_N\}$, $N = 1, 2, \ldots$ are said to be asymptotically equivalent, and denoted by $\{\mathbf{A}_N\} \sim \{\mathbf{B}_N\}$, if the following conditions are satisfied [72]:*

1) $\exists\, Q < \infty$ *such that* $\forall\, N,\ \|\mathbf{A}_N\| < Q$ *and* $\|\mathbf{B}_N\| < Q$

2) $\lim_{N\to\infty} |\mathbf{A}_N - \mathbf{B}_N| = 0.$

where $\|\mathbf{A}\|$ and $|\mathbf{A}|$ denote the strong norm and the weak norm of $\mathbf{A}$ given by [71]

$$\|\mathbf{A}\| = \max_{\underline{x}} \left[(\underline{x}^\dagger \mathbf{A}^\dagger \mathbf{A} \underline{x})/(\underline{x}^\dagger \underline{x})\right]^{1/2},$$
$$|\mathbf{A}| = \left[N^{-1}\, \mathtt{trace}(\mathbf{A}^\dagger \mathbf{A})\right]^{1/2}.$$

It is shown that the eigenvalues of asymptotically equivalent matrices are asymptotically equally distributed [72].

For all absolutely summable infinite complex sequences $\{\gamma_{i,j}(k),\, k \in \mathbb{Z}\}$ with 2π-periodic DTFT, $\Gamma_{i,j}(\omega)$, given in (4.7), there exists a sequence of circulant matrices $\{(\mathbf{\Gamma}_{i,j})_N\}$ asymptotically equivalent to $\{(\hat{\mathbf{\Gamma}}_{i,j})_N\}$ [72] and

$$(\mathbf{\Gamma}_{i,j})_N = \mathbf{U}_N^{\dagger}(\mathbf{\Lambda}_{i,j})_N\mathbf{U}_N, \tag{4.27}$$

where $\mathbf{U}_N$ is the unitary DFT matrix of dimension N given in (4.16) and $(\mathbf{\Lambda}_{i,j})_N$ is a diagonal matrix with the q-th diagonal entry given by

$$(\mathbf{\Lambda}_{i,j})_N(q,q) = \Gamma_{i,j}\left(\frac{2\pi(q-1)}{N}\right),\ q = 1, 2\ldots, N. \tag{4.28}$$

Clearly, for a well-designed waveform with non-zero spectrum over its bandwidth, if the Nyquist sampling frequency $f_s = 2W$ is chosen, there is no deterministic zero in the spectrum of the sequence $\{\gamma_{i,j}(k),\, k \in \mathbb{Z}\}$ and the diagonal entries of $(\mathbf{\Lambda}_{i,j})_N$ are all non-zero bounded values. Since $(\hat{\mathbf{\Gamma}}_{i,j})_N$ and $(\mathbf{\Gamma}_{i,j})_N$ are asymptotically equivalent, in the sequel, for large length codewords, we approximate $\hat{\mathbf{\Gamma}}_{i,j}$ by $\mathbf{\Gamma}_{i,j}$.

Lemma 4.2. *If the shaping waveform has a sub-linear decaying rate in time (i.e., $\psi(t) \leq a/|t/T_s|^{\eta}$, $\eta > 1$, a is a constant), the error of approximating $(\hat{\mathbf{\Gamma}}_{i,j})_N$ by $(\mathbf{\Gamma}_{i,j})_N$ is bounded and goes to zero when $N \to \infty$.*

Proof. Assume $\hat{\mathbf{\Gamma}}_{i,j}$ in (4.26) is approximated by $\mathbf{\Gamma}_{i,j}$ in (4.27) , i.e., $\hat{\mathbf{\Gamma}}_{i,j} \approx \mathbf{\Gamma}_{i,j}$. The approximation error matrix $\mathbf{\Upsilon}$ is defined as

$$\mathbf{\Upsilon} = \mathbf{\Lambda}_{i,j} - \mathbf{U}\hat{\mathbf{\Gamma}}_{i,j}\mathbf{U}^{\dagger}. \tag{4.29}$$

The (q,s)-th entries of $\mathbf{\Lambda}_{i,j}$ and $\mathbf{U}\hat{\mathbf{\Gamma}}_{i,j}\mathbf{U}^{\dagger}$ are respectively given by

$$\mathbf{\Lambda}_{i,j}(q,s) = \begin{cases} \sum_k \gamma_k e^{-\xi\frac{2\pi}{N}(q-1)k}, & q = s \\ 0, & q \neq s, \end{cases}$$

$$\mathbf{U}\hat{\mathbf{\Gamma}}_{i,j}\mathbf{U}^{\dagger}(q,s) = \frac{1}{N}\sum_{j=1}^{N}\sum_{i=1}^{N}\gamma_{i-j}e^{-\xi\frac{2\pi}{N}[(q-1)(i-1)-(s-1)(j-1)]}.$$

If $q = s$, we get

$$\begin{aligned}\mathbf{\Upsilon}(q,q) &= \sum_k \gamma_k e^{-\xi\frac{2\pi}{N}(q-1)k} - \frac{1}{N}\sum_{j=1}^{N}\sum_{i=1}^{N}\gamma_{i-j}e^{-\xi\frac{2\pi}{N}(q-1)(i-j)} \\ &= \sum_{k=-N+1}^{N-1}\frac{|k|}{N}\gamma_k e^{-\xi\frac{2\pi}{N}k(q-1)} + \sum_{|k|\geq N}\gamma_k e^{-\xi\frac{2\pi}{N}k(q-1)}.\end{aligned}$$

Assuming that the shaping waveform is such that $\psi(t) \leq a/|t/T_s|^{\eta}$, where a is a constant, we get

$$\begin{aligned}|\boldsymbol{\Upsilon}(q,q)| &\leq \sum_{k=-N+1}^{N-1} \frac{|k|}{N}|\gamma_k| + \sum_{|k|\geq N} |\gamma_k| \\ &\leq \frac{2a}{N}\sum_{k=1}^{N-1}\frac{1}{k^{\eta-1}} + 2a\sum_{k=N}^{\infty}\frac{1}{k^{\eta}} \end{aligned} \tag{4.30}$$

One can check that for $\eta > 1$, $\lim_{N\to\infty}\frac{1}{N}\sum_{k=1}^{N}\frac{1}{k^{\eta-1}} = 0$. This is because for all N and $\eta > 0$

$$0 = \lim_{N\to\infty}\frac{1}{N}\int_1^N \frac{1}{x^{\eta}}dx < \lim_{N\to\infty}\frac{1}{N}\sum_{k=1}^{N}\frac{1}{k^{\eta}} < \lim_{N\to\infty}\frac{1}{N}\int_1^N \frac{1}{(x-1)^{\eta}}dx = 0.$$

Hence, the first term on the right hand side of (4.30) goes to zero for large values of N. It is also known that the η-series $\sum_{k=1}^{\infty} 1/k^{\eta}$ is convergent for all $\eta > 1$. Hence, the second term is also bounded for $\eta > 1$ and vanishes to zero for large values of N. Therefore, for large length codewords, $|\boldsymbol{\Upsilon}(q,q)|$ is bounded and vanishes to zero if $\eta > 1$.

When $q \neq s$, we get

$$\begin{aligned}\Upsilon(q,s) =& -\mathbf{U}\hat{\mathbf{\Gamma}}_{i,j}\mathbf{U}^{\dagger}(q,s) \\ =& -\frac{1}{N}\sum_{j=1}^{N}\sum_{i=1}^{N}\gamma_{i-j}e^{-\xi\frac{2\pi}{N}[(q-1)(i-1)-(s-1)(j-1)]} \\ =& -\frac{1}{N}\sum_{k=1}^{N-1}\gamma_k e^{-\xi\frac{2\pi}{N}(q-1)k}\sum_{j=k}^{N-1}e^{-\xi\frac{2\pi}{N}(q-s)(j-k)} \\ & -\frac{1}{N}\sum_{k=-N+1}^{-1}\gamma_k e^{\xi\frac{2\pi}{N}(s-1)k}\sum_{j=-k}^{N-1}e^{-\xi\frac{2\pi}{N}(q-s)(j+k)} \\ =& \frac{1}{N}\sum_{k=1}^{N-1}\gamma_k e^{-\xi\frac{2\pi}{N}(s-1)k}\sum_{j=N-k}^{N-1}e^{-\xi\frac{2\pi}{N}(q-s)j} \\ & +\frac{1}{N}\sum_{k=-N+1}^{-1}\gamma_k e^{-\xi\frac{2\pi}{N}(q-1)k}\sum_{j=N+k}^{N-1}e^{-\xi\frac{2\pi}{N}(q-s)j}\end{aligned}$$

Assuming that the shaping waveform is such that $\psi(t) \leq a/|t/T_s|^{\eta}$, where a is a constant, we get

$$\begin{aligned}|\boldsymbol{\Upsilon}(q,s)| &\leq \frac{1}{N}\sum_{k=-N+1}^{-1}|k||\gamma_k| + \frac{1}{N}\sum_{k=1}^{N-1}|k||\gamma_k| \\ &\leq \frac{2a}{N}\sum_{k=1}^{N-1}\frac{1}{k^{\eta-1}} \end{aligned} \tag{4.31}$$

Similarly, one can see that for $\eta > 1$, $|\boldsymbol{\Upsilon}(q,s)|$ is bounded and vanishes to zero for large values of N. This concludes the proof $\square$

Since the communication in this case is carried out over a strictly limited bandwidth W, according to the shift property of the DTFT, we get

$$\mathbf{\Lambda}_{i,j} = \mathbf{\Lambda}_0 \mathbf{E}\big(\hat{\tau}_{i,j}^{[i]}\big), \tag{4.32}$$

where $\hat{\tau}_{i,j}^{[i]} \triangleq \frac{\tau_{i,j}^{[i]}}{T_s}$, $\mathbf{\Lambda}_0$ is defined similar to $\mathbf{\Lambda}_{i,j}$ when $\hat{\tau}_{i,j}^{[i]} = 0$, and

$$\mathbf{E}(\hat{\tau}_{i,j}^{[i]}) = \mathtt{diag}\left\{1, e^{-\xi\frac{2\pi}{N}\hat{\tau}_{i,j}^{[i]}}, e^{-\xi\frac{4\pi}{N}\hat{\tau}_{i,j}^{[i]}}, \ldots, e^{-\xi\frac{2(N-1)\pi}{N}\hat{\tau}_{i,j}^{[i]}}\right\}. \tag{4.33}$$

In the sequel, whenever a band-limited shaping waveform is used, we assume that N is sufficiently large such that $\hat{\mathbf{\Gamma}}_{i,j}$ can be replaced by $\mathbf{\Gamma}_{i,j}$ with a negligible approximation error. In this case, we get

$$\underline{y}'_i = \mathbf{\Lambda}_0 \sum_{j=1}^{K} h_{i,j} \mathbf{E}\big(\hat{\tau}_{i,j}^{[i]}\big)\underline{x}'_j + \underline{z}'_i, \tag{4.34}$$

where $\underline{y}'_i, \underline{x}'_j, \underline{z}'_i$ are respectively the linear transformations of $\underline{y}_i, \underline{x}_j, \underline{z}_i$ by the DFT matrix $\mathbf{U}$.

4.2.3 The Shaping Waveform

It was argued in the previous sections that having a sub-linear decaying rate in time for the shaping waveform is a necessary and sufficient condition to obtain the system models presented in (4.23) and (4.34) respectively for both cases of using time-limited and band-limited systems. A direct consequence of this argument is that the sinc waveform, which has a linear decaying rate in time does not hold a valid approximation with a bounded error. In contrast, the raised-cosine waveform with a non-zero excess bandwidth, which has a decaying rate proportional to $1/|t/T_s|^3$ for large enough values of t, is a good candidate to be used in the structure of the proposed scheme (i.e., using the root-raised cosine waveform as the transmitter and the receiver filters). As can be seen, waveforms with faster decaying rate in time are more appealing to have a faster decaying approximation error with u.

Remark 4.3. *According to the Paley-Wiener Theorem, the spectrum of a signal can not be both time and frequency limited. Hence, using a truncated version of the waveform results in an unlimited support in the frequency domain [73]. For practical values of SNR ($\rho < \infty$), if a well-designed shaping waveform with vanishing spectrums out of bandwidth W is used, depending on the level of the noise at the receivers' side, one may choose u a sufficiently large finite value such that the tails of the spectrum of the transmitted signals lie below the noise level. In this case, the system can be approximated with a bandlimited one. In theoretical analysis, when $\rho \to \infty$, it is not possible to avoid bandwidth expansion when a finite support shaping waveform is used. This is*

both a practical and a theoretical limitation of all communication systems which is characterized by the Paley-Wiener Theorem.

Alternatively, for time-limited signals, where the spectrum has infinite support, a number of bandwidth measures such as the root-mean-square (RMS) bandwidth and the fractional out-of-band energy (FOBE) bandwidth have been extensively used in practice [74]. For a finite energy signal $\psi(t)$, the RMS bandwidth W_{rms} is defined as the standard deviation of the spectrum and is independent of SNR. Clearly, strictly time-limited signals may have finite RMS bandwidth, while they do not have a finite bandwidth. It is shown that the spectrum of a signal with finite RMS bandwidth decays at a rate faster than $1/f^3$ for large frequencies [75, 76]. The rapid decaying of the spectrum with increasing frequency helps to avoid spill over the energy to the adjacent frequency bands. The shaping waveform can be carefully designed such that it has a sub-linear decaying rate in time and it has a finite RMS or a finite FOBE bandwidth.

4.3 Asynchronous Interference Alignment

We propose an interference alignment algorithm which achieves the total $K/2$ DOF over the underlying quasi-static K-user asynchronous interference channel almost surely. Our scheme is similar to the vector interference alignment scheme proposed in [52] for time/frequency/space varying channels wherein the fading coefficients of a link are independently chosen from a continuous probability distribution at the beginning of each symbol interval. In contrast, in our scenario, the communication links are quasi-static. As it was observed in previous sections, using the proposed signaling scheme, they are converted to ISI and accordingly into time varying channels. Hence, the proposed scheme solves the lack of channel variation required for the interference alignment in quasi static scenarios. However, the channel coefficients of the links in this case are not independently chosen from a distribution; rather, they are correlated over the time resulting in a more sophisticated situation. We will show that even under channel correlation, the alignment task can almost always be performed. We proposed our alignment scheme first for a simple three-user interference channel and then generalize it to an interference channel with arbitrary number of users.

When a time-limited shaping waveform is deploy, the practical signaling scheme proposed in Section 4.2.1 is used. However, when it is band-limited, the signaling scheme proposed in Section 4.2.2 is used. In this case, the channel matrices $\hat{\mathbf{\Gamma}}_{i,j}$'s are approximated by their asymptotically equivalent matrices $\mathbf{\Gamma}_{i,j}$'s given in (4.27). Having the same channel model with the same notation for both cases facilitates pursuing a single procedure for both scenarios. In the sequel to avoid

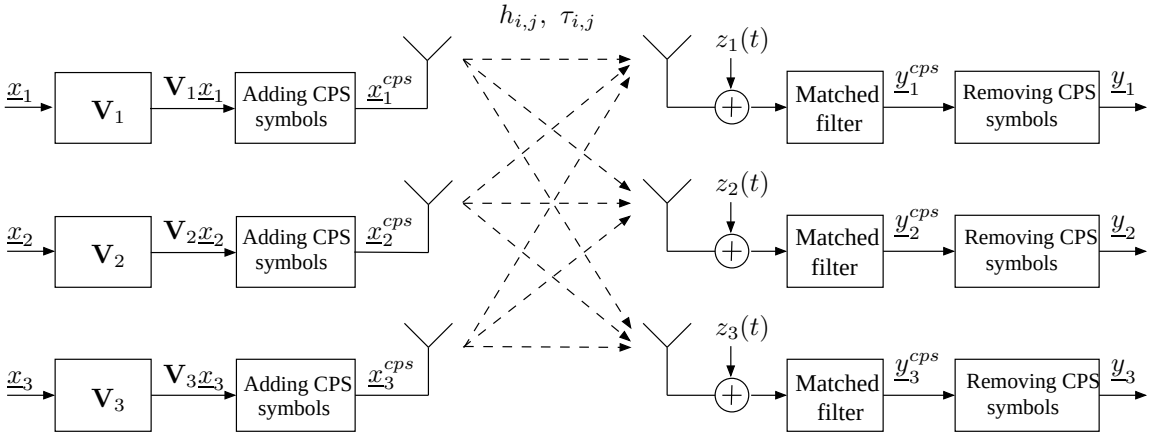

Figure 4.1: Block diagram of the proposed interference alignment scheme over the three-user asynchronous interference channel.

confusion, we detail the scheme for the case that a time-limited shaping waveform is used. The scheme is elaborated for the other case when it is necessary.

4.3.1 Alignment Scheme for the Three-User Asynchronous Interference Channel

In a three-user interference channel in which the transmitters use a shaping waveform of length uT_s, by proceeding in the footsteps of [52], we define a scenario wherein the first transmitter sends $n+1$ independent streams of symbols to the the first receiver via $n+1$ distinct direction vectors, each of length $N = 2n+1$. Each of the two other transmitters sends n streams of symbols via n distinct direction vectors of the same length N. The pre-coding matrix $\mathbf{V}_j,\ j = 1, 2, 3$, at the j-th transmitter node is defined as follows.

$$\mathbf{V}_j \triangleq [\underline{v}_j^1, \underline{v}_j^2, \ldots, \underline{v}_j^s], \tag{4.35}$$

where $s = n+1$ for $j = 1$, and $s = n$ for $j \neq 1$. $\underline{v}_j^k$ of size $N \times 1$ is the k-th direction vector of the j-th transmitter. These vectors are chosen such that at each receiver the interfering signals cast overlapping shadows while the desired signal remains distinct of the interferences. In synchronous quasi-static scenarios wherein the channel coefficients are constant for a long period of time, if the direction vectors are chosen as they are chosen for time/frequency/space varying channels in [52], they all overlap and merge into a single direction vector which contradicts with the main objective of the interference alignment. Our goal is to overcome this shortcoming by deploying asynchronous delays among the received signals at each receiver.

Fig. 4.1 shows the block diagram of the proposed interference alignment scheme for a three-user interference channel. At the j-th transmitter, a vector of information symbols $\underline{x}_j$ is multiplied by a precoding matrix $\mathbf{V}_j$ and then is supported by enough cyclic prefix and cyclic suffix symbols. The resulted sequence is transmitted over the channel. Here, we assume that $\underline{x}_1$ is of length $n+1$ and $\underline{x}_2, \underline{x}_3$ are of length n. The precoding matrix $\mathbf{V}_1$ is of size $N \times (n+1)$ and $\mathbf{V}_2, \mathbf{V}_3$ are of size $N \times n$. At the receivers, the CPS symbols are discarded. According to (4.11) and (4.25), the received signal model at the i-th receiver node is given as follows.

$$\underline{y}_i = \sum_{i=1}^{3} h_{i,j} \mathbf{\Gamma}_{i,j} \mathbf{V}_j \underline{x}_j + \underline{z}_i, \tag{4.36}$$

where $\mathbf{\Gamma}_{i,j}$ is defined in (4.12). At the first receiver, the interfering signals from the second and the third users should be aligned. In other words, the subspaces that are spanned by these signals should completely overlap, i.e.,

$$\texttt{span}\ [h_{1,2}\mathbf{\Gamma}_{1,2}\mathbf{V}_2] = \texttt{span}\ [h_{1,3}\mathbf{\Gamma}_{1,3}\mathbf{V}_3], \tag{4.37}$$

where $\texttt{span}\ \mathbf{X}$ denotes the vector space spanned by the generator matrix $\mathbf{X}$. At the second receiver, the interfering signals from the first and the third transmitters should cast overlapping shadows. Since these signals lie respectively on $n+1$ and n dimensional vector spaces, the direction vectors should be chosen such that the smaller vector space is embedded into the bigger one. Similar argument is valid at the output of the third receiver. Hence,

$$\begin{aligned} \texttt{span}\ [h_{2,3}\mathbf{\Gamma}_{2,3}\mathbf{V}_3] &\subset \texttt{span}\ [h_{2,1}\mathbf{\Gamma}_{2,1}\mathbf{V}_1], \\ \texttt{span}\ [h_{3,2}\mathbf{\Gamma}_{3,2}\mathbf{V}_2] &\subset \texttt{span}\ [h_{3,1}\mathbf{\Gamma}_{3,1}\mathbf{V}_1], \end{aligned} \tag{4.38}$$

where $\subset$ indicates that the left hand side space is a subspace of the right hand side one. In addition, to take advantage of the existing number of DOF, the union of the subspaces of the desired and the interfering signals at each receiver node should span the whole vector space of dimension N, i.e.,

$$\begin{aligned} \texttt{span}\ [h_{1,1}\mathbf{\Gamma}_{1,1}\mathbf{V}_1,\ h_{1,2}\mathbf{\Gamma}_{1,2}\mathbf{V}_2] &= \mathbb{C}^N, \\ \texttt{span}\ [h_{2,2}\mathbf{\Gamma}_{2,2}\mathbf{V}_2,\ h_{2,1}\mathbf{\Gamma}_{2,1}\mathbf{V}_1] &= \mathbb{C}^N, \\ \texttt{span}\ [h_{3,3}\mathbf{\Gamma}_{3,3}\mathbf{V}_3,\ h_{3,1}\mathbf{\Gamma}_{3,1}\mathbf{V}_1] &= \mathbb{C}^N, \end{aligned} \tag{4.39}$$

where $\mathbb{C}$ is the field of the complex numbers.

Remark 4.4. *As can be seen in (4.37)-(4.39), the quasi-static channel coefficients, $h_{i,j}$'s, appear as constant scaling factors of the generator matrices of the vector spaces. Since a vector space is closed under scalar multiplication, it remains the same if the generator matrix is scaled by a*

constant value. Therefore, the fading coefficients do not play any role in aligning interference signals and can be neglected as long as they are non-zero.

To design precoding matrices, a simple choice of the generator matrices is considered.

$$\begin{aligned} \mathbf{\Gamma}_{1,2}\mathbf{V}_2 &= \mathbf{\Gamma}_{1,3}\mathbf{V}_3, \\ \mathbf{\Gamma}_{2,3}\mathbf{V}_3 &\sqsubset \mathbf{\Gamma}_{2,1}\mathbf{V}_1, \\ \mathbf{\Gamma}_{3,2}\mathbf{V}_2 &\sqsubset \mathbf{\Gamma}_{3,1}\mathbf{V}_1, \end{aligned} \tag{4.40}$$

where $\sqsubset$ indicates that the columns of the left hand side matrix is a subset of the columns of the right hand side matrix. These equations can be simplified as follows.

$$\begin{aligned} \mathbf{B} &= \mathbf{TC}, \\ \mathbf{B} &\sqsubset \mathbf{A}, \\ \mathbf{C} &\sqsubset \mathbf{A}, \end{aligned} \tag{4.41}$$

where

$$\begin{aligned} \mathbf{A} &= \mathbf{V}_1, \\ \mathbf{B} &= \mathbf{\Gamma}_{2,1}^{-1}\mathbf{\Gamma}_{2,3}\mathbf{V}_3, \\ \mathbf{C} &= \mathbf{\Gamma}_{3,1}^{-1}\mathbf{\Gamma}_{3,2}\mathbf{V}_2, \\ \mathbf{T} &= \mathbf{\Gamma}_{2,1}^{-1}\mathbf{\Gamma}_{2,3}\mathbf{\Gamma}_{1,3}^{-1}\mathbf{\Gamma}_{1,2}\mathbf{\Gamma}_{3,2}^{-1}\mathbf{\Gamma}_{3,1}. \end{aligned} \tag{4.42}$$

$\mathbf{\Gamma}_{i,j}$'s are full rank and consequently invertible random matrices. Since the asynchronous delays are continuous time independent random variables over a symbol interval, they are distinct with probability one resulting in distinct $\mathbf{\Gamma}_{i,j}$ matrices. As a result, $\mathbf{T}$ is a random invertible circulant matrix. Note that in difference to the vector alignment scheme proposed in [52], $\mathbf{\Gamma}_{i,j}$'s and $\mathbf{T}$ are not diagonal matrices.

If $\mathbf{A}, \mathbf{B}$, and $\mathbf{C}$ are chosen properly such that they satisfy (4.41), the precoding matrices $\mathbf{V}_1, \mathbf{V}_2, \mathbf{V}_3$ are obtained from (4.42). For this sake, let $\underline{w}$ be a vector of size $N \times 1$ and assume $\mathbf{A}, \mathbf{B}$, and $\mathbf{C}$ are chosen as follows.

$$\begin{aligned} \mathbf{A} &= [\underline{w}\ \mathbf{T}\underline{w}\ \ldots\ \mathbf{T}^n\underline{w}], \\ \mathbf{B} &= [\mathbf{T}\underline{w}\ \mathbf{T}^2\underline{w}\ \ldots\ \mathbf{T}^n\underline{w}], \\ \mathbf{C} &= [\underline{w}\ \mathbf{T}\underline{w}\ \ldots\ \mathbf{T}^{n-1}\underline{w}]. \end{aligned} \tag{4.43}$$

It is easily seen that these matrices satisfy the required conditions of (4.41). To show that the precoding matrices (obtained from the above $\mathbf{A}, \mathbf{B}$, and $\mathbf{C}$) perform the alignment task, it is

required to prove that first $\mathbf{A}, \mathbf{B}$, and $\mathbf{C}$ are full column rank matrices and second, the image of the precoding matrices at each receiver node span the whole vector space, i.e., at receiver one, the generator matrix of the resulted space $[\mathbf{\Gamma}_{1,1}\mathbf{V}_1,\ \mathbf{\Gamma}_{1,2}\mathbf{V}_2]$ and equivalently $[\mathbf{V}_1,\ \mathbf{\Gamma}_{1,1}^{-1}\mathbf{\Gamma}_{1,2}\mathbf{V}_2]$ should be a full rank matrix. At the second and the third receivers $[\mathbf{V}_1,\ \mathbf{\Gamma}_{2,1}^{-1}\mathbf{\Gamma}_{2,2}\mathbf{V}_2]$ and $[\mathbf{V}_1,\ \mathbf{\Gamma}_{3,1}^{-1}\mathbf{\Gamma}_{3,3}\mathbf{V}_3]$ should be full rank matrices.

By assuming that a well-designed shaping waveform is used such that equation (4.20) is valid with a negligible approximation error, we get,

$$\begin{aligned}\mathbf{B} &= \mathbf{U}^{\dagger}\mathbf{E}\left(\hat{\tau}_{1,3}^{[2]}\right)\mathbf{U}\mathbf{V}_3,\\ \mathbf{C} &= \mathbf{U}^{\dagger}\mathbf{E}\left(\hat{\tau}_{1,2}^{[3]}\right)\mathbf{U}\mathbf{V}_2,\\ \mathbf{T} &= \mathbf{U}^{\dagger}\mathbf{E}\left(\hat{\tau}_t\right)\mathbf{U},\end{aligned} \tag{4.44}$$

where $\hat{\tau}_{m,j}^{[i]} = \frac{\tau_{m,j}^{[i]}}{T_s}$, $\forall\, i,j,m \in \{1,2,3\}$ and $\hat{\tau}_t = \hat{\tau}_{1,3}^{[2]} + \hat{\tau}_{3,2}^{[1]} + \hat{\tau}_{2,1}^{[3]}$. Note that $\hat{\tau}_t$ and $\hat{\tau}_{m,j}^{[i]}$, $\forall\, i,j,m$, $(j \neq m)$, are independent continuous random variables which are non-zero with probability one.

Proposition 4.2. $\mathbf{A}, \mathbf{B}$, *and* $\mathbf{C}$ *defined in (4.43) are almost surely full column rank matrices.*

Proof. Let $\underline{w}$ be an arbitrary vector such that $\underline{w}' \triangleq \mathbf{U}\underline{w}$ contains only non-zero entries. Let $\hat{\mathbf{T}} \triangleq \mathbf{E}\left(\hat{\tau}_t\right)$. Matrix $\mathbf{A}' \triangleq \mathbf{U}\mathbf{A}$ can be written as follows.

$$\mathbf{A}' = [\underline{w}', \hat{\mathbf{T}}\underline{w}', \hat{\mathbf{T}}^2\underline{w}', \ldots, \hat{\mathbf{T}}^n\underline{w}']. \tag{4.45}$$

Clearly $\mathbf{A}$ and $\mathbf{A}'$ have the same rank order. Because $\hat{\mathbf{T}}$ is a diagonal matrix, $\mathbf{A}'$ can be rewritten as follows.

$$\mathbf{A}' = \mathbf{W}\tilde{\mathbf{T}},$$

where $\mathbf{W} = \mathtt{diag}\{\underline{w}'\}$ and $\tilde{\mathbf{T}} = \left[\underline{t}^0,\ \underline{t}^1,\ \ldots,\ \underline{t}^n\right]$ has size $N \times (n+1)$. $\underline{t}^i$ is a vector of size $N \times 1$ containing the i-th power of the diagonal entries of $\hat{\mathbf{T}}$. i.e.,

$$\underline{t}^i = \left[1, e^{-\xi i \frac{2\pi}{N}\hat{\tau}_t}, \ldots, e^{-\xi i \frac{2\pi(N-1)}{N}\hat{\tau}_t}\right]^T.$$

Since $\mathbf{W}$ is a full rank matrix, $\mathbf{A}$ and $\tilde{\mathbf{T}}$ have the same rank order. Consider any $(n+1)\times(n+1)$ sub matrix of $\tilde{\mathbf{T}}$ (for instant, the top $(n+1)\times(n+1)$ sub matrix). It is a Vandermonde matrix and its determinant is given by the multiplication of all the elements of a set containing the difference of every two non-trivial entries of the generator vector of this matrix. Hence, if the entries of $\underline{t}^1$ are distinct, the determinant of all of the sub matrices is non-zero and $\tilde{\mathbf{T}}$ is a full

column rank matrix. For $q, s \in \{0, 1, \ldots, N-1\}$ and $q \neq s$

$$\begin{aligned} \text{If } \ \underline{t}^1(q) = \underline{t}^1(s) \ &\Rightarrow \ e^{-\xi \frac{2\pi q}{N} \hat{\tau}_t} = e^{-\xi \frac{2\pi s}{N} \hat{\tau}_t} \\ &\Rightarrow \ \frac{2\pi q}{N} \hat{\tau}_t = \frac{2\pi s}{N} \hat{\tau}_t + 2k\pi, \quad k \in \mathbb{Z} \\ &\Rightarrow \ \hat{\tau}_t = \frac{kN}{q-s}, \quad k \in \mathbb{Z}. \end{aligned}$$

Since $\hat{\tau}_t$ is a continuous random variable distributed over $-3 < \hat{\tau}_t < 3$, the probability that $\hat{\tau}_t = \frac{kN}{s-q}$ is equal to zero. Therefore, $\tilde{\mathbf{T}}$ and equivalently $\mathbf{A}$ are almost surely full column rank matrices. Note that, for a finite value of N, $\hat{\tau}_t$ does not necessarily need to be an irrational number to make $\mathbf{A}$ a full rank matrix. Since $\mathbf{B}$ and $\mathbf{C}$ are sub matrices of $\mathbf{A}$, they are also full column rank matrices almost surely. □

Proposition 4.3. *The images of the precoding matrices at each receiver node span the whole vector space of dimension N.*

Proof. The proof is given for the vector space at the receiver one. The generator matrix of the vector space, $[\mathbf{V}_1,\ \mathbf{\Gamma}_{1,1}^{-1}\mathbf{\Gamma}_{1,2}\mathbf{V}_2]$, at this receiver should be full rank. By replacing $\mathbf{V}_1$ and $\mathbf{V}_2$ by their corresponding values from (4.42), it is seen that $[\mathbf{A}, \mathbf{FC}]$ given in the following equation should be a full rank matrix.

$$[\mathbf{A}, \mathbf{FC}] = \left[\underline{w}, \mathbf{T}\underline{w}, \ldots, \mathbf{T}^n\underline{w}, \mathbf{F}\underline{w}, \mathbf{FT}\underline{w}, \ldots, \mathbf{FT}^{n-1}\underline{w}\right],$$

where $\mathbf{F} = \mathbf{\Gamma}_{1,1}^{-1}\mathbf{\Gamma}_{1,2}\mathbf{\Gamma}_{3,2}^{-1}\mathbf{\Gamma}_{3,1}$ is a random circulant full rank matrix. $\mathbf{F}$ is simplified as $\mathbf{F} = \mathbf{U}^\dagger \mathbf{E}\left(\hat{\tau}_f\right)\mathbf{U}$, where $\hat{\tau}_f = \hat{\tau}_{1,2}^{[1]} + \hat{\tau}_{2,1}^{[3]}$. Let $\underline{w}$ be an arbitrary vector such that $\underline{w}' \triangleq \mathbf{U}\underline{w}$ contains no zero entry. Let $\hat{\mathbf{T}} \triangleq \mathbf{E}\left(\hat{\tau}_t\right)$ and $\hat{\mathbf{F}} \triangleq \mathbf{E}\left(\hat{\tau}_f\right)$. By considering that $\hat{\mathbf{T}}$ and $\hat{\mathbf{F}}$ are diagonal matrices, we obtain

$$\begin{aligned} [\mathbf{A}, \mathbf{FC}] &= \mathbf{U}^\dagger \left[\underline{w}', \hat{\mathbf{T}}\underline{w}', \ldots, \hat{\mathbf{T}}^n\underline{w}', \hat{\mathbf{F}}\underline{w}', \hat{\mathbf{F}}\hat{\mathbf{T}}\underline{w}', \ldots, \hat{\mathbf{F}}\hat{\mathbf{T}}^{n-1}\underline{w}'\right] \\ &= \mathbf{U}^\dagger \mathbf{W} \check{\mathbf{T}}, \end{aligned} \tag{4.46}$$

where $\mathbf{W} = \mathtt{diag}\{\underline{w}'\}$. Let $\phi \triangleq e^{-\xi \frac{2\pi}{N} \hat{\tau}_t}$ and $\theta \triangleq e^{-\xi \frac{2\pi}{N} \hat{\tau}_f}$. Matrix $\check{\mathbf{T}}$ of size $N \times N$ is given in equation (4.47). Clearly, $[\mathbf{A}, \mathbf{FC}]$ and $\check{\mathbf{T}}$ have the same rank order.

$$\check{\mathbf{T}} = \begin{bmatrix} 1 & 1 & 1 & \cdots & 1 & 1 & 1 & 1 & \cdots & 1 \\ 1 & \phi & \phi^2 & \cdots & \phi^n & \theta & \theta\phi & \theta\phi^2 & \cdots & \theta\phi^{(n-1)} \\ 1 & \phi^2 & \phi^4 & \cdots & \phi^{2n} & \theta^2 & \theta^2\phi^2 & \theta^2\phi^4 & \cdots & \theta^2\phi^{2(n-1)} \\ \vdots & \vdots & \vdots & \ldots & \vdots & \vdots & \vdots & \vdots & \ldots & \vdots \\ 1 & \phi^{N-1} & \phi^{2(N-1)} & \ldots & \phi^{n(N-1)} & \theta^{N-1} & \theta^{N-1}\phi^{N-1} & \theta^{N-1}\phi^{2(N-1)} & \ldots & \theta^{N-1}\phi^{(N-1)(n-1)} \end{bmatrix} \tag{4.47}$$

$\check{\mathbf{T}}$ is a Vandermonde matrix with $\underline{\check{t}} = [1, \phi, \phi^2, \cdots, \phi^n, \theta, \theta\phi, \theta\phi^2, \cdots, \theta\phi^{(n-1)}]$ of length N as the generator vector. The determinant of this matrix is given by the multiplication of all the elements of a set containing the difference of every two non-trivial entries of $\underline{\check{t}}$. Hence, if the entries of $\underline{\check{t}}$ are distinct, this matrix is full rank and its determinant is non-zero. The elements of the vector $\underline{\check{t}}$ are in the form of $\theta^\alpha \phi^\beta$, where $\alpha \in \{0, 1\}$ and $q \in \{0, 1, \ldots, n\}$ when $\alpha = 0$ and $q \in \{0, 1, \ldots, n-1\}$ when $\alpha = 1$. Note that every element of this vector has a unique (α, β) tuple. If two non-trivial entries of this vector are the same, we obtain

$$\begin{aligned} \theta^\alpha \phi^\beta = \theta^{\alpha'} \phi^{\beta'} \Rightarrow \quad & e^{-\xi \frac{2\pi}{N}(\alpha \hat{\tau}_f + \beta \hat{\tau}_t)} = e^{-\xi \frac{2\pi}{N}(\alpha' \hat{\tau}_f + \beta' \hat{\tau}_t)} \\ \Rightarrow \quad & (\alpha - \alpha')\hat{\tau}_f + (\beta - \beta')\hat{\tau}_t = kN, \quad k \in \mathbb{Z} \end{aligned} \tag{4.48}$$

Since $(\alpha, \beta) \neq (\alpha', \beta')$, this equation cannot trivially hold for $k = 0$. Moreover, Since $\hat{\tau}_t$, $\hat{\tau}_f$ are continuous random variables distributed over $-3 < \hat{\tau}_t < 3$ and $-2 < \hat{\tau}_t < 2$, respectively, the probability that these numbers fit into equation (4.48) is zero. As a sufficient condition, it is seen that if the numbers $\{N, \hat{\tau}_f, \hat{\tau}_t\}$ are algebraically independent over the integers, equation (4.48) does not hold. This concludes the proof. □

According to Propositions 4.2 and 4.3, the proposed scheme performs the alignment task for almost all values of the asynchronous delays. If the channel coefficients, $h_{i,j}$'s, are contributed in design of the preceding matrices, the equivalent channel model at the output of the first receiver node after aligning the interferences is given by

$$\begin{aligned} \underline{y}_1 = \; & h_{1,1}\mathbf{\Gamma}_{1,1}\mathbf{V}_1\underline{x}_1 + h_{1,2}\mathbf{\Gamma}_{1,2}\mathbf{V}_2(\underline{x}_2 + \underline{x}_3) + \underline{z}_1 \\ & \left[h_{1,1}\mathbf{\Gamma}_{1,1}\mathbf{V}_1, h_{1,2}\mathbf{\Gamma}_{1,2}\mathbf{V}_2\right] \begin{bmatrix} \underline{x}_1 \\ \underline{x}_2 + \underline{x}_3 \end{bmatrix} + \underline{z}_1. \end{aligned} \tag{4.49}$$

The equivalent channel matrix $\left[h_{1,1}\mathbf{\Gamma}_{1,1}\mathbf{V}_1, h_{1,2}\mathbf{\Gamma}_{1,2}\mathbf{V}_2\right]$ is full rank. Hence, many decoding schemes can be used to decode the desired samples. The simplest one is the well known zero-forcing algorithm [77].

Corollary 4.1. *The proposed asynchronous interference alignment scheme achieves the total DOF equal to* $3/2$ *over the constant three user interference channel almost surely.*

Proof. According to Propositions 4.2 and 4.3, for a finite value of u, it is shown that $3n + 1$ independent information symbols are transmitted interference free over $2n + 1 + 2(u + 1)$ symbol intervals, where the extra $2(u + 1)$ symbol intervals are due to the transmission of CPS symbols. Hence, the efficiency factor of the transmission scheme is $\frac{3n+1}{2n+1+2(u+1)}$ regardless of the type of the shaping waveform used. For a finite value of u, this factor becomes arbitrary close to $3/2$

for a large value of n. Hence, if a truncated version of the root-square raised cosine filters with a non-zero small excess bandwidth and sufficiently large time support is used, the total DOF arbitrary close to 3/2 can be achieved.

When a band-limited shaping waveform is used, no CPS symbols are used and the efficiency factor is $\frac{3n+1}{2n+1}$ which approaches to 3/2 for large n. In this case the the root-square raised cosine filters with a non-zero small excess bandwidth provide the total DOF arbitrary close to 3/2. This concludes the proof. □

Corollary 4.2. *The DOF region of the underlying constant three-user asynchronous interference channel is almost always the same as that of the corresponding synchronous channel with varying fading coefficients which is given in* (4.2)*.*

Proof. The proof follows in the footsteps of the proof of Theorem 2 of [52]. Let $\mathcal{D}'$ be the DOF region of the underlying channel. Since the underlying constant asynchronous interference channel is modeled by a synchronous interference channel with varying fading coefficients in the frequency domain (see section 4.1.3), $\mathcal{D}' \subset \mathcal{D}$. On the other hand $(0,0,0), (1,0,0), (0,1,0), (0,0,1)$, and $(1/2, 1/2, 1/2)$ which are the corner points of $\mathcal{D}$ are achievable in the underlying channel and hence they are in $\mathcal{D}'$. Since $\mathcal{D}$ is a convex region, any point $(d_1, d_2, d_3) \in \mathcal{D}$ can be written as a convex combination of the corner points. Since the corner points of $\mathcal{D}$ are in $\mathcal{D}'$, any 3-tuple $(d_1, d_2, d_3) \in \mathcal{D}$ can be achieved by time-sharing among the corner points resulting in $(d_1, d_2, d_3) \in \mathcal{D}'$. Hence $\mathcal{D} \subset \mathcal{D}'$. This concludes the proof. □

Remark 4.5. *It is obvious that the proposed scheme does not apply to the case when all the users are fully synchronous, i.e., $\tau_{i,j} = 0, \forall i, j$. Once can check that inserting artificial delays at the transmitters does not help and the scheme applies only to random independent delays. According to the definition of $\hat{\tau}_f$, if $\hat{\tau}_{2,1}^{[1]} = \hat{\tau}_{2,1}^{[3]}$, then $\hat{\tau}_f = 0$ and thus $\hat{\mathbf{F}} = \mathbf{E}(0) = \mathbf{I}_N$ resulting in $\check{\mathbf{T}}$ to be a rank deficient matrix of rank order at most equal to $n+1$. Clearly, when the users are synchronous, $\hat{\tau}_{2,1}^{[1]} = \hat{\tau}_{2,1}^{[3]}$ even if artificial delays are inserted at the transmitters. In the asynchronous system under consideration where the delays are independent random variables due to the random nature of the medium, the relative delays are distinct with probability one.*

4.3.2 Alignment Scheme for the K-User Asynchronous Interference Channel

In a K-user interference channel where the users are not symbol-synchronous, by applying the proposed signaling scheme the underlying quasi-static links are converted to ISI and accordingly into time varying channels. Hence, a similar scheme as the one proposed in [52] for the K-user

synchronous interference channel with varying fading coefficients can be used to perform the alignment task over this channel.

Consider a scenario wherein the first user sends $(n+1)^\kappa$ streams of symbols to the first receiver via $(n+1)^\kappa$ distinct direction vectors each of length $N = (n+1)^\kappa + n^\kappa$, where $\kappa = (K-1)(K-2)-1$. Each of the other transmitters sends n^κ streams of symbols to the corresponding destination via n^κ direction vectors of the same length, N. The precoding matrix $\mathbf{V}_j$ at the j-th transmitter node contains all the corresponding direction vectors as its columns. Each transmitted frame is supported by enough number of CPS symbols. The received signal at the i-th receiver node after discarding the CPS symbols is given by

$$\underline{y}_i = \sum_{j=1}^{K} h_{i,j}\mathbf{\Gamma}_{i,j}\mathbf{V}_j\underline{x}_j + \underline{z}_i. \tag{4.50}$$

To perform the alignment task at the i-th receiver, the following conditions should be satisfied.

$$\mathbf{\Gamma}_{1,2}\mathbf{V}_2 = \mathbf{\Gamma}_{1,3}\mathbf{V}_3 = \cdots = \mathbf{\Gamma}_{1,K}\mathbf{V}_K, \quad i = 1, \tag{4.51}$$

$$\mathbf{\Gamma}_{i,1}^{-1}\mathbf{\Gamma}_{i,j}\mathbf{V}_j \sqsubset \mathbf{V}_1, \quad \forall\, i,j \neq 1,\ i \neq j. \tag{4.52}$$

In addition, the images of the precoding matrices at each receiver node should span the whole vector space of dimension N, i.e., at the i-th receiver

$$\texttt{span}\,[\mathbf{V}_1, \mathbf{\Gamma}_{1,1}^{-1}\mathbf{\Gamma}_{1,3}\mathbf{V}_3] = \mathbb{C}^N, \quad i = 1, \tag{4.53}$$

$$\texttt{span}\,[\mathbf{V}_1, \mathbf{\Gamma}_{i,1}^{-1}\mathbf{\Gamma}_{i,i}\mathbf{V}_i] = \mathbb{C}^N, \quad i \neq 1. \tag{4.54}$$

Equations (4.51) and (4.52) can respectively be simplified as follows.

$$\mathbf{V}_j = \mathbf{S}_j\mathbf{B}, \quad \forall j \in \{2,3,\ldots,K\}, \tag{4.55}$$

$$\mathbf{T}_{i,j}\mathbf{B} \sqsubset \mathbf{A}, \quad \forall i,j \in \{2,3,\ldots,K\}, i \neq j, \tag{4.56}$$

where

$$\begin{aligned}
\mathbf{A} &= \mathbf{V}_1,\\
\mathbf{B} &= \mathbf{\Gamma}_{2,1}^{-1}\mathbf{\Gamma}_{2,3}\mathbf{V}_3,\\
\mathbf{S}_j &= \mathbf{\Gamma}_{1,j}^{-1}\mathbf{\Gamma}_{1,3}\mathbf{\Gamma}_{2,3}^{-1}\mathbf{\Gamma}_{2,1}, \quad \forall j \in \{2,3,\ldots K\},\\
\mathbf{T}_{i,j} &= \mathbf{\Gamma}_{i,1}^{-1}\mathbf{\Gamma}_{i,j}\mathbf{S}_j, \quad \forall i,j \in \{2,3,\ldots K\}, i \neq j.
\end{aligned}$$

Let $\underline{w}$ be an arbitrary vector of length N such that $\underline{w}' \triangleq \mathbf{U}\underline{w}$ contains only non-zero entries, where $\mathbf{U}$ is the DFT matrix of dimension N given in (4.16). Let

$$\mathcal{V}_s \triangleq \left\{ \left(\prod_{i,j=2, i\neq j, (i,j)\neq(2,3)}^{K} \mathbf{T}_{i,j}^{\beta_{i,j}} \right) \underline{w},\ \beta_{i,j} \in \{0,1,\ldots,s\} \right\}. \tag{4.57}$$

$\mathbf{A}$ is chosen as a matrix which contains all vectors in $\mathcal{V}_n$. $\mathbf{B}$ is chosen as a matrix which contains all vectors in $\mathcal{V}_{n-1}$. Clearly, these choices of $\mathbf{A}$ and $\mathbf{B}$ satisfy (4.56). Since $\mathbf{B}$ is known, the precoding matrices $\mathbf{V}_j, j = 2, 3, \ldots, K$ are obtained from (4.55).

Proposition 4.4. *$\mathbf{V}_j,\ j = 1, 2, \ldots, K$, is a full column rank matrix almost surely. Moreover, the images of the precoding matrices at each receiver node span the whole vector space, $\mathbb{C}^N$, with probability one.*

Proof. The proof is given for the first user. We show that the image of the precoding matrices at the first receiver node span the whole vector space. This a priori proves that $\mathbf{V}_1$ is a full rank matrix. At receiver one, $[\mathbf{V}_1, \mathbf{\Gamma}_{1,1}^{-1}\mathbf{\Gamma}_{1,3}\mathbf{V}_3]$ and equivalently $[\mathbf{A}, \mathbf{FB}]$ should be full rank matrices, where $\mathbf{F} = \mathbf{\Gamma}_{1,1}^{-1}\mathbf{\Gamma}_{1,3}\mathbf{\Gamma}_{2,3}^{-1}\mathbf{\Gamma}_{2,1} = \mathbf{U}^\dagger\mathbf{E}(\hat{\tau}_{1,3}^{[1]} + \hat{\tau}_{3,1}^{[2]})\mathbf{U}$. Let $\hat{\mathbf{F}} = \mathbf{E}(\hat{\tau}_f)$, where $\hat{\tau}_f = \hat{\tau}_{1,3}^{[1]} + \hat{\tau}_{3,1}^{[2]}$. $\hat{\mathbf{A}} \triangleq \mathbf{UA}$ and $\hat{\mathbf{B}} \triangleq \mathbf{UB}$, respectively, contain all vectors in $\hat{\mathcal{V}}_n$ and $\hat{\mathcal{V}}_{n-1}$, where $\hat{\mathcal{V}}_s$ is defined as follows.

$$\hat{\mathcal{V}}_s = \left\{ \mathbf{E}\left(\sum_{i,j=2, i\neq j, (i,j)\neq(2,3)}^{K} \beta_{i,j}\hat{\tau}_{t_{i,j}} \right) \underline{w}', \beta_{i,j} \in \{0, 1, \ldots, s\} \right\},$$

where $\hat{\tau}_{t_{i,j}} = \hat{\tau}_{1,j}^{[i]} + \hat{\tau}_{j,3}^{[1]} + \hat{\tau}_{3,1}^{[2]}$. By assuming that the relative delays are independent and distinct continuous random variables, $\hat{\tau}_{t_{i,j}}$'s are independent and distinct random variables for all i and j. Moreover, since the asynchronous delays are random variables of length less than a symbol interval, $-3 < \hat{\tau}_{t_{i,j}} < 3, \forall\, i, j$. Note that $\hat{\tau}_f$ is independent of $\hat{\tau}_{t_{i,j}}$ for all $i, j \in \{2, 3, \ldots, K\}$. Similarly, $\hat{\tau}_f$ is a continuous random variable aver $[-2, 2]$. It is seen that

$$\begin{aligned} [\mathbf{A}, \mathbf{FB}] &= \mathbf{U}^\dagger[\hat{\mathbf{A}}, \hat{\mathbf{F}}\hat{\mathbf{B}}] \\ &= \mathbf{U}^\dagger\mathbf{W}\check{\mathbf{T}}, \end{aligned} \tag{4.58}$$

where $\check{\mathbf{T}} = [\tilde{\mathbf{A}}, \hat{\mathbf{F}}\tilde{\mathbf{B}}]$. $\tilde{\mathbf{A}}$ and $\tilde{\mathbf{B}}$ are defined similar to $\hat{\mathbf{A}}$ and $\hat{\mathbf{B}}$ when $\underline{w}'$ is a vector with all entries equal to one. Clearly, $[\mathbf{A}, \mathbf{FB}]$ and $\check{\mathbf{T}}$ have the same rank order.

Let $\phi_{i,j} \triangleq e^{-\xi\frac{2\pi}{N}\hat{\tau}_{t_{i,j}}}$ and $\theta \triangleq e^{-\xi\frac{2\pi}{N}\hat{\tau}_f}$. The k-th row of $\check{\mathbf{T}}$ has entries of the following forms.

$$\prod_{i,j=2, i\neq j, (i,j)\neq(2,3)}^{K} \phi_{i,j}^{(k-1)\beta_{i,j}},\ \beta_{i,j} \in \{0, 1, \ldots, n\},\ \text{ or}$$

$$\left(\prod_{i,j=2, i\neq j, (i,j)\neq(2,3)}^{K} \phi_{i,j}^{(k-1)\beta_{i,j}} \right) \theta^{k-1},\ \beta_{i,j} \in \{0, 1, \ldots, n-1\}.$$

One can see that $\check{\mathbf{T}}$ is a Vandermonde matrix with the generator vector $\underline{\check{t}}$ containing all the above entries for $k = 2$. In general, the entries of this vector have the following form.

$$\theta^\alpha \left(\prod_{i,j=2, i\neq j, (i,j)\neq(2,3)}^{K} \phi_{i,j}^{\beta_{i,j}} \right),\ \beta_{i,j} \in \{0, 1, \ldots, s\}. \tag{4.59}$$

where $\alpha \in \{0,1\}$, $s = n$ when $\alpha = 0$, and $s = n-1$ when $\alpha = 1$. If two non-trivial elements of $\underline{\check{t}}$ are the same, we get

$$\begin{aligned} & \theta^{\alpha} \prod_{i,j=2, i\neq j, (i,j)\neq(2,3)}^{K} \phi_{i,j}^{\beta_{i,j}} = \theta^{\alpha'} \prod_{i,j=2, i\neq j, (i,j)\neq(2,3)}^{K} \phi_{i,j}^{\beta'_{i,j}}, \\ \Rightarrow \quad & (\alpha-\alpha')\hat{\tau}_f + \sum_{i,j=2, i\neq j, (i,j)\neq(2,3)} (\beta_{i,j}-\beta'_{i,j})\hat{\tau}_{t_{i,j}} = kN, \quad k \in \mathbb{Z} \end{aligned} \tag{4.60}$$

Note that each entry of vector $\underline{\check{t}}$ contains at least one parameter (θ or $\phi_{i,j}$) with different exponent (α or $\beta_{i,j}$) from that of the corresponding parameter in other entries. Therefore, the above equation does not trivially hold for $k = 0$. Moreover, since $\hat{\tau}_f$ and $\hat{\tau}_{t_{i,j}}$'s are continuous independent random variables respectively over $[-2,2]$ and $[-3,3]$ intervals, they do not satisfy equation (4.60) with probability one. This concludes the proof. □ □

Corollary 4.3. *The proposed asynchronous interference alignment scheme achieves the total DOF equal to $K/2$ over the constant K-user asynchronous interference channel almost surely.*

The proof is similar to that of Corollary 4.1 and is omitted for brevity. By combining the upper-bound given in Section 4.1.3 and the result of Corollary 4.3, the proof of Theorem 4.1 is concluded.

4.4 Asynchronous Interference Channel with Multiple Antenna Nodes

In a K-user interference channel with multiple antenna nodes, say M antennas at each node, it is shown in [52] that the total DOF is upper bounded by $MK/2$. For the three-user constant interference channel this upper bound is achieved using the vector alignment scheme proposed in [52] in a finite number of the channel use. However, it is not known if in general for $K > 3$ the same scheme can achieve the total DOF of the channel under quasi-static assumption. For the constant channel scenario, the upper bound is achievable using the real interference alignment technique proposed in [59] when $\rho \to \infty$ and the system has infinite quantization's precision. When the channel coefficients are time/frequency varying, the underlying channel is converted into a single antenna nodes' interference channel with MK independent users. In this case, the vector alignment scheme proposed in [52] is sufficient to achieve the total DOF of the channel.

Similar to the single antenna nodes' interference channel, the asynchronism among the users can be deployed to perform the alignment task under the quasi-static assumption. Theoretically,

the medium can be considered as an asynchronous interference channel with MK independent single antenna users. In this case, by applying the same alignment scheme proposed in Section 4.3, the total $MK/2$ DOF is achievable almost surely. However, since the antennas of each node are co-located, it is more practical to consider the same asynchronous delay for all links between each pair of transmitter-receiver nodes. In this case, the system cannot be considered as a single antenna nodes' asynchronous interference channel with MK independent users.

For such a scenario, assume that at the j-th transmitter node, M independent streams of information symbols, $\underline{x}_j^{[p]}, p = 1, 2, \ldots, M$, each of length s_j, are independently precoded by a matrix $\mathbf{V}_j$ of size $N \times s_j$. Each of the resulted vectors is first supported with enough number of CPS symbols and then is serially transmitted by one of the existing antennas. All the nodes use the same shaping waveform. At the receiver side, the CPS symbols are discarded. Let $\mathbf{H}_{i,j}$ of dimension M be the channel matrix between the j-th transmitter and the i-th receiver nodes. The received signal model at the output of the q-th antenna of the i-th receiver node is given by

$$\underline{y}_i^{[q]} = \sum_{j=1}^{K} \mathbf{\Gamma}_{i,j} \mathbf{V}_j \underline{X}_{i,j}^{[q]} + \underline{z}_i^{[q]}, q = 1, 2, \ldots, M, \tag{4.61}$$

where

$$\underline{X}_{i,j}^{[q]} = \sum_{p=1}^{M} h_{i,j}(q,p) \underline{x}_j^{[p]}. \tag{4.62}$$

$\underline{y}_i^{[q]}$ and $\underline{z}_i^{[q]}$ are respectively the received signal and the noise vectors at the output of the q-th antenna of the i-th receiver node. Matrix $\mathbf{\Gamma}_{i,j}$ given in (4.12) represents the effect of the shaping waveform and the asynchronous delays between the j-th transmitter and the i-th receiver. $h_{i,j}(q,p)$ is the (q,p)-th entry of $\mathbf{H}_{i,j}$ (the entry at the q-th row and the p-th column). $\underline{X}_{i,j}^{[q]}$ is the image of the transmitted vectors from the j-th transmitter node at the q-th antenna of the i-th receiver node.

Since the asynchronous delay is the same, matrix $\mathbf{\Gamma}_{i,j}$ is the same for all links from the j-th transmitter node to the i-th receiver node. The precoding matrix $\mathbf{V}_j$ is also the same for all transmitted streams from the j-th transmitter node. Therefore, if the same precoding matrices as those designed in Section 4.3 for the single antenna nodes' K-user asynchronous interference channel is used, the interfering signals from other users at each receiver antenna are aligned and lie in a subspace of minimum dimension (approximately equal to $N/2$ for large length codewords) which is distinct from that of the desired signals. Hence, $s_1 = (n+1)^\kappa$ and $s_j = n^\kappa$, $j = 2, 3, \ldots, K$, where $\kappa = (K-1)(K-2)-1$. N is chosen as $N = n^\kappa + (n+1)^\kappa$. In this case, each user can almost surely achieve the total $1/2$ DOF in time for large length codewords. By applying the zero-forcing filter at the output of each receive antenna, the interference signals from

other users are discarded. However, the transmitted signals from co-located antennas are aligned at each receiver antenna and they lie in the desired subspace for all co-located receiver antennas. The equivalent channel model in this case is the same as that of an $M \times M$ MIMO channel with total M spatial DOF. Hence, each user can achieve the total $M/2$ DOF with probability one which is tantamount to achieving $MK/2$ DOF for the entire network almost surely. It is worth noting that, in difference to the scheme proposed in [52], using the same precoding matrices as those of the K-user single antenna nodes' interference channel is sufficient to achieve the total DOF of the corresponding multiple antenna nodes' medium. This causes the alignment task to be performed faster (i.e., in less number of channel use) specially for large values of M.

4.5 Discussion and Conclusion

A symbol asynchronous K-user interference channel with quasi-static fading coefficients was considered. It was shown that the total DOF of this channel is the same as that of the corresponding synchronous channel. We proposed a novel alignment scheme for the underlying constant interference channel by deploying the asynchronous delays among the received signals at each receiver node to achieve the total $MK/2$ DOF of this channel almost surely (M is the number of antennas at each node) in the limit of codeword's length. In finite length codewords, however, the existence of CPS symbols avoids achieving the same total DOF of the corresponding synchronous time-varying channel. In the proposed interference alignment scheme, there is no need to have the channel state information of the links at the transmitter side. Instead, the full state of the asynchronous delays is required at all nodes. Although the asynchronous delays are assumed to be less than a symbol interval, generalization to arbitrary values of the delays is straightforward. If we assume that the maximum possible symbol-asynchronous delay among the users is less than b symbol intervals, it is sufficient to support each transmitted frame by $u + b$ cyclic prefix and $u+b$ cyclic suffix symbols. One can use the inverse DFT (IDFT) filter at the transmitters and the DFT filter at the receivers to convert the circulant channel matrices to diagonals ones to simplify the signaling scheme as well as the mathematical analysis. However, the role of the CPS symbols is critical in our proposed scheme in order to mathematically track the underlying problem.

Chapter 5

Future Research Directions

Some interesting problems and ideas that have been emerged from this dissertation are discussed in this chapter.

5.1 Asynchronous Interference Alignment

5.1.1 Alignment with Rational Delay Parameters

The proposed interference alignment scheme achieves the total DOF of the underlying channel when all the delay parameters and the codeword's length N are algebraically independent over the integers. In practice, the channel parameters including the delays are quantized values. Hence, they are rational numbers and they do not satisfy the aforementioned required condition. In this case, the total DOF strictly less than $K/2$ is achieved. However, it is not known what the total DOF of the channel is under this condition. Hence, characterizing the total DOF of the channel and finding a proper achieving scheme in this case are two very interesting topics from the practical point of view.

5.1.2 Relaxing the Condition on the Shaping Waveform

In the proposed alignment scheme, it was seen that the shaping waveform should have a sub-linear decaying rate in the time domain. One may relax this condition by performing the alignment task directly from $\mathbf{\Gamma}_{i,j}$'s and accordingly $\mathbf{\Lambda}_{i,j}$'s matrices (not from their approximations). This may cause a more involved math, however, results in a more general solution for the underlying

problem. One may also deploy the channel fading coefficients or various shaping waveforms for the users to simplify relaxing this condition.

5.2 Application in Other Interference Scenarios

The proposed scheme can be applied to many other quasi-static interference scenarios such as X-Neworks, Z-Networks, and multi antenna nodes interference networks to perform the alignment task and to achieve the total DOF of these channels under quasi-static assumption.

Interference alignment over quasi-static frequency selective networks with finite number of tap delays may also be performed using the proposed scheme. While this can be performed using the vector alignment scheme of [52] when the bandwidth goes to infinity, using the scheme proposed in this thesis, the underlying channel is converted to a time varying fading channel with correlated fading coefficients over time. This may solve the lack of channel variation required for the interference alignment in these networks.

The proposed scheme can also be used to provide secure communications in constant channel scenarios. A secure communication, which is usually obtained by scarifying a portion of the resources, results in a remarkable throughput loss in the system. Using interference alignment, one may provide a sucre communication with the minimum loss of the resources by aligning the interference signals at the desired receivers while accumulating them at the eavesdroppers.

Bibliography

[1] S. Verdu, "The capacity region of symbol asynchronous Gaussian multiple access channel," *IEEE Transactions on Information Theory*, vol. 35, pp. 733–751, July 1989. 2, 33, 82

[2] S. Wei, "Diversity multiplexing tradeoff of asynchronous cooperative diversity in wireless networks," *IEEE Transactions on Information Theory*, vol. 53, pp. 4150–4172, November 2007. 2, 6, 8

[3] K. Barman and O. Dabeer, "Capacity of MIMO systems with asynchronous PAM," *IEEE Transactions on Communications*, vol. 57, pp. 3366–3375, November 2009. 2

[4] J. H. Winters, "The diversity gain of transmit diversity in wireless systems with rayleigh fading," *IEEE Transactions on Vehicular Technology*, vol. 47, pp. 119–123, February 1998. 2

[5] F. Rusek and J. B. Anderson, "On information rates for faster than Nyquist signaling," in *Proc. IEEE Global Telecommunications Conference*, (San Francisco), November 2006. 2

[6] M. Bossert, A. Huebner, F. Schuehlein, H. Haas, and E. Costa, "On cyclic delay diversity in OFDM based transmission schemes," *OFDM Workshop*, 2002. 2

[7] *Wireless LAN medium access control (MAC) and physical layer specifications.* IEEE Std 802.11n/D2.00, Standard, February 2007. 2

[8] Q. Wang, Y. Chang, and D. Yang, "Deliberately designed asynchronous transmission scheme for MIMO systems," *IEEE Signal Processing Letters*, vol. 14, pp. 920–923, December 2007. 2

[9] V. Tarokh, N. Seshadri, and A. R. Calderbank, "Space-time codes for high data rate wireless communication: performance criterion and code construction," *IEEE Transactions on Information Theory*, vol. 44, pp. 744–765, March 1998. 2, 3, 13

[10] H. El-Gamal and A. R. Hammons Jr., "A new approach to layered space-time coding and signal processing," *IEEE Transactions on Information Theory*, vol. 47, pp. 2335–2367, September 2001. 2, 14

[11] A. R. Hammons Jr. and H. El-Gamal, "On the theory of space-time codes for PSK modulation," *IEEE Transactions on Information Theory*, vol. 46, pp. 524–542, March 2000. 2, 4

[12] B. Hassibi and B. Hochwald, "High-rate codes that are linear in space and time," *IEEE Transactions on Information Theory*, vol. 48, pp. 1804–1824, July 2002. 2, 3

[13] H. El-Gamal and M. O. Damen, "Universal space-time coding," *IEEE Transactions on Information Theory*, vol. 49, pp. 1097–1119, May 2003. 2, 4, 5, 16, 23

[14] B. A. Sethuraman, B. S. Rajan, and V. Shashidhar, "Full-diversity, high-rate, space-time block codes from division algebras," *IEEE Transactions on Information Theory*, vol. 49, pp. 2596–2616, October 2003. 2

[15] H. F. Lu and P. V. Kumar, "Unified construction of space-time codes with optimal rate-diversity tradeoff," *IEEE Transactions on Information Theory*, vol. 51, pp. 1709–1730, May 2005. 2, 4

[16] P. Elia, B. Sethuraman, and P. V. Kumar, "Perfect space-time codes with minimum and non-minimum delay for any number of antennas," *IEEE Transactions on Information Theory*, December 2005. 2, 6

[17] S. Tavildar and P. Viswanath, "Approximately universal codes over slow-fading channels," *IEEE Transactions on Information Theory*, vol. 52, pp. 3233–3258, July 2006. 2, 6

[18] A. Sendonaris, E. Erkip, and B. Aazhang, "User cooperation diversity- part I: System description," *IEEE Transactions on Communications*, vol. 51, pp. 1927–1938, November 2003. 2

[19] A. Sendonaris, E. Erkip, and B. Aazhang, "User cooperation diversity part II: Implementation aspects and performance analysis," *IEEE Transactions on Communications*, vol. 51, pp. 1939–1948, November 2003. 2

[20] Y. Jing and B. Hassibi, "Distributed space-time coding in wireless relay networks," *IEEE Transactions on Wireless Communications*, vol. 5, pp. 4–6, December 2006. 3

[21] Y. Jing and H. Jafarkhani, "Using orthogonal and quasi-orthogonal designs in wireless relay networks," *IEEE Transactions on Information Theory*, vol. 53, pp. 6–8, November 2007. 3

[22] S. Wei, D. L. Goeckel, and M. C. Valenti, "Asynchronous cooperative diversity," *IEEE Transactions on Wireless Communications*, vol. 5, pp. 1547–1557, June 2006. 3

[23] Y. Mei, Y. Hua, A. Swami, and B. Daneshrad, "Combating synchronization errors in cooperative relays," in *Proc. IEEE International Conference on Acoustic, Speech, and Signal Processing*, (Philadelphia), March 2005. 3, 4

[24] S. M. Alamouti, "A simple transmit diversity technique for wireless communications," *IEEE Journal of Selected Areas in Communications*, vol. 16, pp. 1451–1458, October 1998. 3

[25] G. S. Rajan and B. S. Rajan, "OFDM based distributed space time coding for asynchronous relay networks," in *Proc. IEEE International Conference on Communications*, pp. 19–23, May 2008. 3

[26] Y. Li, W. Zhang, and X. G. Xia, "Distributive high-rate full-diversity space-frequency codes for asynchronous cooperative communications," in *Proc. IEEE International Symposium on Information Theory*, (Seattle), pp. 2612–2616, July 2006. 3

[27] M. Torbatian and M. O. Damen, "On the design of delay-tolerant distributed space-time codes with minimum length," *IEEE Transactions on Wireless Communications*, vol. 8, pp. 931–939, February 2009. 4

[28] Y. Shang and X. Xia, "Shift-full-rank matrices and applications in space-time trellis codes for relay networks with asynchronous cooperative diversity," *IEEE Transactions on Information Theory*, vol. 52, pp. 3–7, July 2006. 4

[29] Y. Li and X. Xia, "Full-diversity distributed space-time trellis codes for asynchronous cooperative communications," in *Proc. IEEE International Symposium on Information Theory*, pp. 911–915, September 2005. 4, 27

[30] A. R. Hammons Jr., "Algebraic space-time codes for quasi-synchronous cooperative diversity," in *Proc. IEEE International Conference on Wireless Networks, Communications and Mobile Computing*, pp. 11–15, June 2005. 4

[31] A. R. Hammons Jr., "Space-time code designs based on generalized binary rank criteria with application to cooperative diversity," in *Lecture notes in Computer Science*, vol. 399, pp. 60–84, Spring-Verlag, 2006. 4

[32] A. R. Hammons Jr. and R. E. Conklin, "Space-time block codes for quasi-synchronous cooperative diversity," in *Proc. Military Communication Conference*, (Washington DC), October 2006. 4

[33] M. O. Damen and A. R. Hammons Jr., "Delay tolerant distributed TAST codes for cooperative diversity," *IEEE Transactions on Information Theory*, vol. 53, pp. 3755–3773, October 2007. 4, 5, 13, 14, 27

[34] L. Zheng and D. Tse, "Diversity and multiplexing: A fundamental tradeoff in multiple-antenna channels," *IEEE Transactions on Information Theory*, vol. 49, May 2003. 5, 30, 42, 43, 54, 58, 60

[35] T. M. Cover and A. E. Gamal, "Capacity theorems for the relay channel," *IEEE Transactions on Information Theory*, vol. 25, pp. 572–584, September 1979. 5

[36] G. Kramer, M. Gastpar, and P. Gupta, "Cooperative strategies and capacity theorems for relay networks," *IEEE Transactions on Information Theory*, vol. 51, pp. 3037–3063, September 2005. 5

[37] J. N. Laneman and G. Wornell, "Distributed space-time coded protocols for exploiting cooperative diversity in wireless networks," *IEEE Transactions on Information Theory*, vol. 49, p. 24152525, October 2003. 6

[38] J. N. Laneman, D. N. C. Tse, and G. Wornell, "Cooperative diversity in wireless networks: Efficient protocols and outage behavior," *IEEE Transactions on Information Theory*, vol. 50, pp. 3062–3080, December 2004. 6

[39] S. Pawar, A. S. Avestimehr, and D. N. C. Tse, "Diversity-multiplexing tradeoff of the half-duplex relay channel," in *Proc. Allerton Conf. Communication, Control, and Computing*, (Monticello, IL), September 2008. 6

[40] N. Prasad and M. K. Varanasi, "High performance static and dynamic cooperative communication protocols for the half duplex fading relay channel," in *Proc. IEEE Globecom*, (San Francisco, CA), November 2006. 6

[41] M. Yuksel and E. Erkip, "Multiple-antenna cooperative wireless systems: A diversity-multiplexing tradeoff perspective," *IEEE Transactions on Information Theory*, vol. 53, p. 33713393, October 2007. 6

[42] P. Elia, K. Vinodh, M. Anand, and P. V. Kumar, "D-MG tradeoff and optimal codes for a class of AF and DF cooperative communication protocols," *IEEE Transactions on Information Theory*, vol. 55, pp. 3161–3185, July 2009. 6, 7, 42, 43, 48, 54, 60, 61, 63, 67

[43] M. Nahas, A. Saadani, and W. Hachem, "Performance of asynchronous two-relay two-hop wireless cooperative networks," *IEEE Transaction on Wireless Communications*, vol. 9, pp. 1086–1096, March 2010. 6, 7

[44] R. N. Krishnakumar, N. Naveen, K. Sreeram, and P. V. Kumar, "Diversity multiplexing tradeoff of asynchronous cooperative relay networks," in *Proc. Forty-Sixth Annual Allerton Conference*, (Allerton House, UIUC, Illinois, USA), September 23-26 2008. 6, 7

[45] R. N. Krishnakumar, N. Naveen, and P. V. Kumar, "Diversity multiplexing tradeoff of asynchronous cooperative relay networks," *Available on http://arxiv.org/abs/0807.0204*, 2008. 6, 7

[46] S. Yang and J. C. Belfiore, "Towards the optimal amplify-and-forward cooperative diversity scheme," *IEEE Transactions on Information Theory*, vol. 53, pp. 3114–3126, September 2007. 7

[47] T. Han and K. Kobayashi, "A new achievable rate region for the interference channel," *IEEE Transactions on Information Theory*, vol. 27, pp. 49–60, January 1981. 8

[48] A. S. Motahari and A. K. Khandani, "Capacity bounds for the Gaussian interference channel," *IEEE Transactions on Information Theory*, vol. 55, pp. 620–643, February 2009. 8

[49] X. Shang, G. Kramer, and B. Chen, "A new outer bound and the noisy interference sum-rate capacity for Gaussian interference channels," *IEEE Transactions on Information Theory*, vol. 55, pp. 689–699, February 2009. 8

[50] V. S. Annapureddy and V. V. Veeravalli, "Gaussian interference networks: Sum capacity in the low-interference regime and new outer bounds on the capacity region," *IEEE Transactions on Information Theory*, vol. 55, pp. 3032–3050, July 2009. 8

[51] R. Etkin, D. Tse, and H.Wang, "Gaussian interference channel capacity to within one bit," *IEEE Transactions on Information Theory*, vol. 54, pp. 5534–5562, December 2008. 8

[52] V. R. Cadambe and S. A. Jafar, "Interference alignment and the degrees of freedom for the k user interference channel," *IEEE Transactions on Information Theory*, pp. 3425–3441, August 2008. 9, 81, 82, 88, 94, 95, 97, 101, 104, 106, 108

[53] M. A. Maddah-Ali, S. A. Motahari, and A. K. Khandani, "Signaling over MIMO multi-base systems: combination of multi-access and broadcast schemes," in *Proc. IEEE International Symposium on Information Theory*, July 2006. 9

[54] M. A. Maddah-Ali, A. S. Motahari, and A. K. Khandani, "Communication over MIMO X channels: interference alignment, decomposition and performance analysis," *IEEE Transactions on Information Theory*, 2008. 9

[55] B. Nazer, M. Gastpar, S. A. Jafar, and S. Vishwanath, "Ergodic interference alignment," in *Proc. IEEE International Symposium on Information Theory*, (Seoul, Korea), pp. 1769–1773, June 28-July 3 2009. 9

[56] A. Høst-Madsen and A. Nosratinia, "The multiplexing gain of wireless networks," in *Proc. IEEE International Symposium on Information Theory*, 2005. 9, 83

[57] R. Etkin and E. Ordentlich, "The degrees-of-freedom of the k-user gaussian interference channel is discontinuous at rational channel coefficients," *IEEE Transactions on Information Theory*, vol. 55, pp. 4932–4946, November 2009. 9

[58] V. Cadambe, S. A. Jafar, , and C. Wang, "Interference alignment with asymmetric complex signaling: settling the Høst-Madsen-Nosratinia conjecture," *IEEE Transactions on Information Theory*, vol. 56, pp. 4552–4565, September 2010. 9

[59] A. S. Motahari, S. O. Gharan, M. A. Maddah-Ali, and A. K. Khandani, "Real interference alignment: Exploiting the potential of single antenna systems," *submitted to IEEE Transactions on Information Theory*, November 2009. 9, 104

[60] V. R. Cadambe and S. A. Jafar, "Can 100 speakers talk for 30 minutes each in one room within one hour and with zero interference to each other's audience?," in *Proc. 45th Annual Allerton Conference*, October 2007. 10

[61] V. R. Cadambe and S. A. Jafar, "Degrees of freedom of wireless networks - what a difference delay makes," in *Proc. Asilomar Conference on Signals, Systems and Computers*, 2007. 10

[62] L. Grokop, D. N. C. Tse, and R. D. Yates, "Interference alignment for line-of-sight channels," *http://arxiv.org/abs/0809.3035*, September 2008. 10

[63] M. Hazewinkel, *Determinant, Encyclopedia of Mathematics*. Springer, 2001. 15

[64] X. Giraud, E. Boutillon, and J. C. Belfiore, "Algebraic tools to build modulation schemes for fading channels," *IEEE Transactions on Information Theory*, vol. 43, pp. 938–952, May 1997. 16, 20, 23

[65] M. O. Damen, H. El-Gamal, and N. C. Beaulieu, "Systematic construction of full-diversity algebraic constellations," *IEEE Transactions on Information Theory*, vol. 49, pp. 3344–3349, December 2003. 23

[66] M. O. Damen, H. El-Gamal, and G. Caire, "On maximum-likelihood detection and the search for the closest lattice point," *IEEE Transactions on Information Theory*, vol. 49, pp. 2389–2402, October 2003. 24

[67] *The IEEE standard for local and metropolitan areas networks. Part 16: Air interface for fixed and mobile broadband wireless access systems.* www.ieee.org, February, 28 2006. 24

[68] M. O. Damen, *Joint coding/decoding in a multiple access system, application to mobile communication.* Ph.d. dissertation, ENST de Paris, Paris, France, October 1999. 24

[69] A. V. Oppenheim and R. W. Schafer, *Discrete-Time Signal Processing.* Prentice Hall, 2 ed., 1999. 35

[70] H. Gazzah, P. A. Regalia, and J. P. Delmas, "Asymptotic eigenvalue distribution of block toeplitz matrices and application to blind SIMO channel identification," *IEEE Transactions on Information Theory*, vol. 47, March 2001. 35

[71] U. Grenander and G. Szegö, *Toeplitz Forms and Their Applications.* New York, Chelsea, 1984. 35, 90

[72] R. M. Gray, *Toeplitz and Circulant Matrices, A review.* Now, the essence of knowledge, 2006. 40, 41, 57, 62, 86, 90, 91

[73] R. Paley and N. Wiener, *Fourier transforms in the complex domain.* American Mathematical Society, Colloquium Publications, 1934. 93

[74] F. Amoroso, "The bandwidth of digital data signals," *Communications, IEEE Transaction on*, pp. 13–24, November 1980. 94

[75] A. H. Nuttall, "Minimum rms bandwidth of M time-limited signals with specified code or correlation matrix," *IEEE Transactions on Information Theory*, vol. 14, pp. 699–707, September 1968. 94

[76] R. S. Cheng and S. Verdu, "Capacity of root-mean-square bandlimited Gaussian multiuser channels," *IEEE Transactions on Information Theory*, vol. 37, pp. 453–465, May 1991. 94

[77] M. Sellathurai, P. Guinand, and J. Lodge, "Approaching near-capacity on a multi-antenna channel using successive decoding and interference cancellation receivers," *International Journal of Communications and Networks*, vol. 5, pp. 116–123, June 2003. 100